A DISSERTATION FOR THE DEGREE OF DOCTOR OF PHILOSOPHY

Investigation on Recovery, Permittivity and UV Absorption of Acrylic Pressure Sensitive Adhesives for Display Application

디스플레이용 아크릴 점착제의 복원력, 유전율 및 자외선 흡수에 대한 연구

Advisor: Hyun-Joong Kim

by

Jung-Hun Lee

PROGRAM IN ENVIRONMENTAL MATERIALS SCIENCE
GRADUATE SCHOOL
SEOUL NATIONAL UNIVERSITY
JANUARY, 2020

Abstract

Investigation on Recovery, Permittivity and UV Absorption of Acrylic Pressure Sensitive Adhesives for Display Application

Jung-Hun Lee
Program in Environmental Materials Science
Graduate School
Seoul National University

A display device that outputs various information to the screen is called display. Existing displays were limited to TVs and computer monitors, but in the 21st century, the range of applications such as mobile phones and tablets has expended. Accordingly, various functions for the display are required. The existing pressure sensitive adhesives (PSAs) were all responsible for fixing the layers that compose the display. However, various functions are also required for PSAs for the development of displays. The functionalities required for current display PSAs include transparency, flexibility, low permittivity and UV absorption.

Since each layer constituting the display is fixed with an acrylic PSAs, a sufficient adhesion is required. In particular, an acrylic PSAs for flexible displays requires not only adhesion performance but also stretching and recovery characteristics. For this reason, we prepared the

pattern with high/low crosslinking density region on the acrylic PSAs and confirmed the effect of the UV pattern. As result of gel fraction measurement with the content of the crosslinking agent and UV dose, the highest gel fraction value was obtained with the content of 1 phr of the crosslinking agent and UV dose of 1600 mJ/cm^2. To prepare the optimal low crosslinking density region, a pattern film as a function of the contrast of the grey and black patterns was used. As a result of measuring the UV intensity, grey 50% showed the most difference in the degree of crosslinking. For visualization of pattern formation, 2,5-bis(5-tert-butyl-benzoxazol-2-yl) thiophene (BBT), a luminescent compound, was added, and the optimal content was 0.001 phr. As a result of peel strength and full-off measurement of UV patterned acrylic PSAs according to pattern size, it showed a tendency to decrease as pattern was formed. But when the pattern size was reduced to 2 mm, the adhesion increased. On the other hand, as a result of lap shear test, when a pattern was formed, the maximum stress and strain decreased. However, there was no significant difference even when the pattern size was decreased. The measurement results of the recovery via stress relaxation began to withstand a specific strain when the pattern size decreased to 4 mm or less. In addition, the recovery increased to about 60 % when the pattern size was reduced to 2 mm. Therefore, the possibility of the UV pattern on the adhesion performance and recovery of acrylic PSAs was confirmed. However, additional research on pattern shape and size is necessary.

To smoothly drive the touch panel of the smart device, it is necessary to be able to adjust the relative permittivity of the PSA. For these reasons, acrylic prepolymers were synthesized, and four types of

low-*k* monomers were selected. The acrylic prepolymer was mixed with low-*k* monomers and UV-crosslinked to prepare a PSA film. The adhesion performance and relative permittivity of the produced film were measured. As the content of hexamethyldisiloxane (HMDS) increased, the adhesion properties decreased; however, as the content of N-vinylcaprolactam (NVC) increased, the adhesion performance increased. As the content of low-*k* monomer increased, the relative permittivity of the acrylic PSA film showed a tendency to decrease, but other behaviors were shown to vary depending on the type. Through this result, it was confirmed that the adhesion properties and the relative permittivity of the PSA film are adjustable via the type and content of low-*k* monomer due to the difference in the formation of free volume.

Recently, displays are widely used outdoors. For this reason, there is a risk that the display may cause aging and reliability problems due to ultraviolet (UV) irradiation. Because of these problems, the PSA that fixes each layer of the display, also required UV absorption. An acrylic oligomer was prepared through photopolymerization, and an acrylic PSA was prepared using UV absorbers (UVAs) and a crosslinking agent. There was no significant difference in the color change and the transmittance in the visible region depending on the type and content of UVAs. As a result of investigating UV absorption according to the type and content of UVAs, the UV absorption of UVAs with azole group was more effective than those with benzene group. The efficiency of benzotriazole (BTZ) with low molecular weight of UVA with azole group was higher and sooner. There was no significant difference in the measurement results of adhesion properties according to the type and

content of UVAs. However, when the content of triazine (TZ) having a large molecular weight was 3 phr, the adhesion rapidly decreased due to a decrease in cohesion. In other words, a certain amount of UVA content could provide UV absorption without decreasing the adhesion properties and transparency. Among them, the UV absorption of UVA with azole group and low molecular weight was the most effective.

Keywords: Acrylic PSAs, adhesion performance, functionality, crosslinking, pattern, recovery, permittivity, UV absorption

Student Number: 2015-30381

Contents

Chapter 3

Chapter 4

Chapter 6

List of Tables

List of Figures

Chapter 1

Introduction and objectives

1. Introduction

1.1. Pressure sensitive adhesives (PSAs)

Pressure sensitive adhesives (PSAs) are nonmetallic materials used primarily to bond the surfaces of various materials through adhesion and cohesion (Satas, 1999). The function of PSAs is to ensure instantaneous adhesion with the application of light pressure (Czech and Pelech, 2008). Table 1-1 lists the types and properties of PSAs. Among these, acrylic acrylic PSAs are applied in areas, such as splicing tapes, protective foils, films for the graphics market, and a rage of medical products. The common composites used in acrylic PSAs are hard/soft segment monomer, additives and initiators. The roles of the hard segment are to control the adhesive properties of PSAs. An example is acrylic acid (AA), which has a glass transition temperature (T_g) of 106 ^oC. AA possesses carboxyl groups that provide crosslinking sites. Therefore, the cohesion and adhesion properties can be controlled by the AA content. Another important component for controlling tacky property of PSAs is the soft segment, which is a combination of soft and tacky polymers with a low T_g. Commonly reported monomers include alkyl acrylates and methacrylates with 4 -17 carbon atoms, e.g. butyl acrylate, hexyl acrylate, 2-ethylhexyltyl acrylate, isooctyl acrylate, or decyl acrylate. The others are additives, such as plasticizers, inhibitors, and fillers (Li *et al.*, 2001). Therefore, the final property of PSAs is controlled by the optimal fractions of these components (Bae *et al.*, 2013).

Table 1-1. Types and properties of PSAs (Nitto Denko, 2014).

Types	**Materials**	**Properties**	
		Advantages	**Disadvantages**
Rubber	Natural rubber Synthetic rubber	• Low cost	• Small selection of substrates • Weak heat and weather resistance
Acryl	Acrylic ester copolymer	• Excellent transparency • Large selection of substrates • Easy modification by various monomer selection	• Worse heat resistance than silicone PSAs
Silicone	Silicone rubber	• Wide use range of temperatures • Outstanding resistance to heat and cold • Outstanding resistance to chemicals and weather	• Expensive • Weak release force
Urethane	Urethane resin	• Outstanding removability • Only weak of malodor and skin irritation	• Outstanding moisture permeability • Difficult to produce strong adhesion and tack

1.2. Development of display applications

The origin of the display is the Latin word Displico or Displicare, meaning ‘show’, ‘spread’, ‘display’. The most commonly used term is ‘exhibition and display’, but in electronics, display means ‘display device’ as an output device that transmits various information of various electronic devices. Displays have been developed by the invention of projectors through the invention of paper and photography. In the 20th century, display devices currently in contact began to be developed in earnest (Samsung Display Newsroom, 2017a). Starting from a cathode ray tube (CRT) invented by German physicist Karl Ferdinand Braun in 1897, a liquid crystal display (LCD), a plasm display panel (PDP) and organic light emitting diodes (OLEDS) have been developed to express lighter and clearer image quality. Currently, the display is a necessary technology for the trend of the digitized world such as TV, smart phone, monitor, tablet PC, etc. and efforts are made to develop electronic devices through continuous research and development (Samsung Display Newsroom, 2017b).

1.3. Acrylic PSAs in display devices

Acrylic PSAs have advantages not only in adhering the layers of the display device, but also in terms of image quality improvement. In a structure having an air gap, light from the backlight unit affects the refractive index between the air layer and the film layer. As a result, the light is reflected to cause losses, which causes the image quality to deteriorate. In order to improve this, as shown in Figure 1-1, when the air gap is filled with optical clear adhesive (OCA), one of the PSAs, the difference in refractive index between the film layer and the adhesive material is reduced. Light loss from the backlight unit is reduced, allowing a sharp and bright image representation (Park and Kim, 2015). In previous studies, the high refractive index material, phenoxyethyl acrylate (PEA) used to adjust the refractive index of PSAs (Miyamoto *et al.*, 2007). In addition, it is desired to improve the refractive index by using an inorganic chelate curing agent (Kim *et al.*, 2008). On the other hand, in order to develop a low refractive index PSA used for projection screen, the refractive index was lowered using a fluorine-containing monomer (Chang and Holguim, 2005a, 2005b). Thus, since PSA is one of the important component materials that support the improvement for the functionality of the display, research for the improvement of the functionality of the PSA is continuously performed.

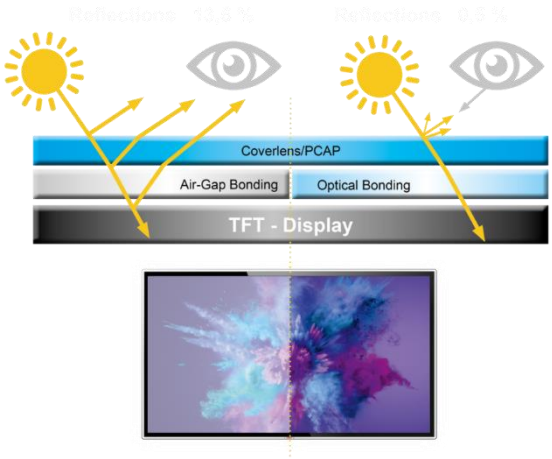

Figure 1-1. Image differences of with and without OCA

(Braunschmweiger system elektronik GmbH, Germany)

2. Required functionality of PSAs for displays

2.1. Flexibility of PSAs in flexible display

The display has been developed from CRT to LCD, PDP and OLED. A typical product, now called future displays, is a flexible display. The flexible display market is changing rapidly, moving away from the traditional curved, small wearable market and making changed to implement the display of new structures. At the current stage, early market evaluation has been made, and a foldable/rollable display is predicted in the final maturity stage. Generally, when the material in bent, a tensile phenomenon will occur in the opposite direction of the compression phenomenon in the bending direction as show in Figure 1-2. Due to the phase difference generated at this time, a strong stress is generated inside the material. This will cause stress in the adhesive material securing each layer of the display. In the case of the optical element and the substrate material, the resistance to internal stress from bending is high, because it is based on the elastic material, and it is characterized by excellent elastic recovery.

On the other hand, the interface fixed by PSAs is likely to cause delamination due to the other elastic force and surface characteristics between the material and the section where foreign materials meet, which may cause a major problem in product reliability. Therefore, there is a need for research into PSAs that can be stretched and recovered to a certain level with respect to the stress generated by bending. Previous studies reported the creep behavior of structural adhesives, but the

flexibility of PSAs have not been studied (Angelidi *et al.*, 2017a, Angelidi *et al.*, 2017b).

Figure 1-2. Compression and tensile phenomenon of PSAs in flexible device.

2.2. Permittivity of PSAs in touch screen panel

Touch screen panel (TSP) is an input device that recognizes the position on the screen when the user clicks on the screen or touches the screen with the finger, and conveys the position to the system. This technology is widely expanded supported by the spread of smart phones. TSP is composed of touch panel, a control IC, a driver SW, and the like. The touch panel is composed of a top plate and a bottom plate on which a transparent electrode (indium tin oxide, ITO) is deposited. Detects the position of the signal generated by the contact or the change of the electric capacity, and transmits the signal to the control IC. The control IC changes the analog signal transmitted from the touch panel to a digital signal and plays a role on the screen. The driver SW is a program that receives a digital signal coming from the control IC and controls the touch panel is realized according to each operating system. The TSP is classified into a resistive touch screen and a capacitive touch screen, and

recently, the capacitive touch screen is widely used for smart devices (INI Research & Consulting, 2014).

In the capacitive touch screen, when weak current is exported on the touch screen, a momentary current flowed when a human finger or a capacitive touch pen touched the screen, and was flowing on the touch screen when the current is discharged, there is a method to find and recognize the position (INI Research & Consulting, 2014).

In order to make the capacitive method more efficient, the capacitance has to be increased. The capacitance (C) is expressed by the following equation:

$$C = k\varepsilon_{\gamma}A/t$$

Where k is the constant value of object, ε_{γ} is the relative permittivity, A is the area and the t is the distance of dielectric.

In other words, in order to increase the capacitance, it is necessary to grow the area, reduce the distance, or increase the permittivity. However, when the size becomes smaller or the thickness becomes thinner, since it does not perform the original function, it tends to increase the permittivity. However, since other substances constituting TSP have no loss during current transfer with a low permittivity, it is necessary to develop an OCA having a low permittivity. Figure 1-3 is the operating mechanism of capacitance type TSP. That is, when not touching, the permittivity of the ITO top and bottom plate should be higher due to save much charge. When touched, the permittivity of OCA should be lower so that charge can flow rapidly.

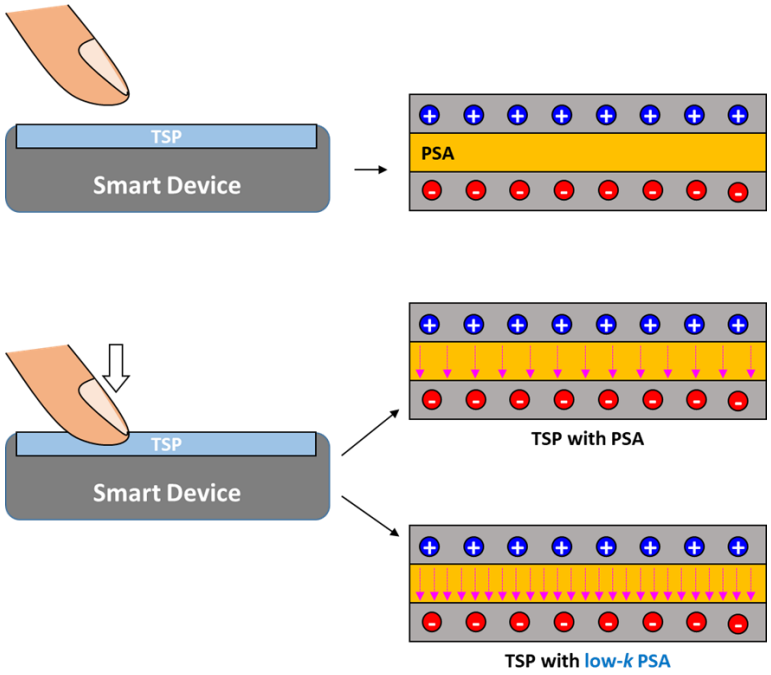

Figure 1-3. Operating mechanism of capacitance type TSP.

The capacitance type TSP used for the current smart device is a mechanism in which the electrostatic capacitance changes when it contacts a conductor such as a finger. This principle is driven when the amount of change in the electrostatic capacity exceeds a specific critical point. For this reason, the OCA used in the capacitance type touch panel is required to have a specific relative permittivity. If the relative permittivity of OCA is too high, noises are negated. On the other hand, if it is too low, the electrostatic capacitance value is not measured, and the signal transmission tends to be delayed. Therefore, adjusting the relative permittivity of OCA is a very important factor in the application of the display market (Jeon *et al.*, 2014).

Several previous researches report that the permittivity behavior of carbon fibre reinforced plastic (CFRP) joint adhesive depending on aging and epoxy resin due to curing system (McConnell and Pethrick, 2010, Garden and Pethrick, 2017). And also, permittivity of glass fiber reinforced polypropylene (GF/PP) was investigated with thermoplastic adhesive layers including different size and contents of SiC, ZnO and anatase TiO_2 particles (Sano *et al.*, 2014, Sano *et al.*, 2015). However, no studies on the permittivity behavior of PSAs have been reported.

2.3. UV absorption of PSAs in displays

The display not only helps to understand information more effectively by transmitting visual information, but also plays an important role in making appropriate decisions. Due to the advantages of these displays, displays have been used for a long time on airport flight information, devices for subway station name notation, and more recently, especially in theaters, fast food store menu boards, displays etc. There is an increasing number of cases where displays in various fields are usefully used. Complex information medium is combined contents, platforms and network installed in public places and commercial spaces to provide media services such as information, advertisement, entertainment, etc. and it is called ‘Digital Signage’. And depending on the form, the video wall, outdoor signage, interactive whiteboard (IWB) can be divided, the display panel mainly used in these products is public information display (PID) immediately. Unlike TVs used in stable spaces like homes, PIDs must be able to operate smoothly outdoors, and at the

same time there should be no problem if used 24 hours a day, 365 days a year, and so on. Its conditions can be operated are required (Samsung Display Newsroom, 2018).

The polymer resin can ensure the reliability of the product whose durability against ultraviolet radiation should be ensured. The absorbed UV energy in not immediately dissipated, causing photolysis and breaking the chemical bonds of the polymer. Photolysis breaks the chains of the polymer to make low molecular weight substances and loses the properties of the polymer. Also, UV energy breaks chemical bonds to generate highly reactive free radicals. As a result, the generated radicals combine with oxygen in the atmosphere to form peroxides, and attack the hydrogen of other polymer chains of this to generate other free radicals while forming hydroperoxides and it will continue to be the propagation of photolysis. For this reason, PSAs for PID applications can be also be exposed to UV light to shorten the product life and to inhibit reliability by photodegradation.

UV cut means that light in the UV region is blocked and light in the visible region is transmitted to maintain transparency, the ideal UV cut is at the wavelength of 400 nm, which is the boundary between UV region and visible light region (Figure 1-4). Ultraviolet absorbers (UVAs) are used for protection against ultraviolet light. UVA is effective in absorbing ultraviolet rays and converting them into harmless thermal energy to maintain product performance and quality. UVA generally has an azo group (N=N), a carbonyl group (C=O), an aromatic group and a double bond structure. It is desirable that UVA absorbs electromagnetic waves in the ultraviolet region and transmits visible light regions, but the

required physical properties vary depending on the application field, and these physical properties change according to the UVA types and contents, so it should be used selectively. Previous works have investigated the UV absorption behavior of various UVA types in TiO_2/polymer nanocomposites, carbon fiber reinforced epoxy resin, graphene oxide nanosheets (Bauh *et al.*, 2018, Hasani *et al.*, 2018, Mahdavian *et al.*, 2018, Wang *et al.*, 2016). However, there have been no studies of PSAs using various UVAs. Therefore, research on the UV absorption behavior of PSAs by UVAs and the influence of adhesion performance in needed.

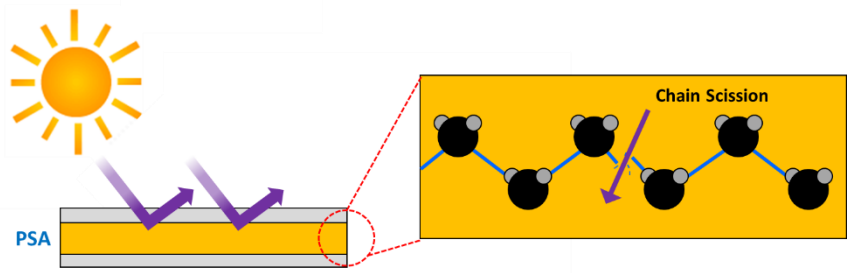

Figure 1-4. Scheme of molecular chain scission by photolysis.

3. Objective

The main purpose of PSAs is to fix each layer of the display. But as displays developed, PSAs required functionality. In the early days, thermal conductivity, which can quickly discharge the heat generated by display device, and transparency and refractive index to improve image quality began to be required. As the display industry continues to develop, there is a need for recovery for flexible display, low permittivity for improving touch sensitivity of touch screen panels, and UV absorption for preventing aging due to UV rays. However, with the current technology, if all the functionality is given to the PSAs, the inherent properties and the original function are gradually reduced, making it difficult to play a role as the PSAs.

Therefore, this study independently conducted the above-mentioned recovery, low permittivity and UV absorption. The objective of this study was to identify the ways to improve the above functionalities and the changes in adhesion property. In addition, I tried to present a reliable quantitative evaluation method for improving the functionality of PSAs.

Chapter 2

Literature review

1. Various factors on properties of acrylic PSAs

Khan and Poh (2011) reported that the dependence of adhesion performance of epoxidized natural rubber (ENR-50) based PSAs on molecular weight and testing rate using coumarone-indene as the tackifying resin. From this research, peel strength and shear strength increase up to an optimum molecular weight of 4.2×10^4 of ENR 50. In peel strength, the results due to the combined effects of wettability and mechanical strength of rubber at the molecular weight. On the other hand, for the shear strength, it is due to the optimum cohesive and adhesive forces that increase the shear resistance of the adhesive. The peel strength and shear strength also increase with increasing the test rate, which is an observation related to the viscoelasticity of the PSAs.

Ito *et al.* (2014) reported that the stringiness of crosslinked polyacrylic PSA was observed during 90 ^{o} peeling under the constant load. The PSA was consisted with random copolymer of butyl acrylate with 5 wt.% acrylic acid crosslinked by N,N,N',N'-tetraglycidy-m-xylenediamine. All stringiness of PSAs was sawtooth-shaped, but it could be classified into three types according to the crosslinking degree. The adhesion form was changed from cohesive failure to interfacial failure as increasing the crosslinking agent. From the results, the shape of stringiness is strongly dependent on the balance between the interfacial adhesion and the cohesive strength of PSA.

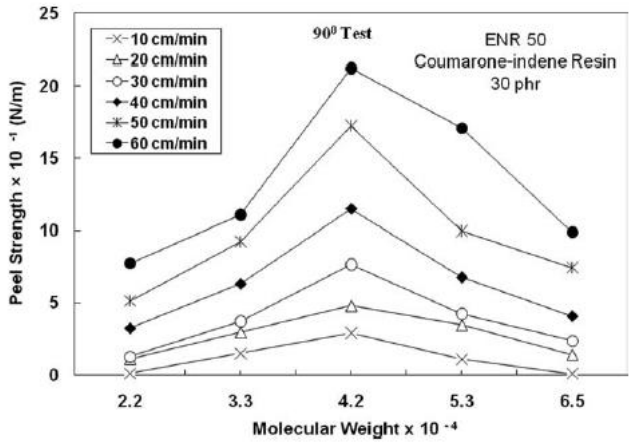

Figure 2-1. Variation of peel strength with molecular weight for various testing rate (Khan and Poh, 2011).

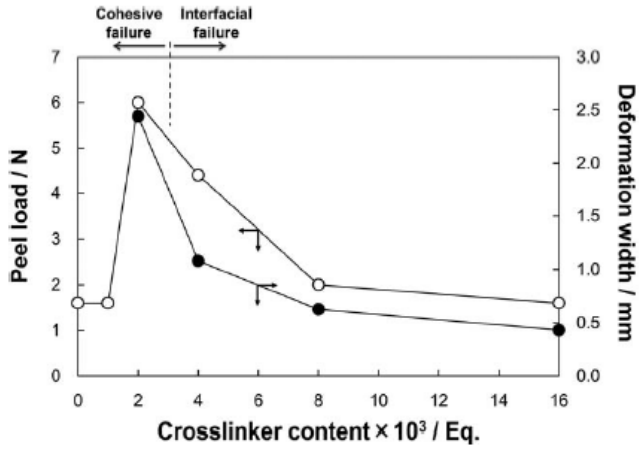

Figure 2-2. Influences of crosslinking agent content on peel load and deformation width (Ito *et al.*, 2014).

Fujita *et al.* (2000) reported that natural rubber (NR) was blended in various ratios with 29 kinds of tackifier resins to confirm miscibility via phase diagrams. Holding time was observed as required time for the PSA tape under shear stress to completely slip away from the adherend. Holding time of miscible PSA tended to decrease as increasing the tackifier content. It is due to a decrease in plateau modulus of the PSA as the tackifier content increased. The observed holding time of various miscible PSA shows different tendency as a function of the kinds of tackifiers due to they have different plateau modulus. In addition, holding time of immiscible PSA increased with increasing tackifier content. It might be caused by different phase separation.

Kajtna *et al.* (2009) reported that the effect of polymer molecular weight and crosslinking reactions on the end-use properties of the microsphere water based acrylic PSA. Polymer molecular weight and microstructure were adjusted using different chain transfer agent (CTA) concentrations and by addition of a diacrylic monomer (MM). The kinetics of suspension polymerization is relatively independent on the amount of CTA and MM. Gel phase of the adhesive reduced as increasing of CTA agent content due to it affected to the polymer molecular weight. For adhesive synthesized solely with CTA, tack decreased with low value of polymer molecular weight and low amount of gel phase. The similar result was also observed in peel strength investigation, but a cohesive failure occurred with low amount of gel phase.

Table 2-1. Tackifiers used for measurement of holding power (Fujita *et al.*, 2000).

Phase Diagram	Raw Materials	Commercial Names of Tackifiers	*Tg* (°C)	*Mn*	Main Components
Completely miscible	Rosin or terpenes	Estergum HP[a]	54.4	685	Pentaerythritol ester of hydrogenated rosin
		Superester A-75[a]	46.6	682	Disproportionated rosin esterified by glycerol, diethyleneglycol
		YS polystar T-130[b]	78.7	765	Terpene phenolic copolymer (phenol 25%)
LCST	Rosin or terpenes	Clearon K-4090[b]	41.8	793	Hydrogenated terpene resin
	Petroleum	ESCOREZ 5320[c]	75.2	395	Hydrogenated petroleum resin
Completely immiscible	Rosin or terpenes	Polypale[d]	60.2	442	25% polymerized rosin
		Estergum AAG[a]	75.7	921	Glycerol ester of rosin
	Petroleum	Kristalex 1120[d]	68.1	873	Polymer from pure aromatic monomer

[a] Supplied by Arakawa Chemical Co., Ltd. (Osaka, Japan).
[b] Supplied by Yasuhara Chemical Co., Ltd. (Fuchu-shi, Hiroshima, Japan).
[c] Supplied by Tonex Co., Ltd. (Kawasaki-shi, Japan).
[d] Supplied by Hercules Co., Ltd. (Wilmington, DE).

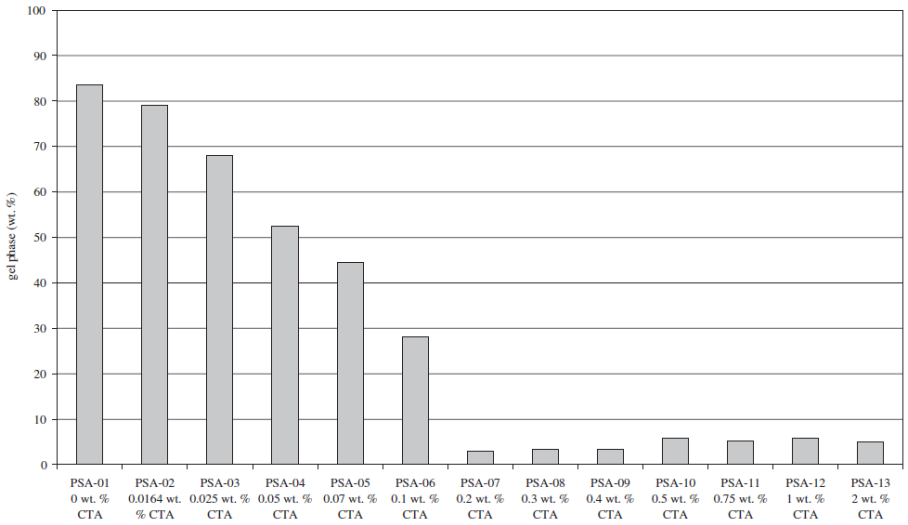

Figure 2-3. CTA effect on gel phase of PSA (Kajtna *et al.*, 2009).

Fang *et al.* (2019) reported that n-dodecyl mercaptan (DDM) chain transfer agent and 1,6-hexanediol diacrylate (HDDA) cross-linker were used to manipulate latex properties in a monomer-starved seeded semi-continuous emulsion polymerization of butyl acrylate (BA), dodecafluoroheptyl methacrylate (DFMA) together with functional monomers acrylic acid (AA) and 2-hydroxyethyl acrylate (HEA). The introduction of DDM and HDDA has no significant effects on the final particle size of the fluorinated PSA latexes. The T_g, thermal stability, surface roughness, modulus of the fluorinated latex PSA were all increased with the introduction of HDDA. Nevertheless, opposite trends were observed for the latex after the addition of DDM. Adhesion performances were considerably increased with DDM content while the shear strength decreased. On the other hand, those were significantly reduced, but shear strength was significantly increased with the increase in HDDA concentration.

Zhang *et al.* (2019a) reported that the thermal stability of acrylic PSAs based on maleimide (Mal) monomer. The heat resistant acrylic PSAs modified by Mal were synthesized successfully. The T_g, adhesion property, molecular weight, viscosity, contact angle and thermal stability of the PSAs were influenced by the content of the Mal. The molecular weight and viscosity of PSAs improved significantly, while the Mal content increased. The T_g increased due to the formation of physical crosslinking networks as well as the heterocyclic structure of Mal. Due to the imide hydrophilic groups of Mal, the contact angle of PSAs was reduced. Adhesion property of PSAs increased first and then decreased.

The Mal content had a significant effect on the thermal stability of PSAs because of the heterocyclic structure which could improve cohesion strength of PSAs. Moreover, there was no residue when the PSAs was peeled from the substrate after 170 ℃ and 3 h, which was 60 ℃ higher than pure PSAs.

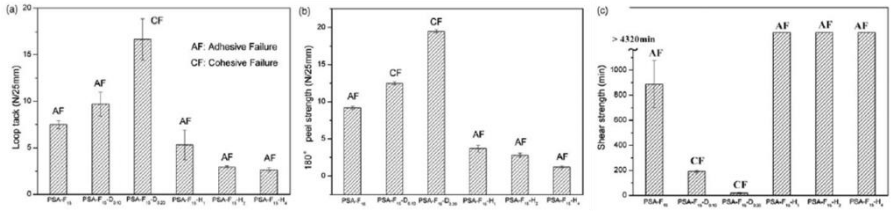

Figure 2-4. Adhesion properties of fluorinate acrylate latex PSAs with different amount of DDM and HDDA (Fang *et al.*, 2019).

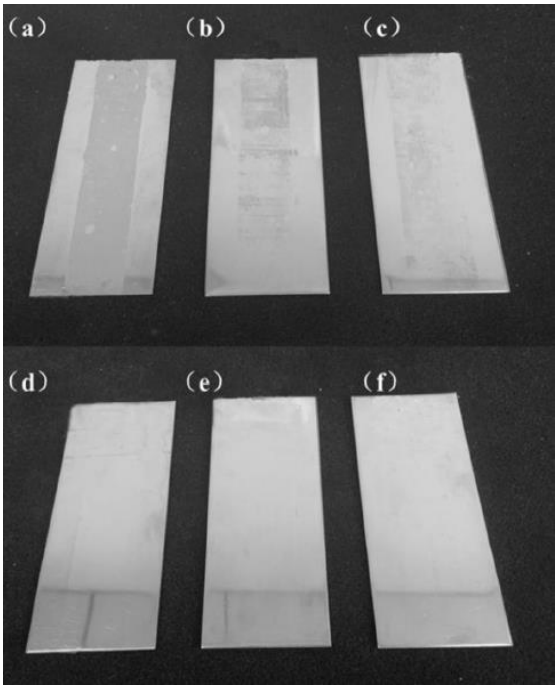

Figure 2-5. Residue situation of the PSA tapes with Mal content (wt.%) on the stainless-steel panel under 170 ^{o}C and 1 h: (a) 0; (b) 1; (c) 2.5; (d) 5; (e) 7.5; (f) 10 (Zhang *et al.*, 2019a).

2. Recovery

Dong *et al.* (1976) reported the performances such as shear modulus, shear strength, creep behavior, and creep recovery, of three commercially available elastomeric adhesives. Because this study is for the applicability of glued wood building system, they compared the physical properties and recovery of shear stress of materials with strong adhesive strength. However, it is the same physical properties required for flexible display PSA. It was confirmed that the materials were compatible with structural wood building components for structural wood building components for roof and floor system by measuring the shear modulus, shear strength, creep, and recovery. This study shows that static tests of shear modulus and strength have not fully evaluated structural elastomeric adhesives. Also, verified the need for sustained loading studies of creep, recovery, and shear strength.

Liu *et al.* (2016) reported that the incorporation of dopamine methacrylamide (DMA) and synthetic nanosilicate (LAPONITE) can be used to construct recoverable double network (DN) hydrogels. Both network-bound DMA and LAPONITE were introduced into the first network and the influence of DMA-LAPONITE interaction on the recovery of the nanocomposites DN hydrogel was evaluated. This nanocomposite DN hydrogel exhibited enhanced mechanical properties when compared to DN that do not contain both DMA and LAPONITE. The reversible DMA-LAPONITE bonds were broken under compressive loading, which dissipated fracture energy. When the nanocomposite DN

was allowed to recover, DMA–LAPONITEs bonds reformed and the hydrogel recovered over 82% of energy dissipated during the successive loading cycles. PSAs also need to measure the recovery of compressive stress as well as the recovery of shear stress. However, it is difficult to make a quantitative evaluation with typical probe and nano tip even though it has tacky.

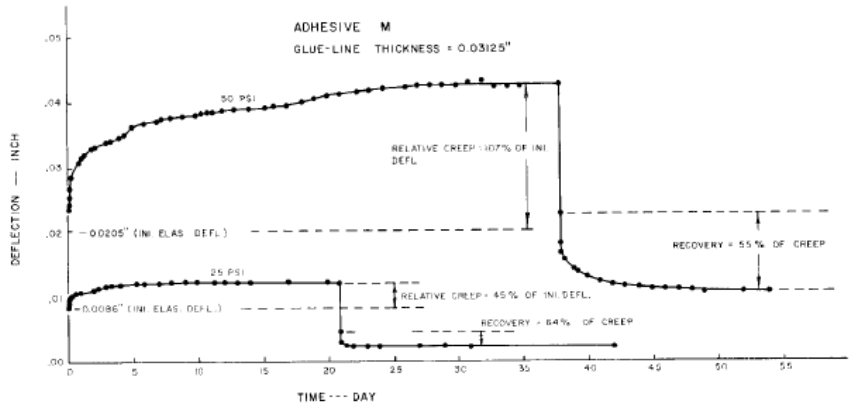

Figure 2-6. Glue-line creep and recovery for adhesive (Dong *et al.*, 1976).

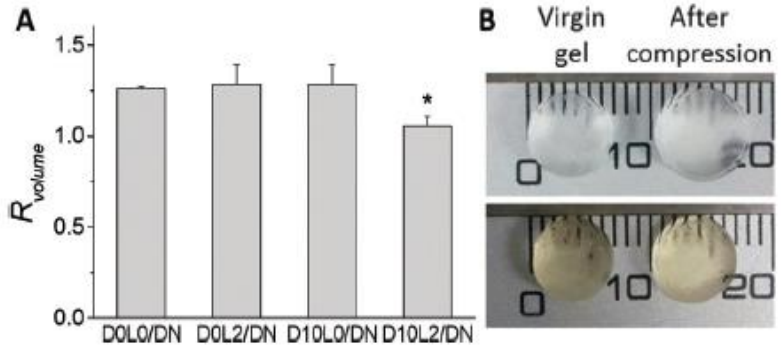

Figure 2-7. The ratio of the volume (R_{volume}) of DN after compression to a strain of 0.5 when compared to virgin DN (A) and photographs of D0L0/DN (top) and D10L2/DN (bottom) in the virgin state and after compression (B) (Liu *et al.*, 2016).

Angelidi *et al.* (2017a) reported that the effects of the loading type (tension or compression) and displacement rate on the non-linear viscoelastic ductile structural adhesive using digital image correlation-based strain fields. The results showed that the Poisson ratio should be based on real strains to take geometry changes into account. For tension, the ratio showed slightly affected to the true strain below the yield point and to the displacement rate and the rate dependency was confirmed with necking, where the ratio locally decreased. In compression, the ratio was affected by out-of-plane deformations of the specimens thus exhibited values above 0.5. The necking in tension and out-of-plane deformations in compression may be attributed to structural effects on the Poisson ration which caused from the changes in the molecular structure of the polymer.

Angelidi *et al.* (2017b) reported that the investigation of the ductility and time-dependent recovery of a ductile acrylic adhesive. The quasi-static true tensile and compressive strain behaviors were experimented at different strain rates, taking large deformations into account. Yield stress, elastic modulus, and failure strain showed a logarithmic dependency on increasing strain rate, while yield strain and stiffness after yield point were insensitive to strain rate. Loading type (tension or compression), the strain rate of loading, and the strain at unloading affected to the time-dependent recovery after unloading. The strain after remove load almost fully recover after 48 h, showing that no residual strain caused from damage or plastic flow occurred.

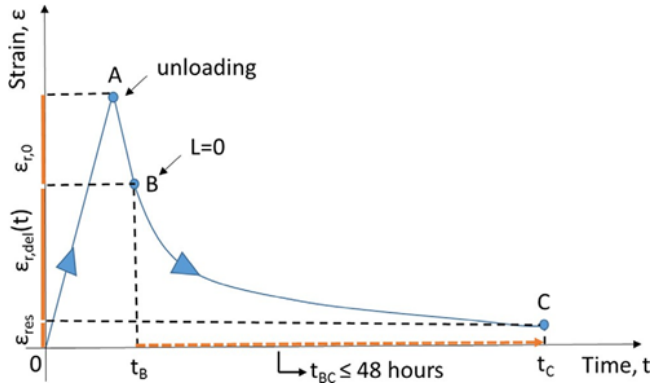

Figure 2-8. Strain recovery after unloading (schematic representation) (Angelidi *et al.*, 2017b).

Lee *et al.* (2017) reported that the acrylic PSAs were crosslinked with various contents of diisocyanate crosslinking agent. The adhesion performance of the crosslinked acrylic PSAs was investigated via peel, tack, and lap shear tests. Stress relaxation test was performed via DMA to evaluate the PSA recovery and to determine their suitability for flexible display applications. The peel strength and probe tack of the crosslinked PSA decreased as increasing the crosslinking agent content due to the decreased wettability caused by the decreasing mobility of polymer chains. Elastic recovery increased, while the residual creep strain decreased with an increase in the PSA crosslinking density. From the obtained results, it was confirmed that the adhesion property and recovery of the acrylic PSA had a conflicting relationship. Stress relaxation test also confirmed the appropriate measurement of recovery for flexible display applications.

Lee *et al.* (2019a) reported that physical properties of the 2-ethylhexyl acrylate-based UV-curable PSAs with respect to incorporation of various acrylic monomers such as methyl acrylate (MA), acrylic acid (AA), acrylamide (AM), and hydroxyethyl acrylate (HEA). The fabricated PSAs were found to have differing properties depending on the type of incorporated acrylic monomers, in terms of peel adhesion and repetitive cycle test results. In this characterization, AA incorporation showed the highest peel adhesion among others. Instantaneous strain reversibility was achieved through the formulation using MA and HEA. Peel adhesion and repetitive cycle test results suggest that the relationship between peel adhesion and strain reversibility is inversely proportional. Moreover, the results of this study can propose a choice of acrylic monomers regarding a targeted purpose.

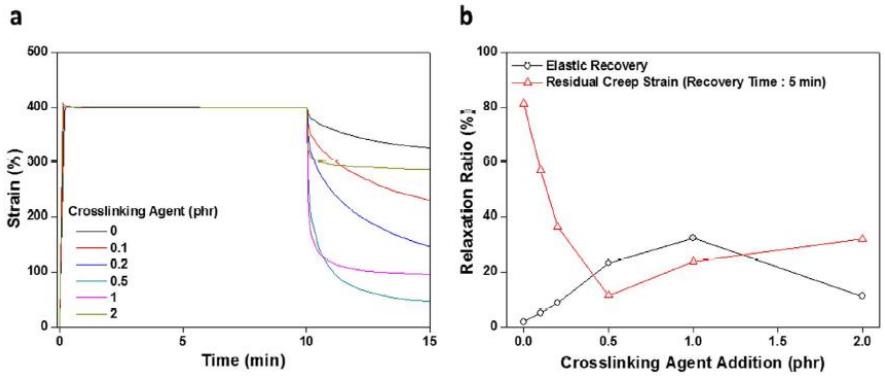

Figure 2-9. Stress relaxation testing of the acrylic PSAs. (a) strain change and (b) degrees of elastic recovery and residual creep strain values measured as functions of the crosslinking agent addition (Lee *et al.*, 2017).

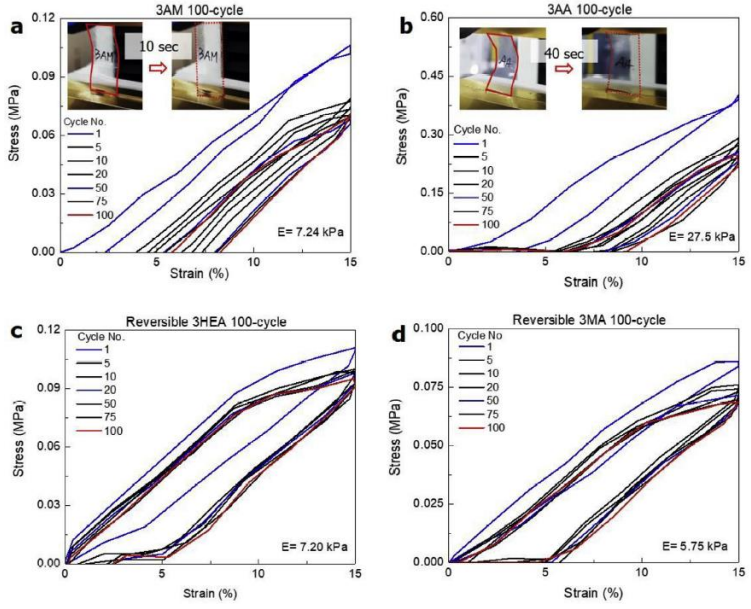

Figure 2-10. The 100-cycle stress-strain curves of acrylate-based PSAs with various acrylic monomers: (a) AM, (b) AA, (c) HEA, and (d) MA (Lee *et al.*, 2019a).

3. Permittivity

Sano *et al.* (2013) reported that investigation of high-frequency welding of polypropylene by melting composite adhesive layers containing dielectric ceramics. Various dielectric ceramics, such as barium titanate ($BaTiO_3$), anatase-titanium oxide (anatase-TiO_2), rutile-TiO_2, Zirconium oxide (ZrO_2), zinc oxide (ZnO), and silicone carbide (SiC) were blended in a polypropylene to prepare the composite adhesive layers, and the relative permittivity was measure using an impedance analyzer. In each case, the relative dielectric permittivity of the composite adhesive layer was higher than that of polypropylene (=2.3) and no frequency dependence was observed.

Sano *et al.* (2014) reported that investigation of high-frequency (HF) welding of glass-fiber-reinforced polypropylene (GF/PP) with thermoplastic adhesive layers including SiC, which is able to heat by HF irradiation. The effect of SiC particle size and content on the dielectric properties of an adhesive layer were confirmed. The relative dielectric permittivity increased with SiC content, and when the SiC increased over 30 vol.%, the relative dielectric permittivity tended to be larger as the particle size increased.

Sano *et al.* (2015) reported that study of HF welding of GF/PP with thermoplastic adhesive layers consisting of SiC, ZnO, and anatase-TiO_2. Effects of the ceramic type and content on the dielectric characteristics of these adhesive layers were evaluated experimentally.

The relative dielectric permittivity increased with SiC content, but no temperature dependence was observed. And also, the adhesive layer with ZnO shows similar tendency to the layer with SiC. However, layers with ZnO exhibited lower relative dielectric permittivity. When 40 vol.% anatase-TiO_2 was mixed with the polypropylene based, the particle aggregation was generated. The relative dielectric permittivity increased with anatase-TiO_2 content and there was no change as a function of temperature, similar to layers with SiC and ZnO. For the same ceramics content, the permittivity of layer with anatase/TiO_2 showed higher value than that with SiC and ZnO.

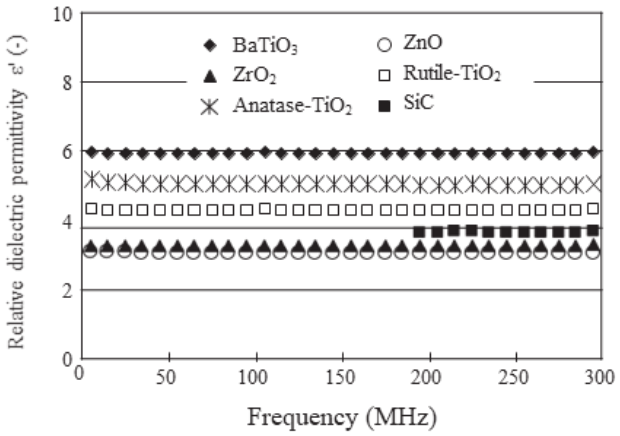

Figure 2-11. Plot of relative dielectric permittivity (ε′) of composite adhesive layers with 20 vol.% dielectric ceramic as a function of frequency (Sano *et al.*, 2013).

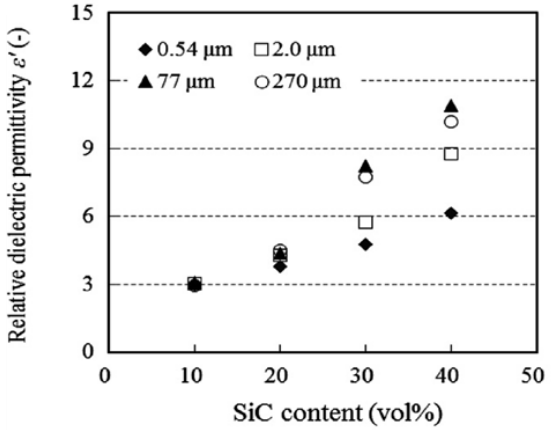

Figure 2-12. Plot of relative dielectric permittivity (ε′) value of thermoplastic adhesive layers (Sano *et al.*, 2014).

Ghosh *et al.* (2008) reported that eight poly(imide siloxane)s copolymers have been prepared by one-pot solution imidization method. The polymers are made by the reaction of bisphenol-A dianhydride (BPADA) with four different fluorinated diamines and amino-propyl terminated polydimethylsiloxane (APPS). In addition, two different levels of siloxane, 20 and 40 wt.% was incorporated. The resulting poly(imide siloxane)s are amorphous as reported and reasonably good thermal stability. The polymer films show low dielectric constant depending on the incorporation of siloxane.

Othman *et al.* (2011) reported that the effect of copolymerization of siloxane units into polyimide. Variation of the silicone content was achieved by utilizing silicone of different disiloxane repeat units. The dielectric constant, refractive index was explored in order to establish their optoelectronic properties. Copolymerization of the silicone unit into the polyimide backbone was successfully performed. Incorporation of silicone unit into the chins considerably reduced the dielectric constant.

Zhang *et al.* (2019b) reported that surface functionalized boron nitride (BN) with grafted hyperbranced polyacrylamide (BN-HBP) were prepared and used to improve the thermal conductivity and low dielectric constant of BN-filled cyanate ester resin (BN-HBP/CE) composites. The composites exhibit a dielectric constant of 3.29 at 1 MHz, a desirable λ of 0.97 W/(m·K) with T_{d5} of 407 ^{o}C as well as the highest T_g of 283 ^{o}C.

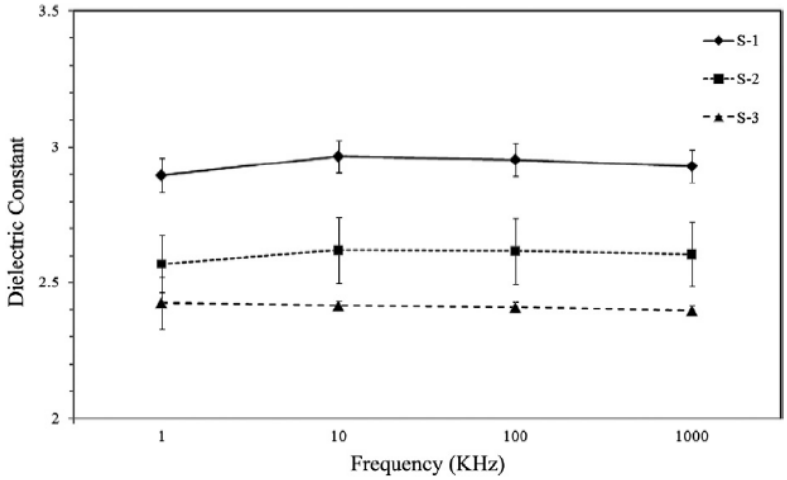

Figure 2-13. Dielectric constant of PI series corresponding to frequency 1 kHz, 100 kHz and 1000 kHz (Othman *et al.*, 2011).

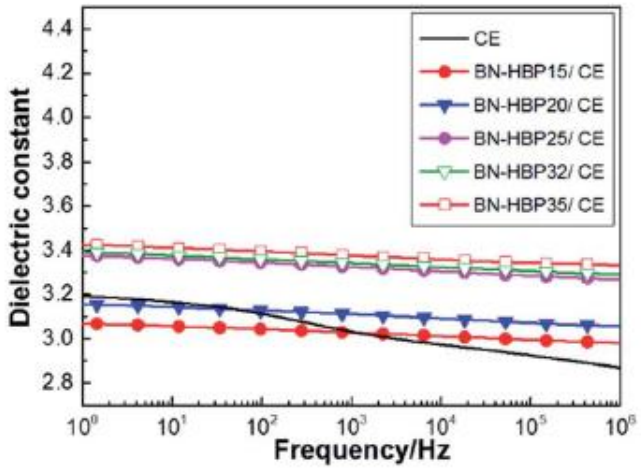

Figure 2-14. Dielectric properties vs. frequency of BN-HBP/CE composites with different content fillers (Zhang *et al.*, 2019b).

4. UV absorption

Wang *et al.* (2016) prepared high performance TiO_2/polymer nanocomposites with enhanced thermal and excellent UV-shielding properties by means of the anatase TiO_2 nanoparticle homogeneously dispersed in the poly (methyl methacrylate/butyl acrylate/methacrylic acid) [P(MMA/BA/MAA)] matrix via a miniemulsion polymerization. UV-vis transmission spectra results indicate that the films with TiO_2 nanoparticles has an excellent UV-shielding property, even at 1.5 wt.% TiO_2 loading can almost block the UV light below 350 nm while still having a high visible transparency.

Mahdavian *et al.* (2018) introduced that a facile approach to synthesize a nano-structure light stabilizer composed of a typical ultra-violet absorber (UVA) and graphene oxide (GO) nano-sheets. By UV-visible analysis, the absorption behavior of GO and UVA in water is investigated. Two absorption peaks for GO at 230 nm and 301 nm, which are respectively attributed to π-π* transition of aromatic C-C bonds, and n-π* transition of carboxylic groups, COOH (Dong *et al.*, 2012, Dong *et al.*, 2015). Three absorption peaks can be seen in the UV-visible spectrum of UVA. One intensive and sharp absorption peat at 218 nm corresponded to π-π* transition of aromatic C-C bonds. In addition, two peaks at 299 and 336 nm which can be assigned to the n-π* transition of –C=N-N=C- group. These results indicate that both GO and UVA show high capability of UBV absorption in both UV-A (315-400 nm) and UV-B (280-315 nm) regions.

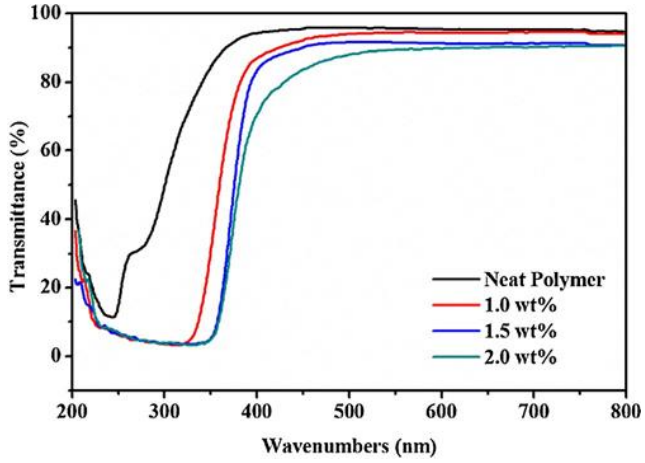

Figure 2-15. UV-vis transmittance spectra of neat P (MMA/BA/MAA) and TiO_2/P (MMA/BA/MAA) nanocomposite films (Wang *et al.*, 2016).

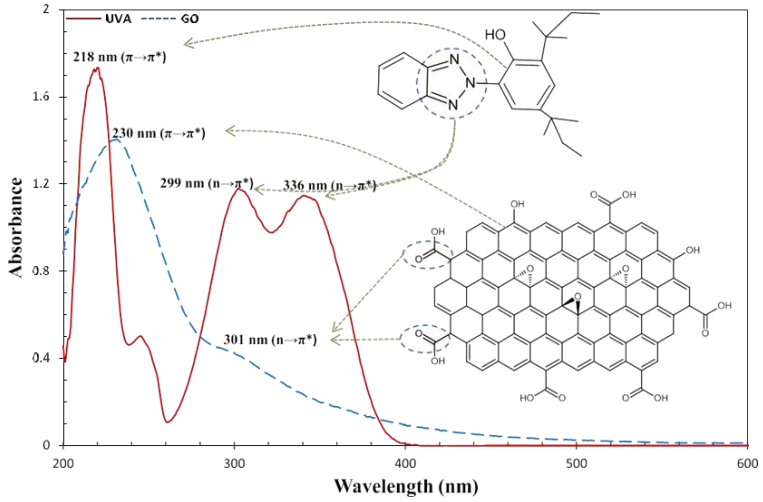

Figure 2-16. UV-visible spectra of individual UVA and GO (Mahdavian *et al.*, 2018).

Huang *et al.* (2016) reported that nontoxic polymeric UV absorbers through covalently attaching a benzophenone derivative onto

the main chain of poly(vinyl chloride) (PVC). Small amounts of PVC-UV were homogeneously mixed with PVC as additive for stabilizing PVC against UV photoaging without degradation and releasing small molecule even after while keeping thermal stability.

Nikafshar *et al.* (2017) reported that the effect of organic UV absorber on the chemical, mechanical and physical properties of cured epoxy structure. Since epoxy resins have a high amount of aromatic rings which can absorb UV light around 300 nm, Tinuvin 1130 was selected as a UV absorber working at UV light in the ranges of 300-350 nm and 350-390 nm. UV-Vis spectroscopy revealed that the epoxy system containing Tinuvin 1130 had a little yellowing after 800 h, whereas the pure epoxy system reached high levels of yellowing after the same duration.

Li *et al.* (2019) reported that poly (p-phenylene benzobisoxazole) (PBO) fibers were functionalized by 3-glycidoxypropyltrimethoxysilane (KH-560) and then coated with 1 H, 1 H, 2 H, 2H-perfluorodecyltrimethoxysilane (HFTES) and UV absorber (UV-328) to improve UV aging resistance. Compared to the pristine PBO fibers, the UV resistance of the PBO treated by the coating are significantly improved. From contact angle results for water, UV-328 has no effect on the hydrophobicity of the fibers.

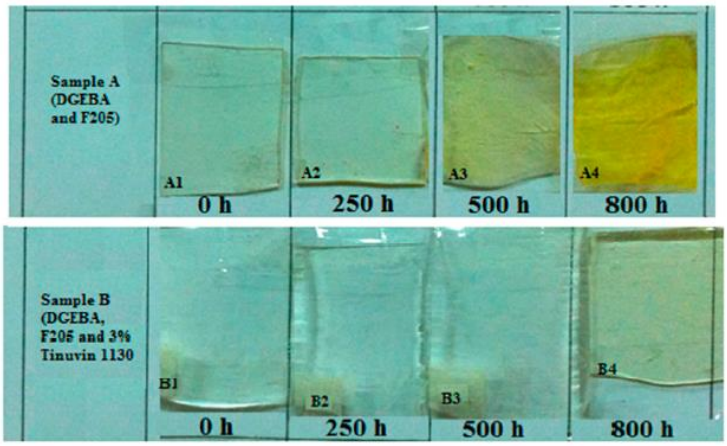

Figure 2-17. Optical images of samples with and without UV absorber after 0, 250, 500, and 800 h of UV radiation (Nikafshar *et al.*, 2017).

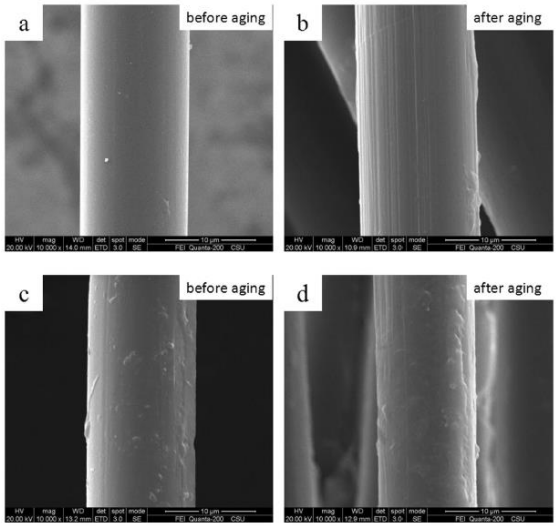

Figure 2-18. SEM images before and after UV exposure of pristine PBO (a,b) and HFTES/UV-328/*f*-PBO (c,d) (Li *et al.*, 2019).

Chapter 3

Analysis methods

1. Gel fraction

To confirm the crosslinking density of acrylic PSAs, gel fraction measurement was used. The gel content depends on the solubility parameter of the solvent. In this work, toluene was selected as the solvent. The gel fractions of the crosslinked acrylic PSAs were determined by soaking samples (approximately 5 g) in toluene, with shaking, for 1 day at room temperature. The soluble part was removed by filtration and dried at 80 ^{o}C to a constant weight. The gel fraction was calculated by the following equation:

$$\text{Gel fraction (\%)} = (W_1/W_0) \times 100$$

where W_o and W_1 are the weights before and after filtration, respectively.

2. Adhesion performance

2.1. Peel strength

The peel strengths of the specimens with widths of 25 mm were investigated using a Texture Analyzer (TA-T2i, Micro Stable Systems, UK). The specimens were pressed onto stainless steel (SUS) substrates by two passes of a 2 kg rubber roller and then aged at room temperature for 24 h. The peel strength magnitude (defined as the average force applied to a PSA specimen during debonding) was determined in accordance with the ASTM D3330 standard at an angle of 180 ° crosshead rate of 300 mm/min, and temperature of 20 ℃. The applied force was recorded for six different runs with an average value of N/25 mm.

2.2. Probe tack

The probe tack was investigated at room temperature in accordance with the ASTM D2979 standard using a Texture Analyzer equipped with a 5 mm SUS cylinder probe. The utilized standard probe tack testing process consisted of the following three stages: approaching the PSA surface, touching the PSA surface and detaching from the PSA surface. The probe rate was 0.5 mm/s, the detaching rate was 10 mm/s, and the contact time with the PSA surface was 1 s at a constant force of 100 g/cm^2. The maximum force generated when the probe was dropped from the surface of PSA was determined five times, and the average

value was calculated as N.

2.3. Pull-off test

The pull-off test was performed using a universal testing machine (AllroundLine Z010, 2000N load cell, Zwick, Ulm, Germany). On the polymethyl methacrylate (PMMA) surface, the UV patterned acrylic PSAs were loaded and crosswise covered with a glass slide (120×25×1 mm^3). The adhesive area was 25×25 mm^2, and pressed with 2 kg weight for 5 min and then aged at room temperature for 24 h. The crosshead speed was 5 mm/min. In the case of UV pattern acrylic PSA, the peel strength measurement result fluctuated and the probe tack measurement had a probe diameter of 5 mm, making quantitative evaluation difficult. Therefore, a pull-off test was added for quantitative evaluation of the adhesion performance of UV pattern acrylic PSAs.

2.4. Lap shear test

Lap shear was measured using the Texture Analyzer. The tested specimens were cut into smaller pieces with widths of 25 mm. After being removed from a silicone release film, each PSA film was attached to another PET substrate (the adhesion cross-sectional area was equal to 25×25 mm^2, and a 2 kg rubber roller was passed over the film surface three times). Lap shear tests were performed at a crosshead rate of 5 mm/min. Shear strain rate values were calculated using the following equation:

$$\text{Shear strain rate (\%)} = \Delta L/t \times 100$$

where ΔL was the moving distance, and t was the thickness of the PSA film.

PSAs for displays are usually subjected to different values of shear strain depending on their structure and radius of curvature. Therefore, investigating the relationship between the shear strain rate and the thickness of the applied PSA films is imperative for their future use in flexible display applications (Lee *et al.*, 2016).

3. Recovery

Recovery of UV patterned acrylic PSAs was investigated by stress relaxation testing using a DMA apparatus (Q-800 TA Instruments, USA). The goal of this experiment was to determine PSA characteristics and their suitability for flexible display applications by measuring the correlation between the deformation and stress with time. During the initial testing period, the investigated PSA samples were stabilized for 1 min, and then, the 300 % strain was applied for 10 min. Afterwards, the studied specimens were recovered for 5 min. Elastic recovery and residual creep strain were obtained from strain of the PSAs as a function of time. The initial stress, final stress, and relaxation ratio were derived from the stress/time graph (Lee *et al.*, 2016).

An initial stress is generated in a material when it experiences a certain deformation. The initial stress begins to decrease over time, shich is due to molecular movement, bond break, and bond interchange (Sperling, 2006). Furthermore, when the specific deformation is eliminated, it is resored by stretching the molecular chain, fixing the molecule by corsslinkiong, and entanglement of the molecular chain. However, a residual creep strain that breaks the bonds within or between molecules can cause a failure of the flexible display.

4. Permittivity

Figure 3-1 shows the equipment used to measure the relative permittivity of the PSA films. It consisted of an impedance analyzer (1260 Impedance Analyser, Solartron Analytical, UK), dielectric interface (1296 Dielectric Interface, Solartron Analytical, UK) and a chamber (micro vacuum probe station, NEXTRON Co., Ltd., Republic of Korea). The impedance analyzer is a device commonly used to measure the permittivity of materials. The reason for using the 1260 Impedance Analyzer in this research was to measure the permittivity in the low-frequency range. Additionally, since the PSA was a material with a high resistance, the investigation was performed while further connected with a dielectric interface, and the research was conducted. The general polymer material used surface/surface probes, and the data reliability was very high. However, we confirmed that since the PSA film is a semi-solid, data reliability and reproducibility were not secured according to the pressure using surface/surface probes. Figure 3-2 shows the results of permittivity measurement according to the thickness of the acrylic PSA and the distance between the probe surfaces. Acrylic PSAs are very sensitive and their physical properties change due to several variables generated in experimental. For this reason, the permittivity of PSA film was measured using the more delicate probe station. The relative permittivity of PSA films as a function of low-*k* monomer and content were measured in the frequency range from 1 to 1000 kHz. The thickness of all PSA films was approximately 400 μm, and the detected sample diameter was fixed at a 10 mm circular cross-section.

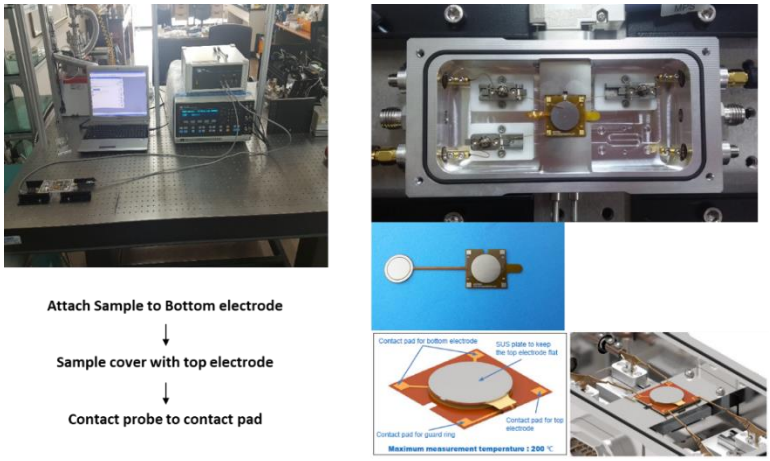

Figure 3-1. Research equipment for permittivity of PSA samples.

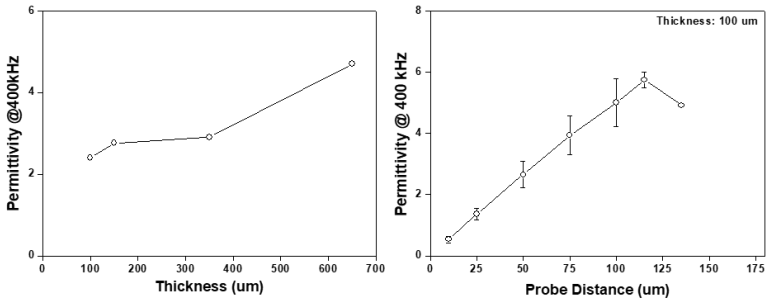

Figure 3-2. Permittivity of pure acrylic PSA as a function of thickness and probe distance.

5. Transmittance

Visible light transmittances for the PSAs as a function of UVAs contents were measured in the wavelength range from 800 to 200 nm using a UV-vis spectrophotometer (Clay 100, Agilent Technologies, USA) to confirm the absorption. The thicknesses of all PSA films were about 400 μm.

6. Color change

Changes in the color of the acrylic PSAs as a function of UVA type and contents were indirectly measured using the spectrophotometer (TECHKON SP 820 λ, TECHKON GmbH, Germany). The lightness (L), redness (a), and Yellowness (b) blues were determined and used to calculate the degree of the color change, ΔE, according to the following equation. The color change data was readjusted with acrylic PSA without UVA value of 100 %.

$$\Delta E = \sqrt{(L_1 - L_2)^2 + (a_1 - a_2)^2 + (b_1 - b_2)^2}$$

Where, L_1, a_1, and b_1 correspond to data of pure acrylic PSA and L_2, a_2, and b_2 correspond to data of acrylic PSAs with UVA (Park *et al.*, 2015, Pfeffer *et al.*, 2012).

Chapter 4

Designing the UV pattern acrylic PSAs and its adhesion performance and recovery for flexible display applications

1. Introduction

In our previous studies, our laboratory conducted research on adhesion performance and recovery of acrylic PSAs as a function of molecular weight, crosslinking density and elastomer (Lee *et al.*, 2016, Lee *et al.*, 2017, Lee *et al.*, 2019). It was confirmed that the adhesion performance and recovery of the acrylic PSAs depending on the molecular weight and the crosslinking density have an opposite relationship in chemical structure. The acrylic PSA applied with the elastomer has improved recovery due to the relatively long chain entanglement phenomenon of the elastomer, confirming the possibility of flexible display application. However, there were limitations due to optical properties.

As described above, the adhesion performance and recovery of the acrylic PSAs have an opposite relationship. A PSA having a low molecular weight has high wettability and improves the adhesion properties, but the recovery is lowered (Lee *et al.*, 2016). On the other hand, even if the recovery is improved by crosslinking, the adhesion properties are lowered (Lee *et al.*, 2017, Zhang *et al.*, 2011). In order to improve the limitation, our laboratory researched to simultaneously satisfy the two different physical properties by providing both high and low crosslinking density region through the UV pattern. The UV dose, crosslinking behavior and adhesion properties were predicted, and the recovery were measured (Back *et al.*, 2019).

In this research, I tried to produce UV pattern acrylic PSA by manufacturing pattern film through contrast pattern printing and

adjusting UV irradiation dose. After confirming the UV pattern formation, I wanted to confirm the effect of pattern size on the adhesion properties and recovery of acrylic PSAs. Acrylic PSAs, which have high and low crosslinking density regions, were expected to have the potential to be flexible PSAs, as each region exhibits both adhesion and recovery.

2. Objective

First, among the functionalities required for PSA for displays, we are conducting research on the recovery required for displays. The roles that PSA of the display component are optical properties, layers adherence, elongation and recovery and protection of adjacent substrates through stress relaxation during deformation. Among these, the layers adherence and the optical characteristics are properties commonly required in the conventional flat display.

PSAs, a viscoelastic material, have both elastic properties that recovered from deformation like springs, and viscosity that is not recovered by absorbing energy during deformation, like dashpot. In PSA for flexible displays that need to maintain low T_g and modulus, methods considered to confer elastic properties that are involved in recovery are methods that impart chemical crosslinking and intermolecular entanglement. These chemical and physical bonds provide properties that can prevent and recover from permanent deformation by preventing slippage between the molecules that make up the PSA during deformation.

Therefore, we have investigated the adhesive performance and recovery according to the molecular weight and crosslinking degree of PSAs (Lee *et al.*, 2016, Lee *et al.*, 2017). As the molecular weight and the degree of crosslinking increase, the adhesive performance increased, but the recovery was decreased. In addition, there was an optimum value in both molecular weight and crosslinking degree. From this result, it was confirmed that there is a limit as PSAs for flexible display only by

adjusting the molecular weight and the degree of crosslinking. In order to improve this, in this research, unlike the existing PSA, we devised an UV patterned acrylic PSA that includes a high crosslinking density region and a low crosslinking density region at the same time, and studied the applicability to flexible display. As mentioned above, the elastic property gives the PSA recovery, buy with this, the range that can be deformed in reduced, which can cause problems that reduce the stress relaxation and adhesion property. Therefore, at the time of manufacturing the pattern acrylic PSA, it is expected that the high crosslinked area is responsible for the recovery, and the low crosslinked area can improve the adhesion and stress relaxation with the substrate. We also wanted to confirm the possibility of applying a flexible display of UV patterned acrylic PSA by adjusting the size of the pattern that plays each role and measuring the adhesion performance and recovery. Ensuring recovery by using these patterns has never been advanced in any laboratory before, and it is a part of the original product that is expected to be applied to actual products in the future.

3. Experimental

3.1. Materials

Acrylic prepolymer (WinnersChem, Republic of Korea) was used without further purification to confirm the designing of UV patterning. Acrylic reactive monomers, including 2-ethylhexyl acrylate (2-EHA, 99.0 % purity, Samchun Pure Chemical, Republic of Korea), isobornyl acrylate (IBA, 99.0 % purity, Samchun Pure Chemical, Republic of Korea), and n-vinylcaprolactam (NVC, 99.0 % purity, Samchun Pure Chemical, Republic of Korea) were used without further purification to synthesis the acrylic prepolymer. Synthesized prepolymer was used to prepare UV patterning acrylic PSA film. The photoinitiator for the acrylic prepolymer synthesis and UV crosslinking was 2-hydroxy-2-methyl-1-phenyl-1-one (Omnirad 1173, IGM Resins, Netherlands). Polyethylene glycol 200 dimethacrylate (PEGDMA, Sartomer, USA) was used as a crosslinking agent. 2,5-Bis(5-tert-butyl-benzoxazol-2-yl)thiophene (BBT, Sigma Aldrich, USA) was used as a luminescent compound to visualized the UV pattern on PSAs.

3.2. Methods

3.2.1. Synthesis of acrylic prepolymer

Acrylic prepolymer was synthesized by bulk polymerization of reactive acrylic monomers via UV irradiation (Park *et al.*, 2016, Czech and Milker, 2003, Czech and Wesolowska, 2007). The reactive acrylic monomers (2-EHA, IBA, NVC) were mixed with an Omnirad 1173 inside a 500-ml four neck round-bottomed flask equipped with a stirrer, thermometer and N_2 purging tube (the formulation of the synthesized acrylic prepolymer is listed in Table 4-1). The mixture was continuously stirred for 20 min at room temperature with N_2 gas. The monomers mixture was synthesized by UV-irradiating using UV-spot cure system (SP-9, USHIO, Japan) under a N_2-rich atmosphere until the temperature of the mixture rose 5 ^{o}C. The above process iterated 5 times and stored in a wide-mouth bottle to protect the acrylic prepolymer from light and air. During the production of UV patterned acrylic PSAs, it needed to maximize the difference in physical properties in high/low crosslinking density regions. Therefore, I designed the acrylic prepolymer T_g as low as possible (approximately 49 ^{o}C). As a result, I tried to increase the difference in each area in the patterning process.

Table 4-1. Formulation of acrylic prepolymer.

Formulation		**Acrylic prepolymer (wt.%)**	**Expected T_g (°C)**
Reactive monomer (wt.%)	2-EHA	75	-49
	IBA	21	
	NVC	4	
Photoinitiator (phr)	1173	1	

Photoinitiator: Omnirad 1173, 2-hydroxy-2-methyl-1-phenyl-1-1-one
Wavelength of UV lamp (nm): ≈365
UV exposure (mW/cm^2): ≈20

3.2.2. UV crosslinking of acrylic PSAs

UV crosslinked acrylic PSAs were prepared by blending 100 wt.% of the acrylic prepolymer or synthesized acrylic prepolymer with 1 phr of PEGDMA and Omnirad 1173 respectively. The mixture syrup was mixed and deformed by paste mixer (SR-500, Thinky, Japan) for 2 min with 800 rpm respectively. At his stage, acrylic PSA for pattern visualization was prepared by adding BBT to the blends. The blends were coated onto the surface of 75 μm thickness corona-treated polyethylene terephthalate (PET) films and covered with silicone release film. In this step, pattern film was covered over silicone release film when the UV patterned acrylic PSAs prepared. The coated acrylic PSAs films were UV crosslinked using conveyor belt-type UV-crosslinking equipment with a 100 W pressure mercury lamp (main wavelength: 340 nm). In order to confirm the crossliking density of the acrylic PSAs, the films were prepared according to the crosslinking agent contents and the UV doses (Table 4-2).

Table 4-2. Formulation of UV crosslinked acrylic PSAs.

Sample Names	Acrylic prepolymer* (wt.%)	Omnirad 1173 (phr)	PEGDMA (phr)	UV Dose (mJ/cm^2)
PSA00	100	1	0	200/400/800/1600/2400
PSA02			0.2	
PSA04			0.4	
PSA06			0.6	
PSA08			0.8	
PSA10			1.0	

Acrylic prepolymer* (WINNERSCHEM, Republic of Korea)

3.2.3. UV design of UV patterned acrylic PSAs

Similar to UV crosslinking, a syrup mixed with the acrylic prepolymer, the crosslinking agent and the photoinitiaor was coated on a PET film and covered with a silicon release film. UV patterned acrylic PSA was prepared via UV irradiation by covering the OHP film on which the pattern was printed (Figure 4-1). This is because, following pattern printing, high and low crosslinking density regions were prepared, the high and low crosslinking density regions provide recovery and adhesion performance respectively. And also, the UV intensity and pattern formation by pattern contrast were investigated. From this result, UV patterned acrylic PSA with different pattern sizes was manufactured.

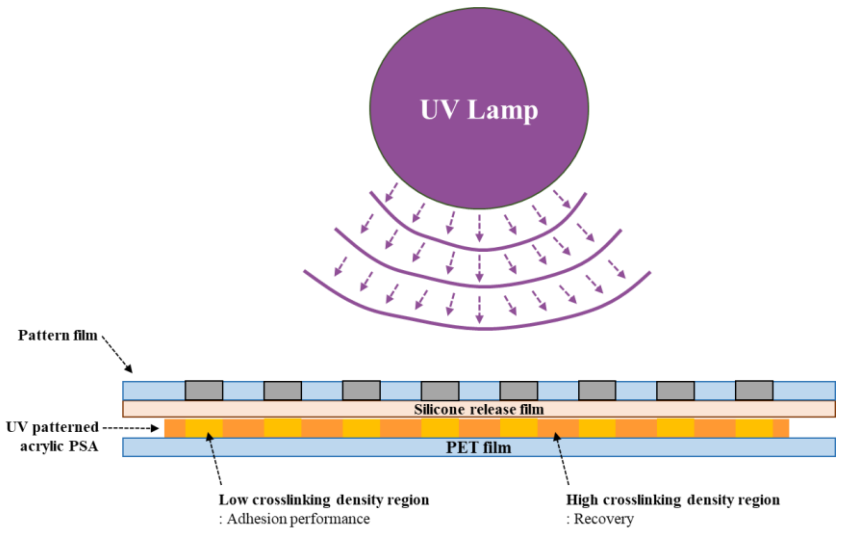

Figure 4-1. Manufacturing of the UV patterned acrylic PSAs.

3.2.4. Visualization of UV patterned acrylic PSAs

For pattern visualization of UV patterned acrylic PSAs, BBT was mixed with the acrylic prepolymer with crosslinking agent and initiator, and prepared via UV crosslinking. As shown in Table 4-3, pattern formation was confirmed by changing the BBT content in order to confirm the optimal content of BBT for visualization. UV pattern acrylic PSAs with BBT added was confirmed via UV light.

Table 4-3. Formulation of UV patterned acrylic PSAs for visualization.

Sample Names	*Acrylic prepolymer (wt.%)	Omnirad 1173 (phr)	PEGDMA (phr)	BBT (phr)
PSA/BBT03	100	1	1	0.0003
PSA/BBT05				0.0005
PSA/BBT07				0.0007
PSA/BBT10				0.001

*Acrylic prepolymer (WINNERSCHEM, Republic of Korea)

4. Results and Discussion

4.1. Gel fraction

In order to confirm the crosslinking density to preparation of the UV patterned acrylic PSAs, the gel fraction as a function of crosslinking agent contents and UV dose were measured. Figure 4- 2 shows the results of gel fraction measurement based on the content of the crosslinking agent contents and UV dose. As the content of the crosslinking agent increased, the gel fraction increased continuously from 200 to 800 mJ/cm^2. However, there was no significant difference when the content of the crosslinking agent was 0.4 phr or more. Also, UV dose of 1600 mJ/cm^2 or higher, no significant difference was shown depending on the content of the crosslinking agent contents, but the highest gel fraction value was obtained with 1 phr of the crosslinking agent content. When preparing UV patterned acrylic PSAs, low crosslinking density region should be crosslink with low UV dose value, because the UV dose has a very low impact. For this reason, the research was carried out with the content of the crosslinking agent fixed at 1 phr and the UV dose at 1600 mJ/cm^2.

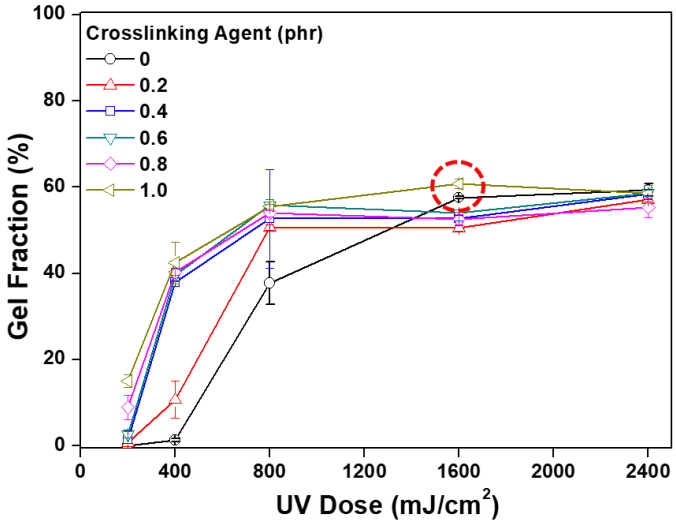

Figure 4-2. Gel fraction as a function of crosslinking agent contents and UV dose.

4.2. UV intensity

Figure 4-3 shows the pattern contrast type and measurement method printed on the pattern film to prepare UV patterned acrylic PSAs. The dark part of the pattern makes low crosslinking density regions on the UV pattern acrylic PSAs and the region performs adhesion. However, the UV intensity should be not be too low because it is hard to maintain the semi-solid in this region when the UV intensity is too low. On the other hand, if the UV intensity is too strong, pattern formation is difficult because there is no discrimination form the high crosslinking density region. Figure 4-4 shows the results of measurement of UV intensity according to pattern contrast and UV distance. In the absence of a film covering the actinometer, the UV intensity was 240 mW/cm^2, the value of the intensity of UV light decreased continuously with increasing UV distance, but maintained about 100 mW/cm^2. On the other hand, when the silicone film or pattern film was covered, the UV intensity decreased rapidly, and in the case of the grey pattern film, it decreased continuously as it became darker, but maintained the level of about 50 mW/cm^2. However, the black pattern film showed a very low UV intensity, and the intensity decreased about 0 mw/cm^2 as the black pattern turn into darker. Therefore, we decided that there was a need to measure the change in adhesion performance according to the brightness of the grey pattern.

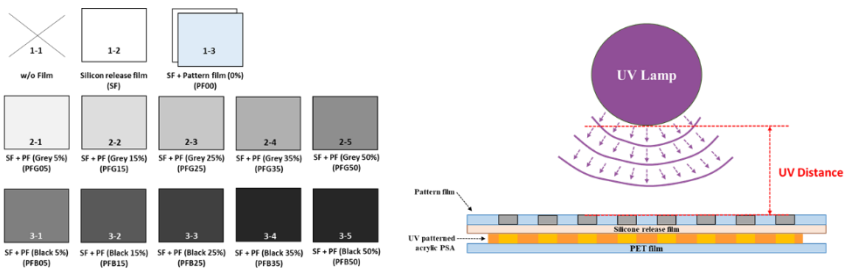

Figure 4-3. Scheme of pattern contrast of pattern film and UV distance.

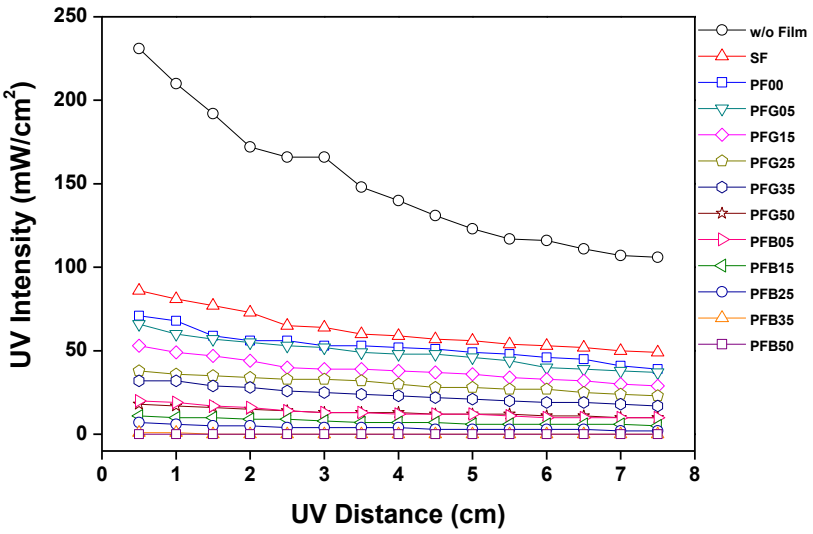

Figure 4-4. UV intensity as a function of pattern contrast and UV distance.

4.3. Peel strength as a function of contrast of grey pattern film

Figure 4-5 shows the result of measuring the change in peel strength by grey contrast. In order to confirm the pattern formation on acrylic PSAs, the acrylic PSAs coated on PET film, covered with half-pattern printed film and UV irradiated to crosslinking. The acrylic PSAs covered with only silicone release film, maintained a constant peel strength value throughout the experiment. Peel strength of acrylic PSAs covered with the grey 5 % pattern film (PFG05) also showed no significant difference. In the case of a grey 15 % pattern film (PFG15), a difference in peel strength gradually began to occur, and as the pattern became darker, the difference in the value began to increase. From these results, it was indirectly confirmed that a difference in the crosslinking density occurred depending on the brightness of the pattern, and the contrast of the pattern was fixed at grey 50 % (PEG50). The pattern region where the UV irradiation amount was low due to the pattern showed a low crosslinking density and a tendency for the peel strength value to increase slightly, and the region with a high crosslinking density decreased slightly. Before proceeding with the research, I anticipated differences in the crosslinking degree depending on the pattern. However, it was confirmed that the crosslinking density of the regions affected by the high crosslinking as the crosslinking degree of the pattern part decreased.

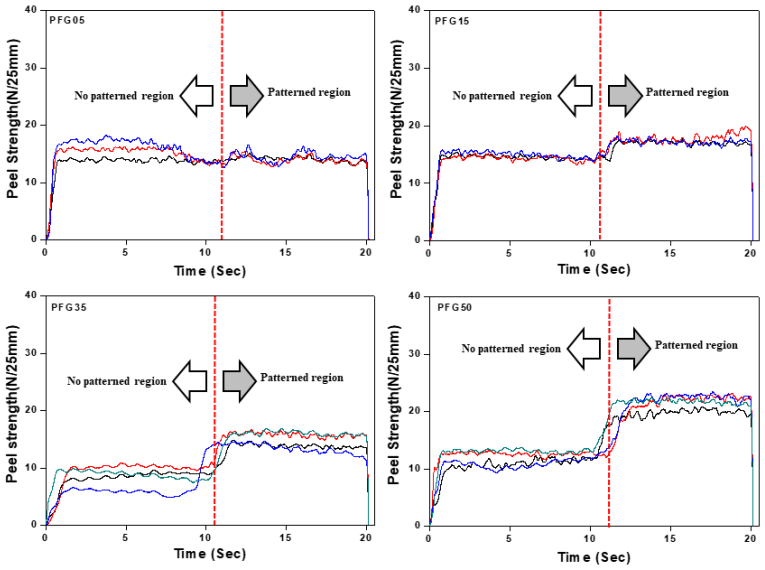

Figure 4-5. Peel strength as a function of grey contrast.

4.4. Visualization of UV pattern as a function of BBT contents

BBT is a luminescent material used as a fluorescent brightener for polymer and fibers. Uniform dispersion is possible because of its high solubility in various organic solvents (Zuo *et al.*, 2016). BBT was dispersed in an acrylic prepolymer and the pattern visualization was confirmed using UV light. Figure 4-6 is a photograph confirming the difference in light emission by UV light of the UV patterned acrylic PSAs according to the BBT contents. With the addition of BBT, a difference in luminescence began to occur due to the difference in the crosslinking density, but the difference was most clear at the 0.001 phr of BBT content. From this result, the content of BBT for visualizing the pattern of the UV patterned acrylic PSAs was fixed at 0.001 phr.

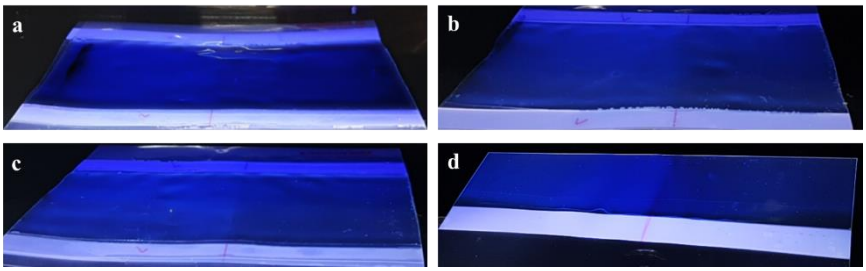

Figure 4-6. Photograph of UV patterned acrylic PSAs as a function of BBT contents. : (a) 0.0003 phr, (b) 0.0005 phr, (c) 0.0007 phr, (d) 0.001 phr

4.5. Visualization of UV pattern acrylic PSAs as a function of pattern sizes

Figure 4-7 is a pattern film photograph to prepare the UV patterned acrylic PSAs having various pattern sizes. The pattern size was adjusted to a maximum of 16 mm and a minimum of 2 mm. Figure 4-8 is a photograph in which the difference in the crosslinking density of the UV patterned acrylic PSAs as a function of the pattern sizes by UV light. As a result of the confirmation, it was confirmed that a difference in the crosslinking density occurred according to various sizes of the pattern film.

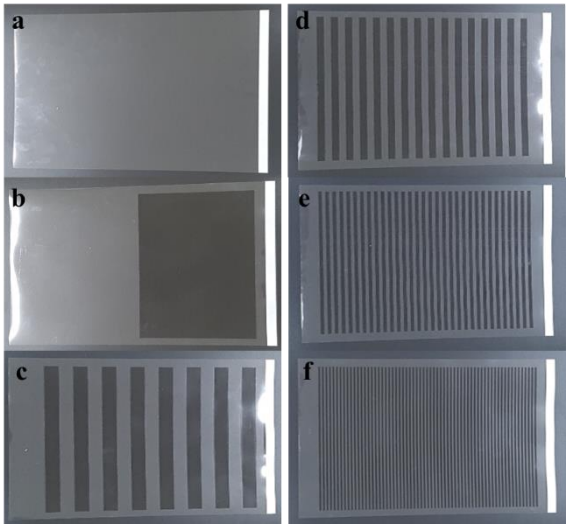

Figure 4-7. Photograph of pattern films as a function of pattern sizes. : (a) w/o pattern, (b) half pattern, (c) 16 mm, (d) 8 mm, (e) 4 mm, (f) 2 mm

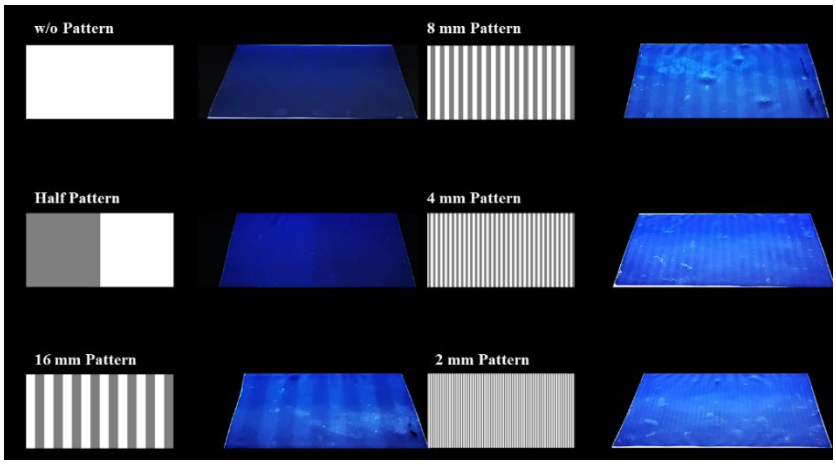

Figure 4-8. Photograph of UV patterned acrylic PSAs as a function of pattern sizes. : (a) w/o pattern, (b) half pattern, (c) 16 mm, (d) 8 mm, (e) 4 mm, (f) 2 mm

4.6. Adhesion performance of UV patterned acrylic PSAs as a function of pattern sizes

Figure 4-9 shows the result of measuring peel strength for which pattern formation is desired to be confirmed through the adhesion properties of the UV patterned acrylic PSAs. When no pattern was applied, peel strength value was at a level of about 2.5 N/25mm and maintained the value depending on distance. When the pattern was applied, the peel strength began to shake and the frequency of rocking increased as the pattern size decreased. In addition, when the pattern size was 2 mm, the maximum peel strength value was increase to about 5.5 N/25mm. The low crosslinking density region to assign adhesion performance to UV patterned acrylic PSA does not mean that the proportion changes according to the pattern size. From the half pattern to the 2 mm pattern, the proportion of the low crosslinking density region is almost the same. Nevertheless, an increase in the peel strength value means that the pattern formation can affect the adhesion property, not the proportion of the region.

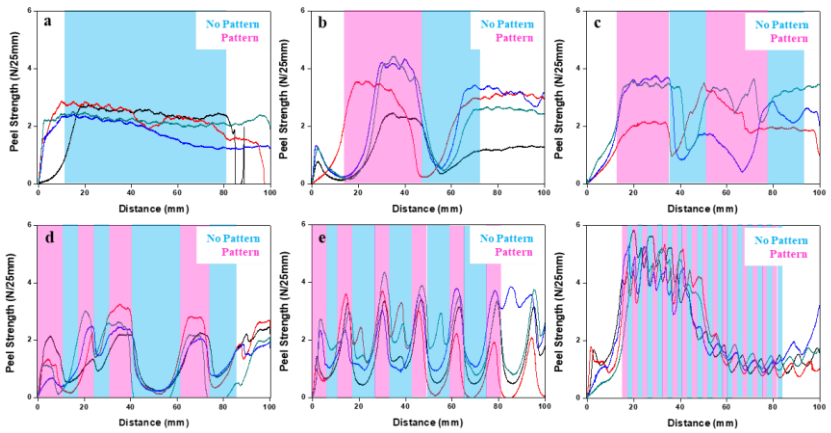

Figure 4-9. Peel strength of UV patterned acrylic PSAs as a function of pattern sizes. : (a) w/o pattern, (b) half pattern, (c) 16 mm, (d) 8 mm, (e) 4 mm, (f) 2 mm

Figure 4-10 shows the result of pull-off test of an UV patterned acrylic PSAs according to the pattern sizes. Peel strength measurement results fluctuated as the pattern was formed, making it difficult to secure quantitative data. Therefore, the pull-off test was used to compare the adhesion performance of acrylic PSAs according to the pattern size. As the pattern was formed, the maximum stress decreased continuously. However, with a pattern size of 8 mm or more, the maximum stress value began to increase. Through this result, it was confirmed that there is a synergistic effect on the adhesion performance as the pattern size decreases and the high/low crosslinking density region becomes denser.

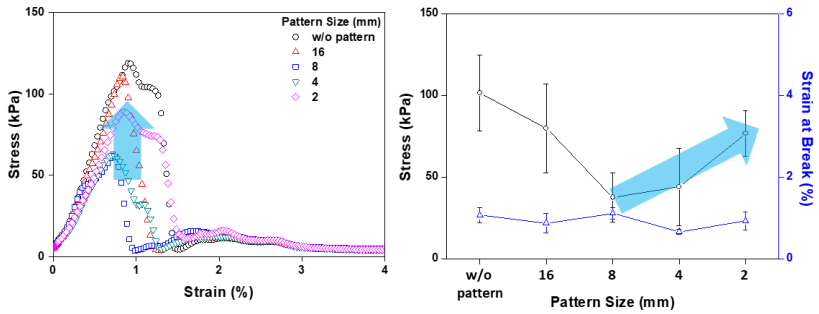

Figure 4-10. Pull-off test results of UV patterned acrylic PSAs as a function of pattern sizes.

Figure 4-11 shows the results of a lap shear test of the UV patterned acrylic PSAs as a function of the pattern sizes. As the pattern was formed, the maximum stress decreased slightly and the strain decreased considerably. However, the maximum stress and strain according to the pattern sizes were not significantly different. As mentioned above, there is no big difference in the proportion of high/low crosslinking density region depending on the pattern size. For these reasons, unlike the pull-off test results, the shear stress and shear strain do not show a large difference depending on the pattern size. The maximum stress means adhesion against endure the stress generated from shear deformation, and a decrease in strain means that the modulus of the PSAs is improved. Improvement in modulus is a phenomenon advantageous for recovery, but disadvantageous phenomenon for elongation.

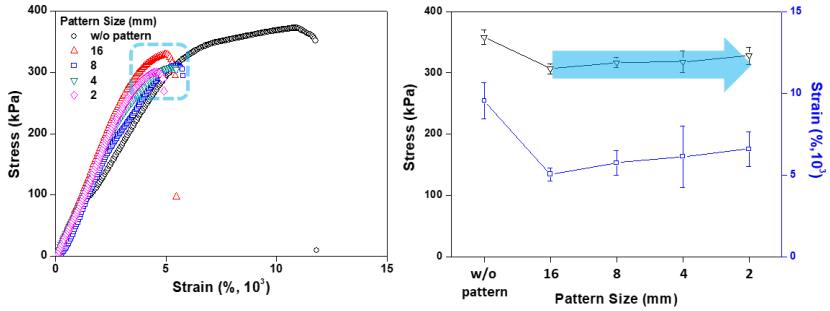

Figure 4-11. Lap shear test results of UV patterned acrylic PSAs as a function of pattern sizes.

4.7. Recovery of UV patterned acrylic PSAs as a function of pattern sizes

A stress relaxation test was performed to measure the recovery of the UV patterned acrylic PSAs. Figure 4-12 shows the result of changing the strain of the UV patterned acrylic PSAs according to the pattern sizes. The acrylic PSAs with no pattern endured a specific strain, but it was not recovered because it moved to the plastic region when the strain was removed. In the case of the acrylic PSAs with pattern, when the pattern sizes were 8 mm and 16 mm, it could not withstand a specific strain and was separated. Interestingly, the results of the lap shear test did not show a large difference between the maximum stress and strain at maximum stress depending on the pattern size, but different results were obtained in recovery after specific deformation from stress relaxation test. The UV patterned acrylic PSAs with 2 mm and 4 mm pattern size began to recover when the specific strain was removed. The elastic recovery of the UV pattern acrylic PSA having a 4 mm pattern size was about 24 %, and the recovery after 5 min was about 44 %. Also, the elastic recovery of the PSA with 2 mm pattern size increased to about 30 % and the recovery increased to about 60 %. This result is due to the synergistic effect of the high crosslinking density region, similar to the pull-off test result. This is because the pattern of the high crosslinking density region responsible for the recovery became dense, and the recovery of the UV patterned acrylic PSAs were added. Figure 4-13 shows the result of the stress change for the UV patterned acrylic PSAs according to the pattern size. UV patterned acrylic PSAs with pattern

size of 8 mm and 16 mm could not be measured due to the specimens were destroyed during the specific strain loading. Acrylic PSAs with pattern size of 2 mm and 4 mm have increased modulus and, for certain strain, the initial stress increased to about 3.7 N and 2.8 N, respectively. Unlike the results of the lap shear test, the recovery of UV patterned acrylic PSAs after specific deformation showed the effect of the modulus of the high crosslinking density region below the specific pattern size.

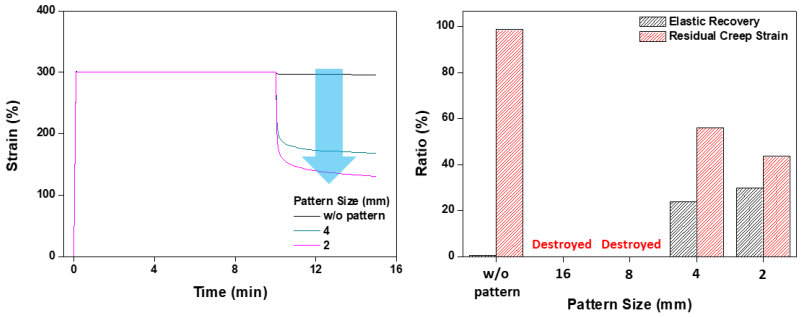

Figure 4-12. Stress relaxation test results of UV patterned acrylic PSA as a function of pattern size: (a) strain change and (b) elastic recovery and residual creep strain.

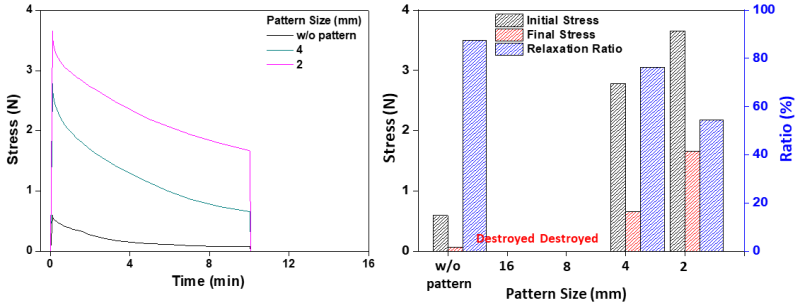

Figure 4-13. Stress relaxation test results of UV patterned acrylic PSA as a function of pattern size: (a) stress change and (b) initial stress, final stress, and relaxation ratio.

5. Conclusions

In order to confirm the applicability of the flexible display applications, the UV curable acrylic PSAs were formed with another crosslinking density, and the adhesion performance and recovery were measured. As a result of measuring the difference between the crosslinking agent contents and the crosslinking density by UV dose, the highest gel fraction value was obtained at 1 phr of crosslinking agent content and UV dose 1600 mJ/cm^2. In order to prepare the optimal low crosslinking density region, the UV intensity was measured according to the pattern contrast and the UV distance. In the case of a black pattern film, an UV intensity value close to 0 mW/cm^2 was shown. In the case of the grey pattern film, it decreased with increasing darkness, but maintained about 50 mW/cm^2. From the measurement result of the peel strength according to the lightness and darkness of the grey pattern, the pattern contrast was fixed at grey 50 % at which the difference in the crosslinking density occurred clearly. In addition, the BBT content was adjusted for pattern visualization, and the pattern formation of the UV pattern acrylic PSA with 0.001 phr of BBT was most distinct. The pattern size was adjusted to prepare the UV patterned acrylic PSAs, and it was confirmed that the pattern was formed using UV light. The peel strength of UV pattern acrylic PSAs as a function of pattern size began to shake as the pattern was formed and showed the highest value at 2 mm pattern size. From the pull-off test results, the cohesion of the acrylic PSAs in low crosslinking density region decreased and the stress decreased, but the PSA with the pattern size of 2 mm began to increase. As a result of

lap shear test, the maximum stress decreased slightly, but the strain decreased greatly. However, it did not show much difference depending on the pattern size. The recovery via stress relaxation test could not withstand specific strain as the pattern was applied. However, when the pattern size decreased to 4 mm or less, it began to endure specific strain, and the recovery of the 2 mm pattern size increased to about 60 %. From this research, the possibility of applying a flexible display of UV pattern acrylic PSAs was confirmed. We also confirmed the need for further research on acrylic PSAs according to the shape and size of the pattern.

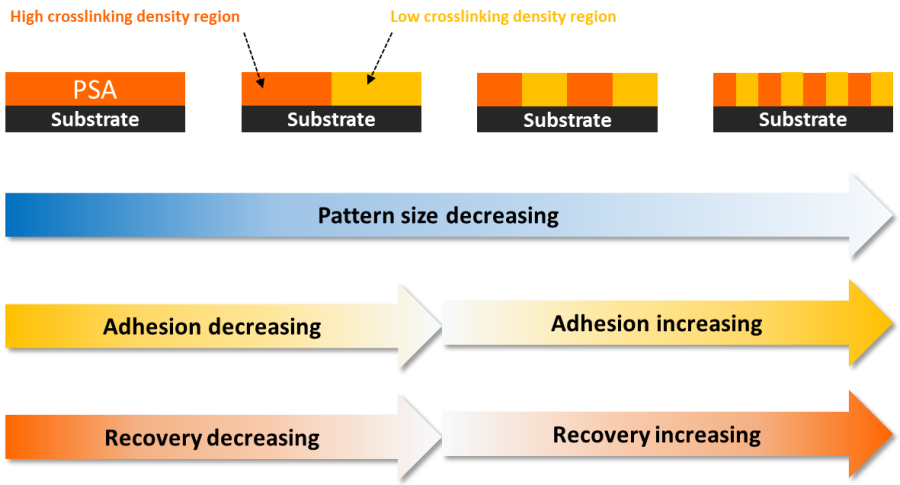

Figure 4-14. Schematic diagram of UV patterned acrylic PSAs with different pattern size and its adhesion and recovery.

Chapter 5

Adhesion performance and permittivity of acrylic PSAs/various low-*k* monomers via UV crosslinking for touch screen panel

1. Introduction

Optical clear adhesives (OCAs) refer to PSAs having a transmittance of more than 90 % in the visible-light region. Because acrylic PSAs possess a high transmittance, they are most widely used for OCAs. The transmittance of the adhesive is a very important factor for display applications. Since an OCA is used especially for the cover window and the transparent electrode, there are limits to its application when transparency is not necessitated (Keizai, 2011, Lee *et al.*, 2014).

A touch-screen panel (TSP) is an input device that recognizes the position on the screen where the user clicks or touches with a finger and conveys the position to the system. This technology has been widely expanded and supported by the spread of smart phones. A TSP is composed of a touch panel, a control integrated circuit (IC), a driver software, and the like. The touch panel is composed of a top plate and a bottom plate on which a transparent electrode (indium tin oxide, ITO) is deposited. And each layer is fixed using PSAs (Figure 5-1). The position of the signal is generated by detecting the contact or change the electric capacity, and the signal is transmitted to the control IC. The control IC changes the analog signal transmitted from the touch panel to a digital signal that plays a role on the screen. The driver software is a program that receives a digital signal coming from the control IC, controls the touch panel and is realized according to each operating system. TSPs are classified into resistive touch screens and capacitive touch screens, and recently, capacitive touch screens have been widely used for smart devices.

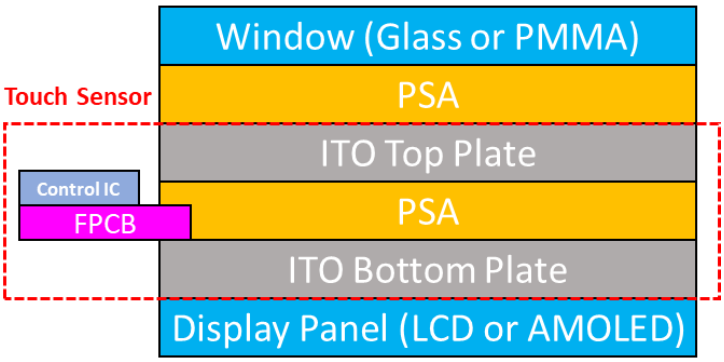

Figure 5-1. Structure of capacitance type touch screen panel (TSP).

The permittivity is a degree that generates dielectric polarization. When an electric field is applied to the outside of the dielectric, a dielectric polarization phenomenon occurs, and an electric field changed due to polarization is generated in a direction opposite to the external electric field, so that the electric field of the dielectric changes (Figure 5-2). The flow of current having a high relative permittivity is interrupted. Since, the flow of current having a high relative permittivity is cut off, the electric field strength decreases, the charge amount increases, and the capacitance of the dielectric increases. That is, a high relative permittivity means that the capacitance that can be stored increases (Bora, 2018). The capacitance (C) is expressed by the following equation:

$$C = k\varepsilon_{\gamma}A/t$$

where k is a constant value of the object, ε_{γ} is the relative permittivity, A is the area, and the t is the distance of the dielectric interface.

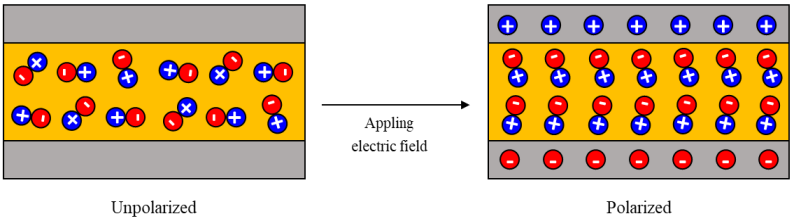

Figure 5-2. Schematic of dielectric polarization phenomenon.

The relative permittivity, so called dielectric constant, means the ratio of the permittivity of vacuum to the permittivity, and has no unit. That is, the relative permittivity changes according to the permittivity of the dielectric (Figure 5-3) (Hummel, 2011). The relative permittivity is expressed by the following equation:

$$\varepsilon_\gamma = \varepsilon/\varepsilon_0$$

The capacitance-type TSP used for the current smart device adopts a mechanism in which the electrostatic capacitance changes when it contacts a conductor, such as a finger. This principle is driven by the amount of change in the electrostatic capacity exceeding a specific critical point. For this reason, the PSA used in the capacitance-type touch panel is required to have a specific permittivity. If the permittivity of the PSA is too high, the noise is negated. On the other hand, if the permittivity is too low, the electrostatic capacitance value is not measured, and the signal transmission tends to be delayed. Therefore, adjusting the permittivity of the PSA is a very important factor in the display application market (Jeon *et al.*, 2014).

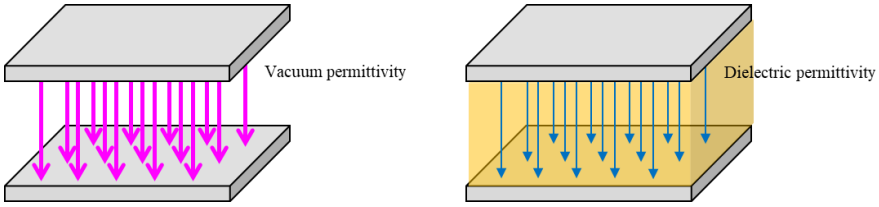

Figure 5-3. Schematic of permittivity of vacuum (ε_0) and permittivity (ε).

Research on low permittivity (low-*k*) materials has been steadily advanced to lower the permittivity of dielectrics. Various efforts for the research were actively made in academia and industry in the 1990s (Hatton *et al.*, 2006, Long and Swager, 2003, Maier, 2001, Miller, 1999, Volksen *et al.*, 2010). Compared to inorganic dielectrics, organic dielectrics have various advantages, such as low fair price, combining with flexible electronics, and possibility of chemical modification (Kohl *et al.*, 2011, Morgen *et al.*, 2000, Shamiryan *et al.*, 2004). Therefore, various polymer materials, such as polybenzobisoxazole (Ishida and Low, 1997, Tao *et al.*, 2010), polysilsesquionxane (Kessler *et al.*, 2009), SILK (k=2.65, Dow Chemical), and polyimide (PI) (Hougham *et al.*, 1994, Lee *et al.*, 1995, Liaw *et al.*, 2012, Liu *et al.*, 2012, Liu *et al.*, 2015, Pellerin *et al.*, 1997, Sydlik *et al.*, 2011), have been studied as low-*k* materials. And also, to reduce the *k* value about 1.0, nanosized air voids have been introduced in to the low-*k* polymer materials (Grosso *et al.*, 2007, Meador *et al.*, 2012). Recently, research has been reported that the permittivity can be effectively reduced by increasing the free volume. This is because providing a free volume can dilute the polar molecule concentration, weaken the interaction between polymer chains, and reduce the permittivity (Chern *et al.*, 1997, Chern *et al.*, 1998, Lew *et al.*,

2008, Wang *et al.*, 2017, Yuan *et al.*, 2013, Zhang *et al.*, 2017). However, introduction of free volume has a complicated molecular structure of the dielectric, has difficulty in manufacturing, and can affect the intrinsic physical properties of the dielectric (Qian *et al.*, 2019). Moreover, since the role of PSA fixes substrate materials, sufficient adhesion property is required.

In this research, permittivity measurements using probe station to minimize the variables generated by existing surface/surface methods to ensure reliable permittivity data for semi-solid acrylic PSAs. An acrylic prepolymer was synthesized with acrylate monomers. In addition, low-*k* monomers were selected and blended with the prepolymer. I selected four types with low-*k* monomers, which have silane group, nitrogen group, high-branched side group and long alkyl side group. Recently, decreasing permittivity of materials is achieved by reducing the interaction between polymer chains by diluting the polar molecule concentration by forming a free volume. Therefore, I wanted to confirm that low-*k* monomers with different chemical structure can reduce the permittivity of acrylic PSAs by effectively forming free volume. The free volume was also expected to affect the adhesion property of acrylic PSAs. In detail, it is expected to affect the side that degrades the specific characteristics of PSA and in the case of silane, which has no reaction point, the effect is expected to be larger. An acrylic PSA film was prepared via UV crosslinking with a crosslinking agent and photoinitiator. The crosslinking degree was confirmed via gel fraction, and the transmittance was measured using a UV-vis spectrophotometer. The adhesion performance was investigated via the peel strength, probe

tack and lap shear tests. The permittivity was measured using an impedance analyzer, the dielectric interface and a micro vacuum probe station.

2. Objective

The definition of dielectric constant is related to the permittivity of the materials. Permittivity refers to the degree to which a material is polarized by the application of an electric field. Polarization is applied by an electron cloud when an electric field is applied and moves with the nucleus in the opposite direction of the field. This separates the positive and negative charges, making the molecule act like an electric dipole. There are three mode of polarizations (Blythe *et al.*, 2005).

i) Electronic polarization
: slight displacement of electrons to the nucleus
ii) Atomic polarization
: distortion of atomic position in a molecule or lattice
iii) Orientational polarization
: In the case of polar molecules, permanent dipoles tend to be sorted by the electric field and give net polarization in that direction

Certain structures and elements are more polar than other structures. Aromatic rings, sulfur, iodine and bromine have the higher polarity. The presence of this group induces an increase in dielectric constant. Polarization is easy because the π bond of the aromatic ring is attached

more loosely than the σ bond. For large atoms such as bromine and iodine, the electron cloud is too large and away from the effects of positive nuclear electrostatic forces. In the case of fluorine with a small atomic radius and concentrated negative charges, the electron cloud can be fixed much more firmly, so the polarity is low. It can induce lower dielectric constants. In this way, it was predicted that the tendency of PSA with lower T_g would be displayed differently compared to general polymers with higher T_g due to the large influence of molecular fluidity. However, no studied related to permittivity of PSAs have been reported.

Table 5-1 shows the dielectric constant values of several inorganic materials and polymers. Thus, permittivity of the material varies depending on the chemical composition and structure. In particular, materials with ions and polarity have high dielectric constant values. For this reason, inorganic materials with ions and polar polymer have high dielectric constant.

Table 5-1. Dielectric constant of several polymers and inorganic materials (Ren *et al.*, 2008, Silaghi, 2012).

Materials	**Dielectric constant, ε**	**Materials**	**Dielectric constant, ε**
TiO_2	100	Fluorinated polyimide	2.5-2.9
H_2O	78	Methylsilsesquioxane	2.6-2.8
Neoprene	9.8	Polyarelene ether	2.8-2.9
PVDF	6.0	Polyethylene	2.3-2.7
SiO_2	3.9-4.5	Polystyrene	2.5-2.9
Fluorosilicate glass	3.2-4.0	Teflon AF	2.1
Polyimide	2.8-3.2	Air	1.02

Depending on the application in the electronic industry, both high and low permittivity are required. A material with a low permittivity enables resistance-capacitance (RC) time delays, crosstalk and power dissipation in the high density and speed integration through the isolation of signal conductors, rapid signal propagation, and interlayer dielectrics (Tummala *et al.*, 1989). Also, since all electronic devices are miniaturized, reducing the permittivity can reduce the harmful effects of stray and coupling capacitances. For these reasons, it is necessary to reduce the permittivity of acrylic PSAs used in electronic devices.

According to Maxwell-garnet theory, the presence of a low dielectric constant second phase in a composite material greatly reduces the dielectric constant (Bergman *et al.*, 1992). The concept is to create a foam structure by introducing air-filled pores. Permittivity of the pores generated in this way is about 1, which means that the overall permittivity decreases. However, the pore distribution must be uniform, and in the case of acrylic PSAs, the pores can affect optical property and adhesion performance.

The purpose of this research is to set a highly reliable permittivity evaluation method for PSA. Since the permittivity measuring equipment for general materials is solid by the surface/surface method, it is possible to secure reproducible data. However, PSA is semi-solid and the molecular structure is also less uniform than the typical polymer, so it is difficult to ensure reliable data with conventional methods. In order to improve such problems, we tried to minimize the variables that can occur during analysis using probe station. Four types with low-*k* monomer, silane group, nitrogen group, high branched group

and long alkyl side group were selected. I tried to confirm the effects of different chemical structures of each low-*k* monomer on the transparency, adhesion performance and permittivity of acrylic PSA.

3. Experimental

3.1. Materials

Acrylic monomers, 2-hydroxyethyl acrylate (2-HEA, 99.0 % purity, Samchun Pure Chemical, Republic of Korea), 2-ethylhexyl acrylate (2-EHA, 99.0 % purity, Samchun Pure Chemical) and isobutyl acrylate (IBA, 99.0 % purity, Samchun Pure Chemical) were used as received without further purification to prepare the acrylic prepolymers. The low-*k* monomers hexamethyldisiloxane (HMDS, Silane monomer, monomer Sigma-Aldrich, USA), N-vinylcaprolactam (NVC, Nitrogenous monomer, Tokyo Chemical Industry Co., Ltd, Japan), tert-butyl acrylate (TBA, High-branched side group monomer, Sigma-Aldrich, USA) and isooctadecyl acrylate (ISTA, Long alkyl side group monomer, Nippon Shokubai Co., Ltd, Japan) were used to adjust permittivity of the acrylic PSA (Figure 5-4). The photoinitiator for the acrylic prepolymer synthesis was 2-hydroxy-2-methyl-1-phenyl-1-one (Omnirad 1173, IGM Resins, Netherlands). Phosphine oxide (Omnirad 2100, IGM Resins, Netherlands) was used as photoinitiator for UV crosslinking, and 1,6-hexanediol diacrylate (HDDA, Sigma-Aldrich, USA) was used as a crosslinking agent.

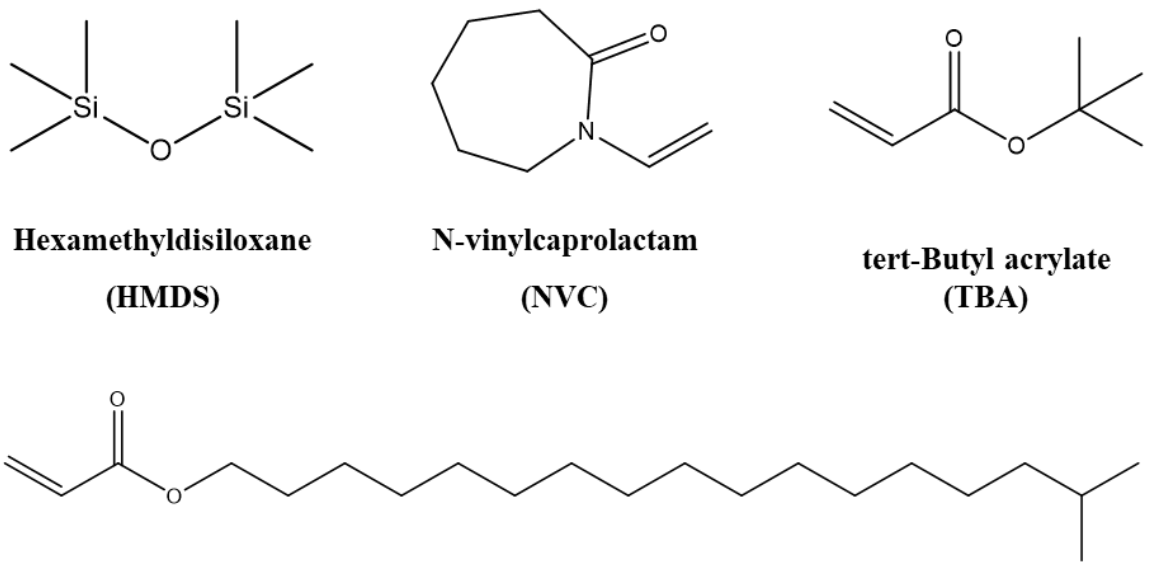

Figure 5-4. Chemical structure of low-*k* monomers.

3.2. Methods

3.2.1. Synthesis of acrylic prepolymer

The acrylic monomers (2-HEA, 2-EHA and IBA) were mixed with an Omnirad 1173 inside a 500 ml four-neck round-bottomed flask equipped with a stirrer, thermometer and N_2 purging tube (the formulation of the synthesized acrylic prepolymer is listed in Table 5-2). The mixture was continuously stirred for 20 min at room temperature with N_2 gas. The monomer mixture was synthesized by UV irradiating using UV-spot cure system (SP-9, USHIO, Japan) under a N_2-rich atmosphere until the temperature of the mixture rose 5 °C. The above process was iterated 5 times, and the product was stored in a wide-mouth bottle to protect the acrylic prepolymer from light and air. In this study, I wanted to confirm the adjustment of the permittivity of typical acrylic PSA and the change in adhesion performance due to low-*k* monomers. Therefore, instead of using the acrylic prepolymer used in UV pattern research, acrylic prepolymer with a common T_g value (approximately -40 ^oC) was synthesized and used.

Table 5-2. Formulation of acrylic prepolymer.

Formulation		**Acrylic prepolymer (wt.%)**	**Expected T_g (°C)**
Reactive monomer (wt.%)	2-HEA	20	-40
	2-EHA	60	
	IBA	20	
Photoinitiator (phr)	Omnirad 1173	1	

Photoinitiator: Omnirad 1173, 2-hydroxy-2-methyl-1-phenyl-1-1-one
Wavelength of UV lamp (nm): ≈365
UV exposure (mW/cm^2): ≈20

3.2.2. UV crosslinking of acrylic PSAs with low-*k* monomers

Crosslinked PSAs with low-*k* monomers were prepared by blending 100 wt.% of the synthesized acrylic prepolymer with 1 part per hundred resin (phr) of HDDA and Omnirad 2100 as a function of the low-*k* monomer content (Table 5-3). The mixture was combined and deformed using a paste mixer (SR-500, Thinky, Japan) for 4 min. The blends were coated onto the surface of corona-treated polyethylene terephthalate (PET) films, 50 μm in thickness, and crosslinked by a black-light lamp, approximately 1600 mJ/cm^2.

Table 5-3. Formulation of crosslinked acrylic prepolymer with low-*k* monomers.

Sample Names	Acrylic prepolymer (wt.%)	Photoinitiator (phr)	Crosslinking agent (phr)	Low-*k* Monomer (phr)			
		Omnirad 2100	HDDA	HMDS	NVC	TBA	ISTA
PSA-HMDS	100	1	1	2/4/6/8/10	-	-	-
PSA-NVC				-	2/4/6/8/10	-	-
PSA-TBA				-	-	2/4/6/8/10	-
PSA-ISTA				-	-	-	2/4/6/8/10

Omnirad 2100: Blend of ethyl phenyl(2,4,6-trimethylbenzoyl)phosphinate and phenyl bis(2,4,6-trimethylbenzoyl)-phosphineoxide
HDDA: Hexanediol diacrylate
UV lamp: Black light
Exposure time: 5 min

4. Results and Discussion

4.1. Gel fraction

The crosslinking density for the crosslinked PSAs can be measured indirectly by calculating the corresponding gel content from the insoluble fraction (Joo *et al.*, 2007). The gel fraction was measured to confirm the degree of crosslinking of acrylic PSA depending on the type and the content of the low-*k* monomers. Figure 5-5 reveals the gel fraction results depending on the type and content of low-*k* monomers. The crosslinked acrylic PSA exhibited a gel fraction value of approximately 97 %, regardless of the type and content of low-*k* monomers. However, in the case of PSA-HMDS, the gel fraction value decreased as the content of HMDS increased, decreasing to approximately 90 % at the maximum. Low-*k* monomers were added to the acrylic prepolymer with both crosslinking agent and photoinitiator and then the mixture was undergoing crosslinking reaction. At this time, the HMDS has no sites that can react with the prepolymer and the crosslinking agent, so the gel fraction value decreases. Early in the research design, this was taken into account, but it was determined that silane, a relatively heavy atom, could not participate in the crosslinking reaction, but could exist between crosslinked acrylic PSAs. Research was conducted to reduce the permittivity of the Si-C bond, and I wanted to confirm the results of the permittivity and adhesion performance when used for acrylic PSAs (Suyal *et al.*, 1999, Chen *et al.*, 2019).

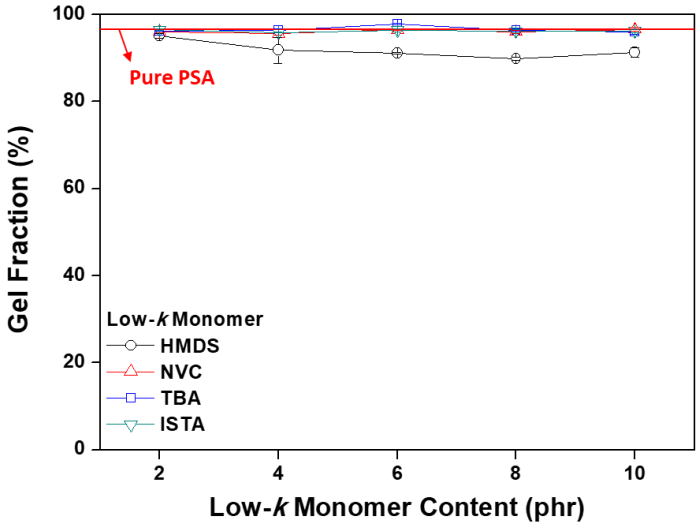

Figure 5-5. Gel fraction of crosslinked acrylic PSA as a function of low-*k* monomer types and contents.

4.2. Transmittance

The transparency of an acrylic PSA is a very important factor for applications in the display field. The transmittance was measured to confirm the transparency of the acrylic PSA in the visible-light region. Figure 5-6 shows the transmittance measurement results according to the type and content of low-*k* monomer. All acrylic PSA samples utilizing a low-*k* monomer showed permeability values similar to that of the pure acrylic PSA level. However, the transmittance of PSA-HMDS with an HMDS content of 10 phr decreased to approximately 85 %. This is because the miscibility of silane of HMDS with acrylic PSA has decreased. However, the nitrogen atom of NVC, the branched side group of TBA, and the long alkyl chain of ISTA had no problem maintaining the transparency of acrylic PSA.

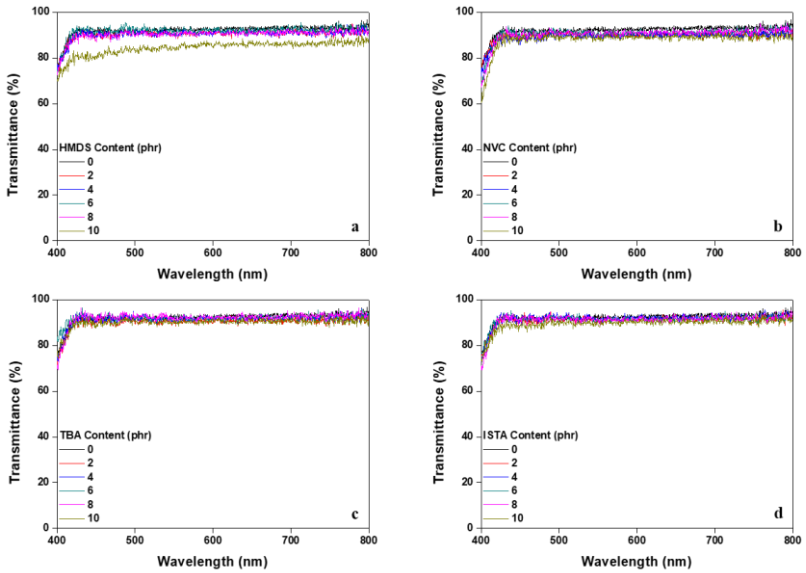

Figure 5-6. Transmittance from UV-vis spectrophotometer of crosslinked acrylic PSA as a function of low-*k* monomer types and contents: (a) PSA-HMDS, (b) PSA-NVC, (c) PSA-TBA, (d) PSA-ISTA.

4.3. Adhesion performance

Peel strength, probe tack and lap shear tests were performed to confirm the adhesion performance of the acrylic PSA depending on the type and content of the low-*k* monomer. As confirmed by the gel fraction results, to confirm the physical properties at the same degree of crosslinking, the contents of the crosslinking agent and photoinitiator were fixed at 1 phr.

Figure 5-7 reveals the peel strength and the probe tack measurement results of the acrylic PSAs according to the type and content of low-*k* monomer. The adhesion of PSA-HMDS decreased continuously as increasing HMDS content with silane groups. On the other hand, the adhesion value of PSA-NVC increased consistently with the NVC content. This result is due to the improved intermolecular interactions caused by the NVC with a relatively high polarity. The high polarity is due to the presence of the nitrogen atom, because it plays a role in improving the cohesion of the acrylic PSA (Czech and Kurzawa, 2007, Park *et al.*, 2015). In the cases of PSA-TBA and PSA-ISTA, they showed a tendency to rise slightly as the content of low-*k* monomer increased, but did not show large differences. However, in the case of ISTA having a relatively large molecular weight, the wettability of the acrylic PSA was greatly affected and showed an increase in value but remained lower than that of TBA. By adding low-*k* monomers, the permittivity can be reduced. However, it is not a combination of acrylic monomers that make up acrylic PSA, but a substance with another chemical composition is mixed, so it was predicted that there is a big

decreasing on the adhesion performance. Contrary to expectations, the adhesion property was not significantly reduced, but rather increased in the case of NVC. However, as predicted by the silane group, the miscibility was reduced.

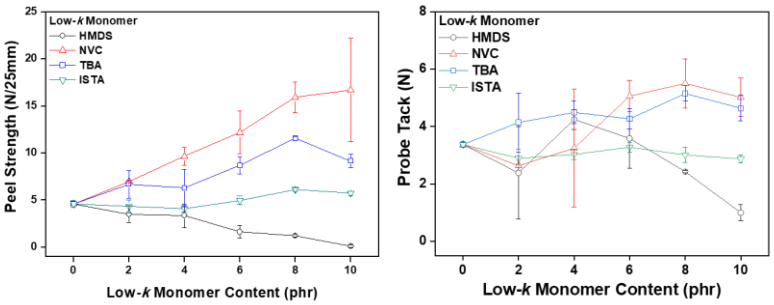

Figure 5-7. Peel strength and probe tack of crosslinked acrylic PSA as a function of low-*k* monomer types and contents.

Figure 5-8 is the lap shear test results for the acrylic PSAs according to the type and content of low-*k* monomer. From this result, the maximum stress and strain at maximum stress was confirmed. As the content of HMDS increased, the maximum stress and strain at maximum stress decreased continuously. HMDS with silane groups was not miscible with the acrylic PSA, and as the content increased, the shear adhesion decreased. This result is because, as confirmed by the gel fraction results, HMDS exists in an unreacted state with acrylic PSA, which has no functional group to participate in the crosslinking reaction, and bubbles generated by the heat generated during the crosslinking process (Figure 5-9). On the other hand, as the content of NVC, TBA and ISTA increased, the maximum stress and strain at maximum stress did

not show any significant changes. This is because the low-*k* monomers having a functional group reacted with the prepolymer and HDDA to reduce bubble formation. When the initial acrylic prepolymer was crosslinked, it was predicted that HMDS with a relatively heavy atom could exist between the crosslinked molecular chains. As expected, HMDS was not bound and was present, but generated bubbles which reduced the adhesion performance of the acrylic PSAs. In general, the results of lap shear tests on acrylic PSAs show different behavior to peel strength and probe tack results due to it is relate to shear direction. The values according to the type and content of the low-*k* monomers do not show a significant difference. In particular, the decrease in maximum stress due to immiscibility between acrylic PSA and the silane group showed the same result as peel strength and probe tack.

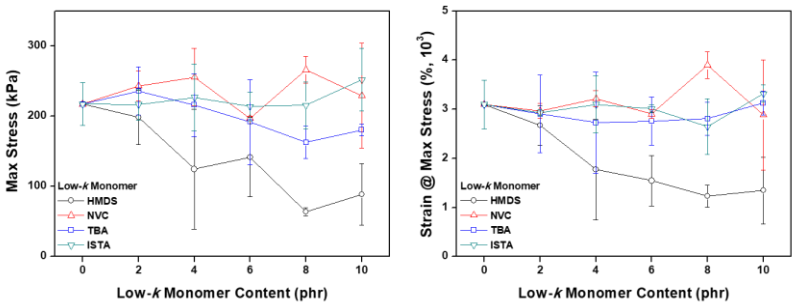

Figure 5-8. Max stress and strain at max stress from lap shear test of crosslinked acrylic PSA as a function of low-*k* monomer types and contents.

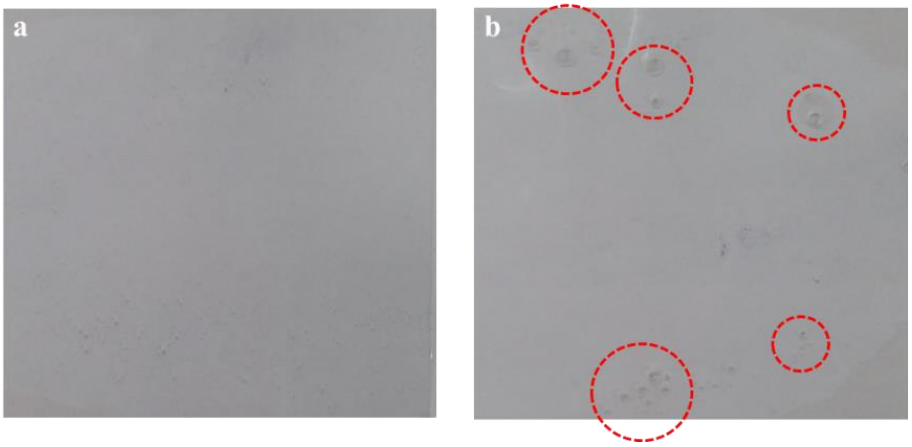

Figure 5-9. Pictures of crosslinkined acrylic PSA film

: (a) pure acrylic PSA, (b) PSA-HMDS (10 phr).

4.4. Permittivity

The quantification of the electric field dielectric can be summarized in the Clausius-Mossotti equation.

$$P = (\varepsilon_\gamma\text{-}1/\varepsilon_\gamma+2)\cdot(M/\rho) = N_a\alpha/3\varepsilon_0$$

P is the molar polarizability, ε_γ is the relative permittivity, ε_0 is the permittivity in vacuum, M is molecular weight of a repeat unit, ρ is density, α is polarizability, N_a is the Avogadro constant. This equation implies that the dielectric constant depends on the polarizable free volume of the components present in the material. Polarization describes the proportionality constant for dipole formation under the influence of an electric field. Therefore, its value is affected by different types of atoms or molecules (Indulkar *et al.*, 2008). The relationship between the permittivity and the polarizability of a substance can be expressed by the following equation.

$$\varepsilon_\gamma = 1 + N_a\alpha/\varepsilon_0$$

In other words, the relative permittivity is the ratio of the total permittivity of one mole of substance in vacuum. Therefore, the relative permittivity is a value included in the free volume of one mole of the substance. In addition, the molar volume is a unique feature of each different type of atom or molecule.

Figure 5-10 presents the measurement results of the permittivity

of the acrylic PSA/low-*k* monomer blends according to the frequency. As shown in the graph, the permittivity decreased continuously as the content of all low-*k* monomers increased. This result is because the addition of the low-*k* monomer reduced the density of acrylic PSA because the organic material was interposed between the molecular chains of the acrylic prepolymer (Maex *et al.*, 2003, Jousseaume *et al.*, 2005, Chen *et al.*, 2019). In other word, it is due to a free volume is formed by the low-*k* monomer and the dielectric constant of the dielectric is lowered (Chern *et al.*, 1997, Chern *et al.*, 1998, Lew *et al.*, 2008, Wang *et al.*, 2017, Yuan *et al.*, 2013, Zhang *et al.*, 2017). However, although there was a difference depending on the type of monomer, the permittivity increased with certain contents over others. The permittivity of acrylic PSA/low-*k* monomers blends started to increase with an HMDS content of 8 phr or more, NVC content of 4 phr or more, TBA content of 8 phr or more and ISTA content of 4 phr or more. Through these results, it was confirmed that a certain amount or more of low-*k* monomer reduces the distribution of free volume. Also, there was a difference in the optimal amount depending on the chemical structure of the low-*k* monomer. In particular, it was confirmed that NVC with a nitrogen group and ISTA with a long alkyl chain were effective for the formation efficiency of free volume to lower the permittivity of acrylic PSA. HMDS is also expected to be present in small amounts in acrylic PSA, as confirmed by the gel fraction results. However, the permittivity achieved similar results when compared to other monomers. From these results, it was confirmed that the miscibility with acrylic PSA was reduced, but it was very effective in forming a free volume to lower the

permittivity. However, lower values than the permittivity of the pure acrylic PSA was provided by all low-*k* monomer types and contents.

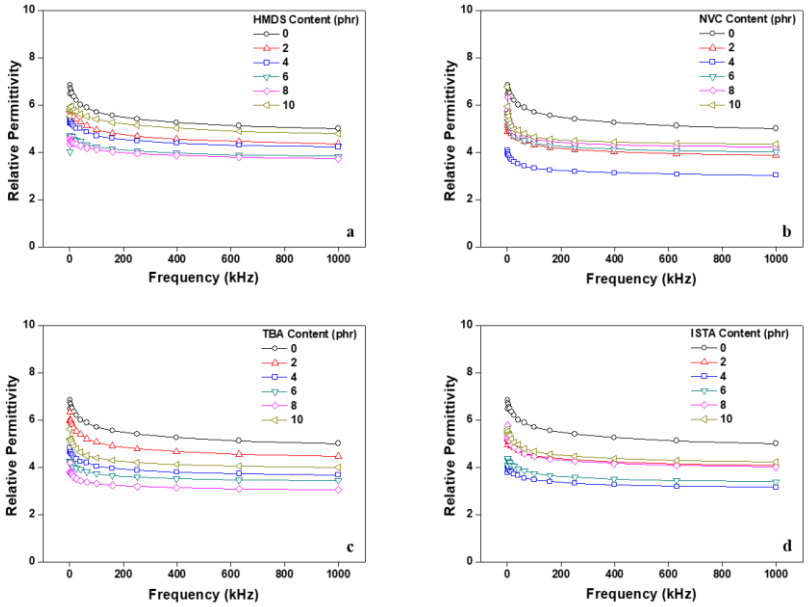

Figure 5-10. Permittivity of crosslinked acrylic PSA as a function of low-*k* monomer types and contents: (a) PSA-HMDS, (b) PSA-NVC, (c) PSA-TBA, (d) PSA-ISTA.

Figure 5-11 is a graph showing the average value of the relative permittivity of an acrylic PSA depending on the type and content of low-*k* monomer in the low-frequency region of 400 kHz. As mentioned above, as the content of monomer increased, an overall lower relative permittivity value than that of pure PSA was permitted. However, when the content of a monomer was above a certain level, this value began to increase. This result is a consequence of bubbles forming by heat

generated during the UV-crosslinking process, similar to the lap shear measurement result. In addition, the bubbles generated in the acrylic PSA film exerted a large influence on the result of the relative permittivity rather than the adhesion properties. According to the previous research reported that the presence of the air gaps affected the relative permittivity of poly (tetrafluoroethane) (PTFE). The measured relative permittivity of PTFE was slightly different than the reported values, which was a result from air gaps due to imperfections in the machined PTFE samples (Chang *et al.*, 2019, Geyer and Krupka, 1995, Lu *et al.*, 2009).

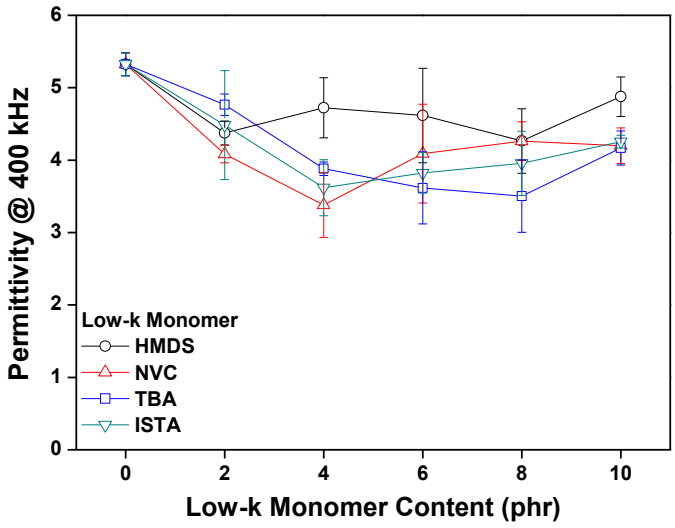

Figure 5-11. Permittivity at 400 kHz of crosslinked acrylic PSA as a function of low-*k* monomer types and contents.

5. Conclusions

To confirm the applicability of PSAs for display, four types of low-*k* monomer were selected to produce an acrylic PSA film according to the contents. In this research, the adhesion performance corresponding to low-*k* monomer type and content was confirmed via peel strength, probe tack and lap shear tests. Furthermore, the permittivity of the produced acrylic PSA films was measured using probe station. Due to the material properties of the semi-solid PSA, our measurements were very sensitive to the permittivity.

As a result of the gel fraction measurement, there was no difference in the degree of crosslinking among all low-*k* monomer types and contents. However, the value decreased from 10 phr of HMDS content to approximately 90 %. Additionally, the transmittance of the acrylic PSA film did not differ depending on the low-*k* monomer type and content, but it decreased at 10 phr of HMDS content down to approximately 85 %. As a result of measuring the adhesion performance of acrylic PSA depending on the type and content of low-*k* monomer, the adhesion properties decreased with increasing HMDS content, which has silane groups. When the content of HMDS was increased, bubble was generated due to unreacted the monomer, which affected the lap shear results. On the other hand, as the content of NVC with high polarity increased, the adhesion performance increased. TBA having branched side group affected the cohesion of the acrylic PSA, and ISTA with an alkyl chain had no significant effect on the adhesion performance. As the content of low-*k* monomer increased, the measurement results of

permittivity showed lower values than the permittivity of pure acrylic PSA. This result is because a free volume is formed by the low-*k* monomer. However, depending on the type of monomer, the permittivity began to increase above a certain content of monomer. The result is that as the content of low-*k* monomer increases, the efficiency of non-uniform free volume distribution decreases, and also the proportion of free volume decreases. Through this result, it was confirmed that certain amount or more of low-*k* monomer reduces the formation of free volume.

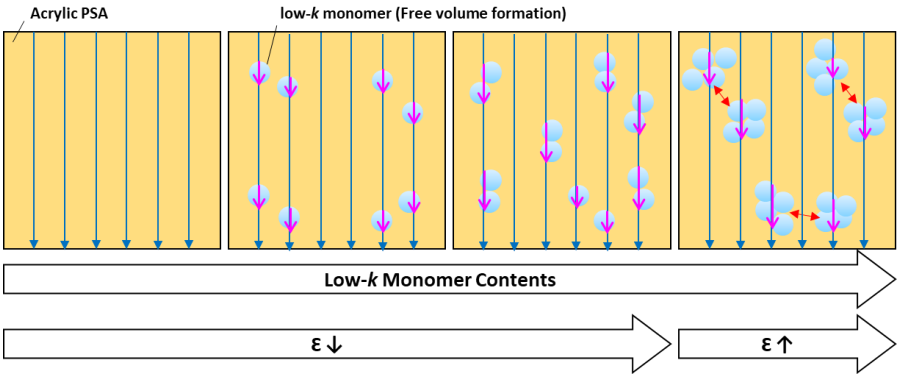

Figure 5-12. Schematic of free volume distribution in acrylic PSAs as a function of low-*k* monomer content.

Chapter 6

Transparency, adhesion performance and UV absorption of acrylic PSAs with various UV absorbers for display

1. Introduction

Display is a very important element for information output of electronic devices. In particular, displays such as smart phones, automobile displays, and outdoor advertisement displays are often used while being exposed to the outside. As a result, the display may be exposed to UV and aged due to chemical decomposition, which greatly affects the reliability and life of the product (Wang *et al.*, 2010). Therefore, the display is actively researched on the UV protection for preventing aging (Li *et al.*, 2019, Liang *et al.*, 2019, Lim *et al.*, 2019, Yuan *et al.*, 2019). UV protection is commonly called UV cut in the industry, and PSA having UV protection property is called UV cut PSA. Materials for imparting UV absorption are classified into inorganic agents and organic agents (Alebeid and Zhao, 2017). ZnO and TiO_2 are the most widely used inorganic agents, but they have a problem of reliability because of their photocatalytic reaction (Chen *et al.*, 2018, Huang *et al.*, 2016, Mai *et al.*, 2018, Zhu *et al.*, 2017). Moreover, the optical characteristic of the PSA for displays can be inhibited. Nanosilica, one of the inorganic UV protective agent, is nontoxic and nonphotocatalytic reaction, but weak in UV absorption (Xiong *et al.*, 2019). UVA is an organic agent for UV absorption, and there are benzophenones, benzotriazoles and substituted triazine derivatives. UVAs can be applied to various plastics and organic substances such as acrylic polymer, unsaturated polyester, polyvinyl chloride, polyolefin, polyurethane, polyacetal, polyvinyl butyral, elastomer and adhesive. Therefore, UVA is widely used to protect UV-induced degradation of

paints, industrial and automotive coatings, sealants, lubricants and like (Wypych *et al.*, 2015). The main purpose of UVA is to improve the UV absorption, but it affects the main physical properties of the materials, so it is applied by adjusting the type and content depending on the application field.

Since the researches of UV absorption are concentrated on general polymers and fibers, research on UV absorption and adhesion property of acrylic PSA is needed. Because inorganic UVA can hinder the transparency of acrylic PSA, organic UVA was conducted on this research. UVA exhibits UV absorption by releasing the energy of UV light as heat through a conjugation system in which double and single bonds cross. This system shows the difference in UV absorption depending on the movement of π electron. Also, it was predicted that the addition of UVA would change the adhesion property of acrylic PSAs. Therefore, this study tried to study the effect of organic UVA having different chemical structure with benzene group and azole group on UV absorption and adhesion performance of acrylic PSAs.

Acrylic oligomers were produced via photopolymerization, and syrups were prepared for the production of acrylic PSA. Acrylic PSAs were prepared by adjusting the type and content of UVA to the acrylic oligomer and adding a crosslinking agent and a photoinitiator. The UV absorption of acrylic PSAs according to the type and content of UVA were confirmed. Moreover, the change behavior of transparency and adhesion properties of acrylic PSA due to functional addition were investigated. Gel fraction was measured to investigate crosslinking density of acrylic PSA with UVA. Texture Analyzer was used to measure

peel strength, probe tack, and lap shear test, and UV-vis spectrophotometer was used to investigate transparency and transmittance along wavelength.

2. Objective

All commonly used plastics are known to degrade due to sunlight. This is why the light stability of polymers is an important property. There are various UVAs that can absorb UV rays in order to improve the UV absorption of common polymers.

UVA is broadly divided in to two types: organic and inorganic. Inorganic UVA is a variety of metal oxides, including zinc oxide (zincite), titanium dioxide (titania), cerium dioxide (ceria), and Various iron oxides and oxide-hydroxides. The UV absorption effect is exerted by a convenient band gap in the range of 3.0-3.4 eV corresponding to wavelengths below 400 nm due to particle scattering and reflection. However, there is a concern that the emergence of common product nanoparticles is not environmentally friendly, as high specific surface area and small particle size can definitely spread to the environment. Metal oxides are materials that can be photocatalytically activated (Asl *et al.*, 2012, Peng *et al.*, 2011). Therefore, it is an exciting substance in various application fields such as wastewater treatment and air pollution reduction (Kristensen *et al.*, 2011, Lei *et al.*, 2010, Xu *et al.*, 2008). However, this materials can cause degradation of the polymer matrix due to its photocatalytic activity when used for UV absorption of normal polymers. Organic UVA is a molecule with a conjugated π electron

system that can absorb UV radiation like various methoxycinnamate derivative. However, this molecule has a lifetime problem because it can be photodegraded by the generation of radicals from the degradation of the polymer matrix (Gerlock *et al.*, 1995, Rodil *et al.*, 2009). For the above reasons, research in ongoing to improve this.

However, there is a lack of research on UV absorption of PSA. The types of UVA that can be added to acrylic PSA are limited. Inorganic UVA is effective for UV absorption but it can inhibit the transparency of PSA for display. Therefore, in this study, experiments were designed using organic UVA. In recent industries, photo curable acrylic PSA using UV rays is indispensable to speed up the process. UV cut by UVA can hinder the UV curing of acrylic PSA due to insufficient UV energy. Therefore, UV absorption should be applied and at the same time do not cause any problems in UV curing acrylic PSA. For this reason, the type of initiator and the crosslinking density have to analyze for the UV curing of acrylic PSA with UVA added. The UV absorption of organic UVA is that heat is dissipated by a resonance system using UV energy. There are several types of organic UVA, but the most common are the benzophenones and phenylbenzotriazoles (Riedel *et al.*, 1994). Therefore, 4 types of UVA with benzene and azole groups were selected. I would like to confirm the effects of the different chemical structures of each UVA on transparency, adhesion performance and UV absorption of acrylic PSA.

3. Experimental

3.1. Materials

Reactive acrylic monomers, 2-hydroxyethyl acrylate (2-HEA, 99.0 % purity, Samchun Pure Chemical, Republic of Korea), 2-ethylhexyl acrylate (2-EHA, 99.0 % purity, Samchun Pure Chemical) and isobutyl acrylate (IBA, 99.0 % purity, Samchun Pure Chemical), were used as received without further purification to prepare acrylic prepolymer. Chemical types of UVAs, hydroxybenzoate (HB, SONGSORB®2908, SONGWON, Republic of Korea), benzophenone (BP, SONGSORB®8100, Republic of Korea), benzotriazole (BTZ, SONGSORB®3280, Republic of Korea), triazine (TZ, SONGSORB®CS400, Republic of Korea) were used to enhance the UV absorption (Figure 6-1). The photoinitiator to synthesize the acrylic prepolymer was 2-hydroxy-2-methyl-1-phenyl-1-one (Omnirad 1173, 1173, IGM Resins, Netherlands). 1-hydroxy-cyclohexyl-phenyl-ketone (Omnirad 184, 184, IGM Resins, Netherlands) and ethyl (2,4,6-trimethylbenzoyl)-phenyl-phosphinate (Omnirad TPO-L, TPO-L, IGM Resins, Netherlands) were used to identify the most appropriate photoinitiator to UV crosslinking for UV cut PSAs (Figure 6-2). 1,6-hexanediol diacrylate (HDDA, Sigma-Aldrich, USA) was used as a crosslinking agent.

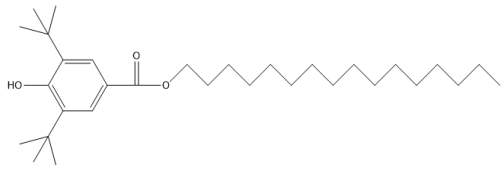

Hytdroxybenzoate (HB)

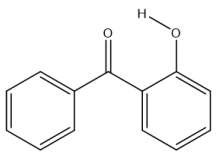

Benzophenone (BP)

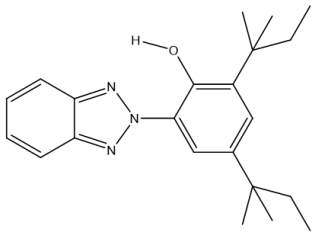

Benzotriazole (BTZ)

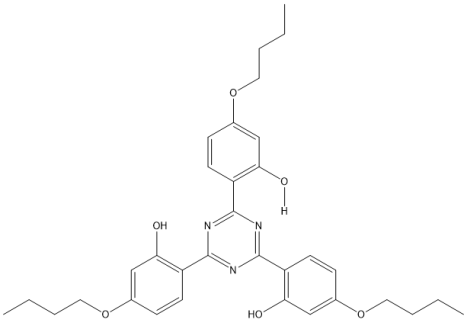

Triazine (TZ)

Figure 6-1. Chemical structure of UVAs.

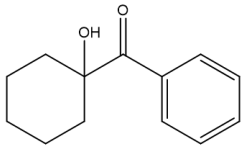

1-Hydroxy-cyclohexyl-phenyl-ketone

Omnirad 184

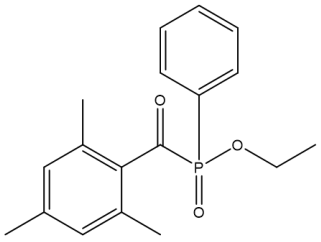

Ethyl (2,4,6-trimethylbenzoyl)-phenyl-phosphinate

Omnirad TPO-L

Figure 6-2. Chemical structure of photoinitiators to UV crosslinking for UV cut PSAs.

3.2. Methods

3.2.1. Synthesis of acrylic prepolymer

The acrylic monomers (2-HEA, 2-EHA and IBA) were mixed with an Omnirad 1173 inside a 500-ml four neck round-bottomed flask equipped with a stirrer, thermometer and N_2 purging tube (the formulation of the synthesized acrylic prepolymer is listed in Table 6-1). The mixture was continuously stirred for 20 min at room temperature with N_2 gas. The monomers mixture was synthesized by UV-irradiating using UV-spot cure system (SP-9, USHIO, Japan) under a N_2-rich atmosphere until the temperature of the mixture rose 5 ^oC. The above process iterated 5 times and stored in a wide-mouth bottle to protect the acrylic prepolymer from light and air. In this study, I tried to confirm the enhancement of the UV absorption of typical acrylic PSA and the behavior of adhesion performance according to organic UVA type and content. Therefore, instead of using the acrylic prepolymer used in UV pattern research, acrylic prepolymer with a common T_g value (approximately -40 ^oC) was synthesized and used.

Table 6-1. Formulation of acrylic prepolymer.

Formulation		**Acrylic prepolymer (wt.%)**	**Expected T_g (^oC)**
Reactive monomer (wt.%)	2-HEA	20	-40
	2-EHA	60	
	IBA	20	
Photoinitiator (phr)	Omnirad 1173	1	

Photoinitiator: Omnirad 1173, 2-hydroxy-2-methyl-1-phenyl-1-1-one
Wavelength of UV lamp (nm): ≈365
UV exposure (mW/cm^2): ≈20

3.2.2. Fabrication of UV cut PSAs

Crosslinked PSAs with UVAs were prepared by blending 100 wt.% of the synthesized acrylic prepolymer with 1 phr of HDDA. First, in order to confirm the optimal photoinitiator types and contents, the content of benzotriazole fixed at 3.0 phr, and the contents of Omnirad 184 and Omnirad TPO-L was adjusted from 0.5 phr to 3.0 phr to prepare PSA films (Table 6-2). The crosslinking reaction for the preparation of acrylic PSA is triggered by UV light. However, when UVA imparts UV absorption, the photoinitiator cannot initiated, and as a result, it is difficult to sufficiently crosslink the acrylic PSA. Therefore, even if UVA was overdosed, it was necessary to investigate the type and content of the initiator capable of sufficient crosslinking reaction. Second, UV cut PSA was manufactured according to the type and content of UVA (Table 6-3). The blend was mixed and deformed using paste mixer (SR-500, Thinky, Japan) for 4 min. The blends were coated onto the surface of 50 μm thickness corona-treated polyethylene terephthalate (PET) films and crosslinked by black light lamp, approximately 1600 mJ/cm^2. The dry thickness of UV cut PSA was about 100 μm.

Table 6-2. Formulation of acrylic PSA as a function of photoinitiator types and contents.

Sample Names	Acrylic prepolymer (wt.%)	UVA (phr)	Crosslinking agent (phr)	Photoinitiator (phr)	
		BTZ	HDDA	Omnnirad 184	Omnirad TPO-L
184 series	100	3	1	0.5/1.0/2.0/3.0	-
TPO-L series				-	0.5/1.0/2.0/3.0

UV lamp: Black light
Exposure time: 5 min

Table 6-3. Formulation of acrylic PSA as a function of UVA types and contents.

Sample Names	Acrylic prepolymer (wt.%)	Photoinitiator (phr)	Crosslinking agent (phr)	UVA (phr)
		TPO-L	HDDA	HB/BP/BTZ/TZ
Neat acrylic PSA	100	3	1	-
HB series	100	3	1	0.5/1.0/2.0/3.0
BP series				
BTZ series				
TZ series				

UV lamp: Black light
Exposure time: 5 min

4. Results and Discussion

4.1. Optimum initiator for UV cut PSA

Figure 6-3 shows gel fraction results according to the type and content of photoinitiator of acrylic PSA containing UVA. By adding the TPO-L initiator, the gel fraction value of the acrylic PSA was maintained at about 90 % or more. On the other hand, in the case of 184, the 0.5 phr content was not crosslinked and increased as the initiator content increased above 1 phr, but only up to about 60 %. In other words, UVA absorbed UV energy, thereby suppressing initiation of the crosslinking agent by the initiator. TPO-L absorbs UV light having a wavelength longer than 184. 184 has UV absorption peaks of 246, 280, and 333 nm, and TPO-L has the peaks of 295, 368, 380, and 393 nm. TPO-L, which absorbs long wavelength UV energy, has been confirmed to be advantageous for the production of UV cut PSA. From these results, it was confirmed that the type and content of photoinitiaotr are important factors for the application of photocurable acrylic prepolymer in the preparation of UV cut PSA. UV light is divided into UVA (315-400 nm, Long wave), UVB (280-315 nm, Medium wave), UVC (100-280 nm, Short wave) according to the wavelength range. For UVA applied to UV crosslinked acrylic PSA, there is a photoinitiator that can be initiated by UVA, ie, long wavelength.

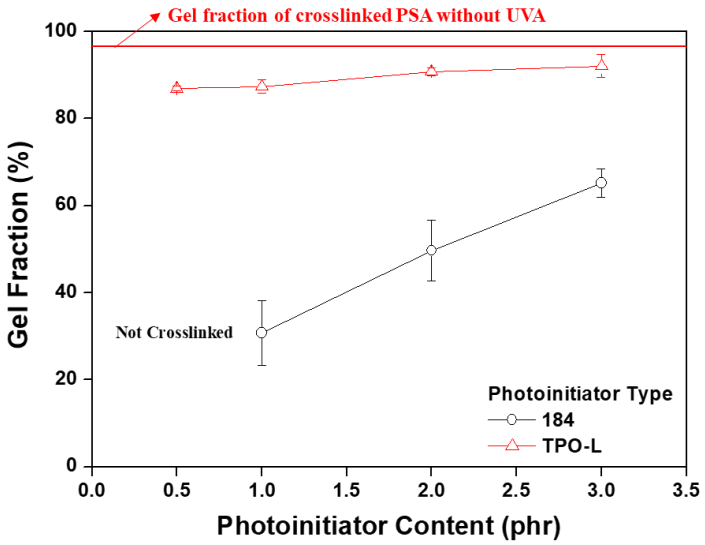

Figure 6-3. Gel fraction results according to the type and content of photoinitiator of acrylic PSA containing UVA.

Figure 6-4 shows peel strength measurement results according to the type and content of photoinitiator of acrylic PSA containing UVA. The acrylic PSA to which 184 initiator was added was not crosslinked and could not be measured. On the other hand, in acrylic PSA containing TPO-L, the value of peel strength continuously increased as the initiator content increased. This result is because the cohesion of acrylic PSA was improved as the content of the initiator was increased to improve the crosslinking density. Crosslinking reaction is one of the important factors that determine the adhesion property of acrylic PSAs. In other words, even if the UV absorption through organic UVA are improved, adhesion performance must be maintained in order to play a primary role as PSA, and this property is exhibited by sufficient crosslinking.

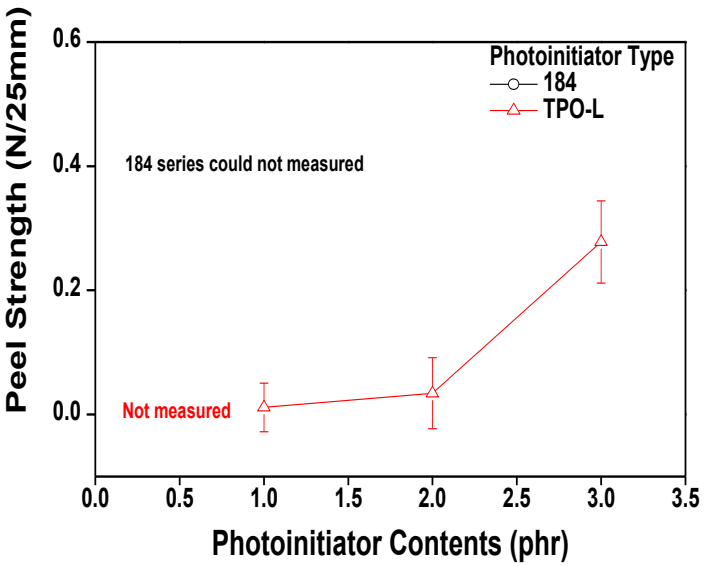

Figure 6-4. Peel strength measurement results according to the type and content of photoinitiator of acrylic PSA containing UVA.

4.2. UV cut PSAs with various UVAs

4.2.1. Gel fraction

Figure 6-5 shows the gel fraction results of acrylic PSA according to UVA type and content. It was confirmed that the gel fraction value of acrylic PSA according to the type and content of UVA was maintained at about 90 % or more and did not affect the crosslinking density. However, the gel fraction value of acrylic PSA with 3 phr of triazine content decreased sharply to about 52 %.

From these results, it was confirmed that sufficient crosslinking was possible according to the type and content of organic UVA when using a long wavelength initiator. In particular, for UVA with benzene group, the molecular weight and the number of benzene units do not affect the crosslinking density. On the other hand, in the case of triazine in the UVA with azole group, when the triazine content was increased to 3 phr, the starting reaction was hindered due to the large molecular weight and chemical structure, and it was difficult to sufficiently crosslink between the prepolymer and the HDDA.

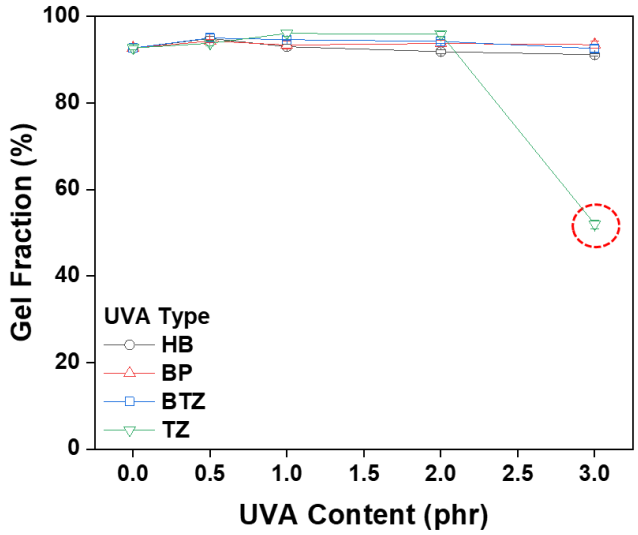

Figure 6-5. Gel fraction results of acrylic PSA according to UVA type and content.

4.2.2. Color change

Figure 6-6 shows the calculation result of the change in color according to the type and content of UVA. Calculations were made with the color of neat acrylic PSA not added to UVA fixed at 100 % as described section 2.3. All UVA types and contents showed the almost same value as neat acrylic PSA color. It means that the UVA used in this study did not affect the transparency of acrylic PSA.

The reason for choosing organic UVA instead of inorganic UVA in the experimental design is that even if the adhesion property of acrylic PSA changed due to the addition of UVA to improve UV absorption and maintain the transparency. Using the above results, it was confirmed that organic UVA maintains transparency regardless of the chemical group and chemical structure that express the resonance system.

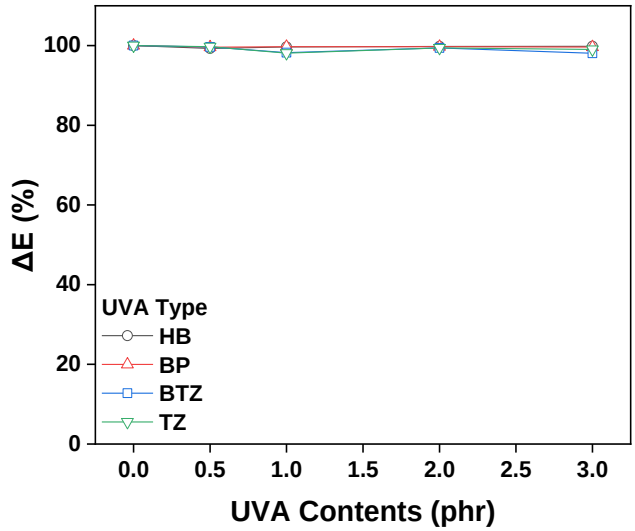

Figure 6-6. Calculation result of the change in color according to the type and content of UVA.

4.2.3. Adhesion performance

Figure 6-7 shows the peel strength measurement results of acrylic PSA according to the type and content of UVA. As the content of all UVAs increased, the peel strength value of acrylic PSA tended to decrease slightly, but no significant difference was observed. However, the peel strength of acrylic PSA with a triazine content of 3 phr increased rapidly and a cohesive failure occurred. This is because, like the gel fraction result, triazine having a large molecular weight hinders the crosslinking of HDDA, and the cohesion with the acrylic prepolymer chain is reduced (Czech, 2007, Czech *et al.*, 2011, Vu *et al.*, 2019).

Figure 6-8 shows the results of probe tack of acrylic PSA according to the type and content of UVA. Although it showed a tendency to decrease slightly as the content of all UVAs increased, it did not show a significant difference, similar to the peel strength result. However, the tack value of acrylic PSA with a triazine content of 3 phr increased to about 5.7 N. This result is also because the stickiness of PSA became stronger due to the inhibition of the crosslinking reaction (Czech *et al.*, 2015).

These results confirm that the UVA does not significantly affect the peel strength and probe tack values exhibited by wetting and cohesion. Nikafshar *et al*. reported that cured epoxy resin with 3 % UVA investigated the tensile properties according to UV irradiation time. There was no significant difference when UVA was added, but there was a tendency to decrease slightly (Nikafshar *et al.*, 2017). But unlike solid epoxy resins, the semi-solid acrylic PSAS shows more of an effect.

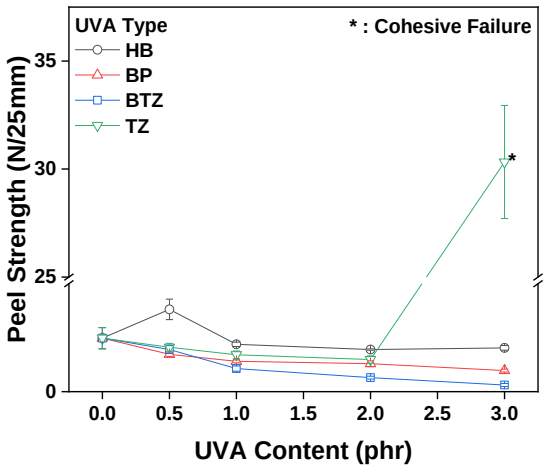

Figure 6-7. Peel strength measurement results of acrylic PSA according to the type and content of UVA.

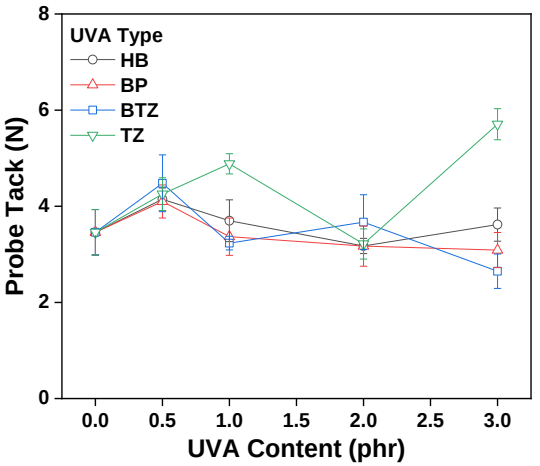

Figure 6-8. Probe tack measurement results of acrylic PSA according to the type and content of UVA.

Figure 6-9 shows the lap shear test result of acrylic PSA according to the content of UVA with benzene group. As each UVA content increased, the maximum shear stress and strain did not differ greatly. In addition, it was confirmed that the long alkyl chain of hydroxybenzoate does not significantly affect the shear adhesion property of acrylic PSA. This result means that the shear adhesive force can be maintained while the UV absorption ability is improved. As the benzotriazole content increased, the maximum shear stress and strain also did not change considerably. On the other hand, it was confirmed that the maximum shear stress slightly increased as the triazine content increased. This result is due to an increase in cohesion due to the polarity of nitrogen possessed by triazine (Park *et al.*, 2015, Kuo *et al.*, 2018). However, with the triazine content of 3 phr, the maximum shear stress decreased rapidly, as did the results of gel fraction, peel strength, and probe tack. That is, as the content of UVA increases, the energy absorption of UV rays increases and sufficient crosslinking is impossible.

Shear stress and strain are determined based on the cohesion of acrylic PSA, which is controlled by the crosslinking density. We tried to confirm how the organic UVA selected in this study affects the cohesion of crosslinked acrylic PSAs. In the case of UVA with benzene group, as the content increased, it tended to increase slightly, but did not show a significant difference, and did not significantly affect cohesion based on the chemical structure. UVA with azole group can improve the cohesion by the polarity of nitrogen group, and benzotriazole with small molecular weight was expected to be more effective. The maximum stress and the strain at the maximum stress of acrylic PSA when benzotriazole was

added tended to decrease slightly. On the other hand, the maximum stress of acrylic PSA with triazine added was rather increased. This result is because the polarity of the hydroxyl group of triazine affected the cohesion of the PSA. However, as the triazine content was 3 phr, the maximum stress was sharply reduced due to the decrease in crosslinking due to the inhibition of the initiation reaction as confirmed from the results of gel fraction, peel strength and probe tack.

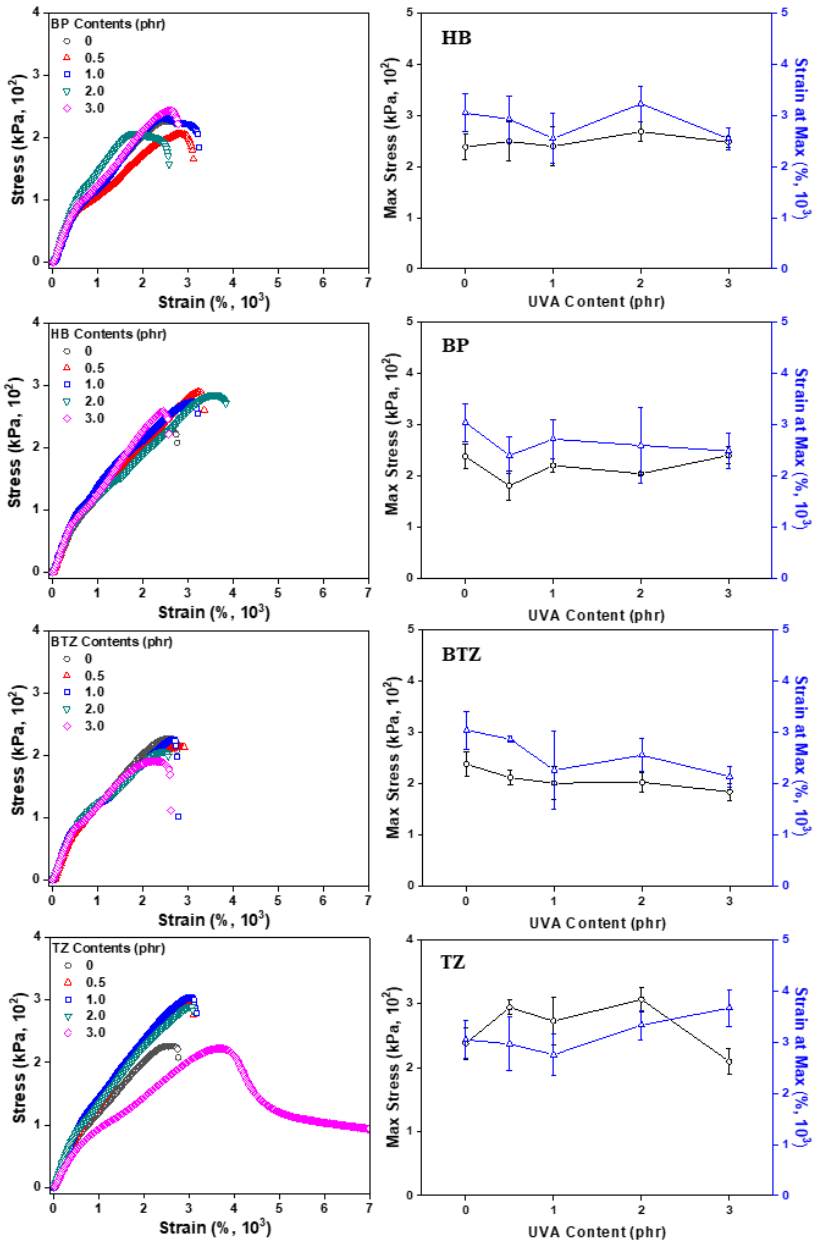

Figure 6-9. Lap shear test results of acrylic PSA according to the content of UVA.

4.2.4. Transmittance

Figure 6-10 shows the resonance system mechanism according to the type of UVA. UVA absorbs the energy of UV rays and generated heat through the resonance system, and repeats this to exert the UV ray protecting effect. UVA with benzene and azole group can see the difference in generation of resonance system based on chemical structure. Also, it was expected that there would be a difference in UV absorption because the distance between the atoms at which the π electrons move based on the chemical structure changes.

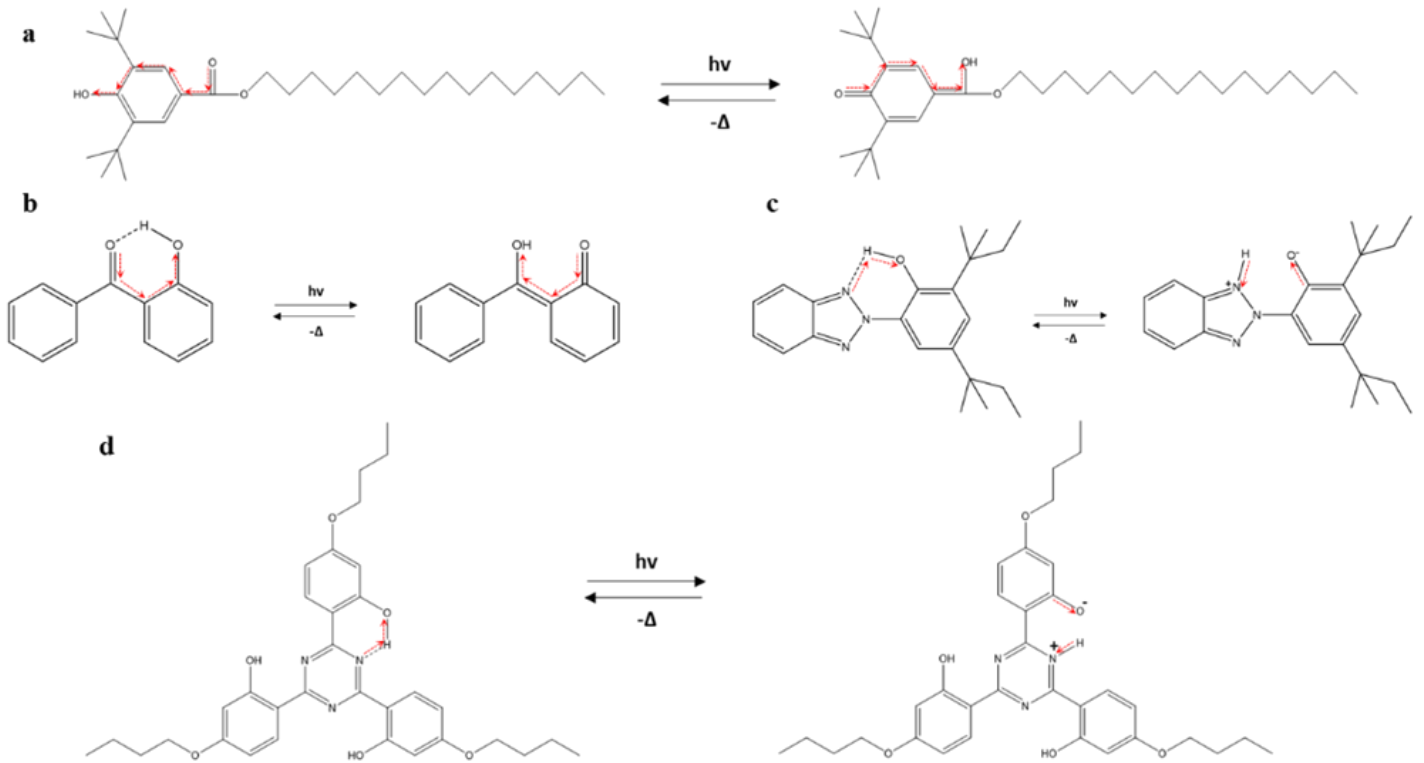

Figure 6-10. Resonance system mechanism according to the type of UVA:

(a) hydroxybenzoate, (b) benzophenone, (c) benzotriazole, (d) triazine.

Figure 6-11 shows the transmittance measurement results of acrylic PSA according to the type and content of UVA. Acrylic PSA of all UVA types and contents satisfied both about 95 % in the visible light region above 400 nm, consistent with this color change data. However, the transmittance in the rage of 200 to 400 nm, which is the UV region, showed a difference in the results depending on the type and content of UVA. UVA with benzene group had lower UV cut effect than that with azole group. The UV absorption of UVA is that the double bond present in UVA absorbs UV energy and is released as heat by the resonance effect. From these results, it was confirmed that the chemical structure of azole group in UVA is advantageous in absorbing UV rays. Moreover, it was confirmed that benzophenone, which has a short electron transfer distance of UVA having a benzene group, is more effective. On the other hand, hydroxybenzoate, in which the moving distance of the π electrons is longer than benzophenone, does not exhibit UV absorption. Based on these results, it was confirmed that the UV absorption by the resonance system showed a difference based on the chemical group, and that the migration distance of π electrons due to the chemical structure was an important factor in determining the UV absorption of acrylic PSAs.

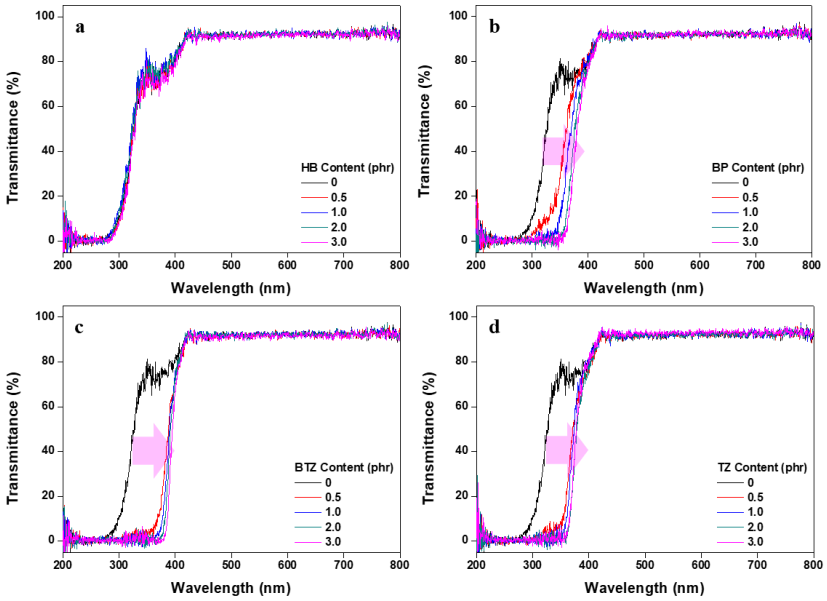

Figure 6-11. Transmittance measurement results of acrylic PSA according to the type and content of UVA: (a) hydroxybenzoate, (b) benzophenone, (c) benzotriazole, (d) triazine.

Figure 6-12 summarizes the transmittance according to the wavelength of the UV-vis spectrophotometer. The acrylic PSA containing hydroxybenzoate did not generated UV absorption according to the wavelength. However, in the case of benzophenone, the UV transmittance continuously decreased as the UVA content increased. In other words, UVA having a benzene group has a resonance system, and the shorter the interatomic distance to transfer π electrons, the more excellent the UV absorption effect. Acrylic PSA containing benzotriazole and triazine showed a sharp decrease in UV transmittance in the UV region, and decreased slightly as the content increased. From these results, it was confirmed that UVA with azole group has higher UV protection effect than UVA with benzene group. However, it was confirmed that benzotriazole, which has a low overall molecular weight, is more effective in UV absorption than triazine in UVA with azole group. This result is because triazine having three hydroxyl group to generate resonance system in one molecule and relatively high molecular weight required more UV energy to operate resonance system than benzotriazole.

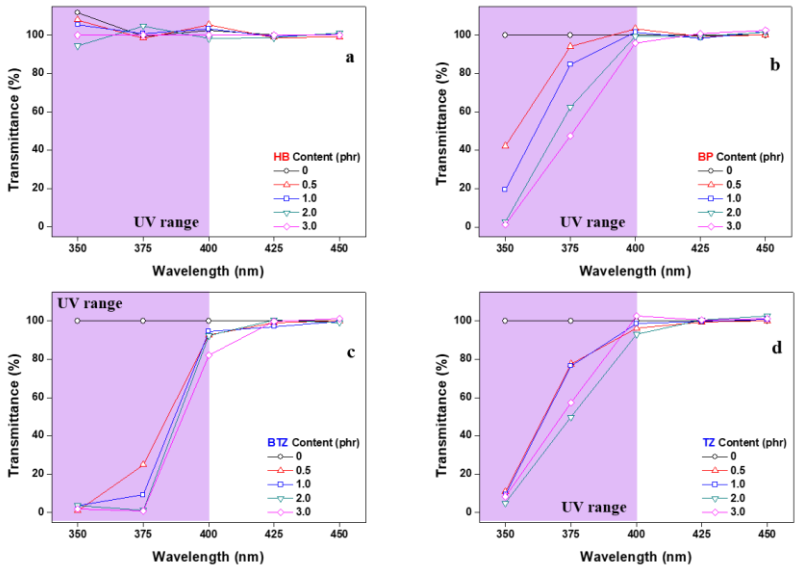

Figure 6-12. Transmittance according to the wavelength of the UV-vis spectrophotometer.

5. Conclusions

In this study, UVAs with benzene and azole group were selected in order to confirm the UV absorption and adhesion properties of acrylic PSA for display.

In order to confirm the inhibition of the crosslinking of UV cut acrylic PSA by UVA absorption, gel fraction was measured according to the contents of 184 and TPO-L initiator. As a result of the measurement, inhibition of the crosslinking density could be avoided when TPO-L absorbing long wavelength UV rays was added. As for the peel strength measurement result, PSA containing 184 showed no adhesion. However, in the case of TPO-L, the value of peel strength continuously increased as the content increased.

As a result of gel fraction measurement according to the type and content of UVA, the value of about 90 % or more of all types and contents of UVA was maintained. However, at a triazine content of 3 phr, the value dropped sharply to about 52 %. As a result of measuring the change in color according to the type and content of UVA, all samples showed values similar to neat acrylic PSA. The transmittance in the visible light region was all about 95 % as a function of UVA type and content, as was the result of measuring the color change. However, it showed the difference in UV absorption characteristics in the UV region. Compared with UVA with benzene group, the UV absorption of UVA with azole group is more effective. The efficiency of benzotriazole with low molecular weight of UVA with azole group was higher and sooner. hydroxybenzoate having a large molecular weight of UVA with benzene

group and a long alkyl chain exhibited almost no UV absorption. In other words, it was confirmed that the UV absorption of UVA is determined by the electron movement distance, molecular weight, and side chain. Peel strength, probe tack, and lap shear test results were confirmed for acrylic PSA adhesion properties according to UVA type and content. The adhesion properties did not show a big difference, but the adhesive strength decreased rapidly when the content of triazine with the highest molecular weight of UVA was 3 phr. This result is because as increase in the content of UVA having a molecular weight above a certain level affects the crosslinking of acrylic PSA. Also, the decrease in adhesive force can be explained from a result of gel fraction.

Through this research, the UV absorption of benzotriazole with azole group and relatively low molecular weight is the best. Moreover, there was almost no influence which reduced the adhesion properties of acrylic PSA. From this result, benzotriazole was confirmed to be most advantageous to enhance the UV absorption of acrylic PSA. In addition, it was confirmed that triazine with three hydroxyl group to generate resonance system in on molecule and relatively large molecular weight could be used for the production of UV cut PSA when added in small amounts for its adhesion performance.

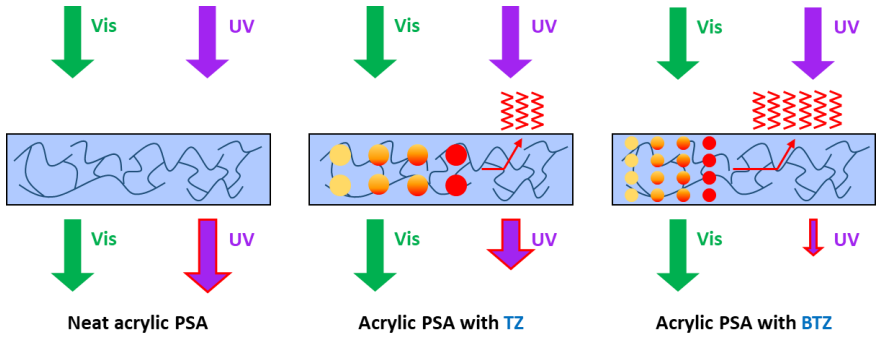

Figure 6-13. Scheme of the resonance system comparison according to the chemical structure of UVA with azole group.

Chapter 7

Concluding remarks

This study confirmed the method of improving recovery, low permittivity and UV absorption of acrylic PSAs, and the resulting change in adhesion performance. I also established a reliable quantitative evaluation method for improving the functionality of acrylic PSAs.

Patterned acrylic PSAs through UV crosslinking have improved recovery and adhesion performance as the size of the pattern becomes smaller. The probe station was used to measure the reliable permittivity of the PSAs. The permittivity of the acrylic PSAs using low-*k* monomers differed depending on the chemical structure of the monomers and decreased to below a certain content. In addition, the adhesion performance of the PSAs changed according to the chemical group of the low-*k* monomers. The UV absorption of acrylic PSAs with UVA have azole group and small molecular weight is the most excellent. Unexpectedly, UVA did not significantly affect the adhesion performance as long as it did not affect the crosslinking density of the acrylic PSAs.

The study was conducted independently due to current technical limitations. Future development of the display requires the development of a PSAs with simultaneous recovery, low permittivity and UV absorption. As a result of this research, in order to develop PSAs for displays with various functionalities, research to improve the adhesion performance inherent to PSAs is required in addition to controlling molecular weight and crosslinking density. Maximizing the adhesion performance will make it easier to choose a method and simultaneously implement functionality to apply acrylic PSAs to display application.

References

Alebeid, O.K., Zhao, T. (2017) Review on: developing UV protection for cotton fabric. *Journal of The Textile Institute.* 108(12): 2027-2039.

Angelidi, M., Vassilopoulos, A.P., Keller, T. (2017a) Displacement rate and structural effects on poisson ratio of a ductile structural adhesive in tension and compression. *International Journal of Adhesion and Adhesives.* 78: 13-22.

Angelidi, M., Vassilopoulos, A.P., Keller, T. (2017b) Ductility, recovery and strain rate dependency of an acrylic structural adhesive. *Construction and Building Materials*. 140: 184-193.

Asl, S.K., Sadrnezhaad, S.K., Rad, M.K., Uner, D. (2012) Comparative photodecolorization of Red Dye by Anatase, Rutile (TiO_2), and Wurtzite (ZnO) using response surface methodology. *Turkish Journal of Chemistry.* 36: 121-135.

Back, J.-H., Baek, D., Sim, K.-B., Oh, G.-Y., Jang, S.-W., Kim, H.-J., Kim, Y. (2019) Optimization of recovery and relaxation of acrylic pressure-sensitive adhesives by using UV patterning for flexible displays. *Industrial & Engineering Chemistry Research.* 58(10): 4331-4340.

Bae, K.-Y., Lim, D.-H., Park, J.-W., Kim H.-J., Jeong H.-M., Takemura, A. (2013) Adhesion performance and surface characteristics of low surface energy PSAs fluorinated by UV polymerization. *Polymer Engineering and Science.* 53(9): 1968-1978.

Bauh, B., Kreling, S., Kolb, M., Geistbeck, M., Boujenfa, S., Suess, M., Dilger, K. (2018) UV-laser cleaning and surface characterization of an aerospace carbon fibre reinforced polymer. *International Journal of Adhesion and Adhesives.* 82: 50-59.

Bergman, D.J., Stroud, D. (1992) Physical properties of macroscopically inhomogeneous media. *Solid State Physics.* 46: 147-269.

Blythe, T., Bloor, D. (2005) Electrical Properties of Polymers, 2nd Ed., Cambridge University Press, UK.

Bora, J. (2018) Fabrication and characterization of D-glass fibers with low dielectric constant (Master Thesis, Hanyang University, Republic of Korea).

Braunschmweiger system elektronik GmbH, “Optical Bonding for Industrial/Medical”, 2019년 11월 21일 접속, https://www.systemelektronik.de/en/optical-bonding/.

Chang, E.P., Holguin, D. (2005a) Curable optically clear pressure-sensitive adhesives. *The Journal of Adhesion.* 81: 495-508.

Chang, E.P., Holguim, D. (2005b) Electrooptical light-management material: Low-refractive-index adhesives. *The Journal of Adhesion.* 81: 925-939.

Chang, K., Luo, H., Geise, G.M. (2019) Water content, relative permittivity, and ion sorption properties of polymers for membrane desalination. *Journal of Membrane Science.* 574: 24-32.

Chen, D.Z., Mai, Z.H., Liu, X., Ye, D.Z., Zhang, H.W., Yin, X.Z., Zhou, Y.S., Liu, M., Xu, W.L. (2018) UV-blocking, superhydrophobic and robust cotton fabrics fabricated using polyvinylsilsesquioxane and nano-TiO_2. *Cellulose.* 25: 3635-3647.

Chen, J., Calvin, J.J., King, S.W., Woodfield, B.F., Navrotsky, A. (2019) Energetics of porous amorphous low-*k* SiOCH dielectric films. *Journal of Chemical Thermodynamics.* 139: 105885.

Chern, Y.-T., Shiue, H.-C. (1997) Low dielectric constants of soluble polyimides based on adamantine. *Macromolecules.* 30: 4646−4651.

Chern, Y.-T., Shiue, H.-C. (1998) High sunglass transition temperatures and low dielectric constants of polyimides derived from 4,9-bis(4-aminophenyl) diamantine. *Chemistry of Materials.* 10: 210−216.

Crawford, J. (1999) 2(2-Hydroxyphenyl)2H-benzotriazole ultraviolet stabilizer. *Progress Polymer Science.* 24: 7-43.

Czech, Z. (2007) Synthesis and cross-linking of acrylic PSA systems. *Journal of Adhesion Science and Technology.* 21(7): 625-635.

Czech, Z., Butwin, A., Kabatc, J. (2011) Photoreactive UV-crosslinkable acrylic pressure-sensitive adhesives containing type-II photoinitiators. *European Polymer Journal.* 47: 225-229.

Czech, Z., Kabatc, J., Kowalczyk, A., Sowa, D., Madejska, E. (2015) Application of selected 2-methylbenzothiazoles AS cationic photoreactive crosslinkers for pressure-sensitive adhesives based on acrylics. *International Journal of Adhesion and Adhesives.* 58: 1-6.

Czech, Z., Kurzawa, R. (2007) Acrylic pressure-sensitive adhesive for transdermal drug delivery systems. *Journal of Applied Polymer Science.* 106: 2398-2404.

Czech, Z., Milker, R. (2003) Solvent-free radiation-curable polyacrylate pressure-sensitive adhesive systems. *Journal of Applied Polymer Science.* 87(2): 182-191.

Czech, Z., Wesolowska, M. (2007) Development of solvent-free acrylic pressure-sensitive adhesives. *European Polymer Journal.* 43: 3604-3612.

Czech, Z., Pelech, R. (2008) The thermal degradation of acrylic pressure-sensitive adhesives based on butyl acrylate and acrylate and acrylic acid. *Progress in Organic Coatings.* 65: 84-87.

Dong, C.C., Hoyle, R.J. (1976) Elastomeric adhesive properties – shear strength, shear modulus, creep, and recovery. *Wood and Fiber.* 8(2): 98-106.

Dong, L.M., Shi, D.Y., Wu, Z., Li, Q., Han, Z.D. (2015) Improved solvothermal method for cutting graphene oxide into praphene quantum dots. *Digest Journal of Nanomaterials and Biostructures.* 10(3): 855-864.

Dong, Y., Shao, J., Chen, C., Li, H., Wang, R., Chi, Y., Lin, X., Chen, G. (2012) Blue luminescent graphene quantum dots and graphene oxide prepared by tuning the carbonization degree of citric acid. *Carbon.* 50(12): 4738-4743.

Fang, C., Liu, Z., Zhu, X., Cao, Y., Dong, X. (2019) Manipulation of chain transfer agent and cross-linker concentration to modify the performance of fluorinated acrylate latex pressure sensitive adhesive. *Journal of Adhesion Science and Technology.* Online published.

Fujita, M., Takemura, A., Ono, H., Kajitama, M., Hayashi, S., Mizumachi, H. (2000) Effects of miscibility and viscoelasticity on shear creep resistance of natural-rubber-based pressure-sensitive adhesives. *Journal of Applied Polymer Science.* 75: 1535-1545.

Garden, L., Pethrick, R.A. (2017) Critique of dielectric cure monitoring in epoxy resins – Does the method work for commercial formulations? *International Journal of Adhesion and Adhesives.* 74: 6-14.

Gerlock, J.L., Tang, W. (1995) Reaction of benzotriazole ultraviolet light absorbers with free radicals. *Polymer Degradation and Stability.* 48: 121-130.

Geyer, R.G., Krupka, J. (1995) Microwave dielectric-properties of anisotropic materials at cryogenic temperatures. *IEEE Transactions on Instrumentation and Measurement.* 44(2): 329-331.

Ghosh, A., Banerjee, S. (2008) Thermal, mechanical, and dielectric properties of novel fluorinated copoly(imide siloxane)s. *Journal of Applied Polymer Science.* 109:2329-2340.

Grosso, D., Boissière, C., Sanchez, C. (2007) Ultralow-dielectric-constant optical thin films built from magnesium oxyfluoride vesicle-like hollow nanoparticles. *Nature Materials.* 6: 572−575.

Hasani, M., Mahdavian, M., Yari, H., Ramezanzadeh, B. (2018) Versatile protection of exterior coatings by the aid of praphene oxide nanosheets; Comparison with conventional UV absorbers. *Progress in Organic Coatings.* 116: 90-101.

Hatton, B.D., Landskron, K., Hunks, W.J., Bennett, M.R., Shukaris, D., Perovic, D.D., Ozin, G.A. (2006) Materials chemistry for low-*k* materials. *Materials Today.* 9: 22-31.

Hougham, G., Tesoro, G., Shaw, J. (1994) Synthesis and properties of highly fluorinated polyimides. *Macromolecules.* 27: 3642−3649.

Huang, Z., Ding, A., Guo, H., Lu, G., Huang, X. (2016) Construction of nontoxic polymeric UV-absorber with great resistance to UV-photoaging. *Scientific Reports.* 6: 25508.

Hummel, R.E. (2011) Electronic Properties of Materials. 4th ed. Springer, Berlin, Germany.

Indulkar, C.S., Thiruvengadam, S. (2008) An Introduction to Electronic Emgineering Materials. Chand and Company, India.

INI Research & Consulting (2014) "터치스크린 패널의 원리 및 기술별 종류", 2014년 9월 15일, 2019년 5월 9일 접속, https://www.inirnc.com:40126/prop/bbs/board.php?bo_table=ini_column&wr_id=20&page=40.

Ishida, H., Low, H.Y. (1997) A study on the volumetric expansion of benzoxazine-based phenolic resin. *Macromolecules.* 30: 1099-1106.

Ito, K., Shitajima, K., Karyu, N., Fujii, S., Nakamura, Y., Urahama, Y. (2014) Influence of the degree of crosslinking on the stringiness of crosslinked polyacrylic pressure-sensitive adhesives. *Journal of Applied Polymer Science.* 131(11): 40336.

Jeon, H., Kim, S., Lee, S., Lee, J., Kho, D. (2014) Low dielectric pressure-sensitive adhesive film for capacitive touch screen panel, KR101572010B1.

Joo, H.-S., Park, Y.-J., Kim, H.-S., Kim, H.-J., Song, S.-J., Choi, K.-Y. (2007) The curing performance of UV-curable semi-interpenetrating polymer network structured acrylic pressure-sensitive adhesives. *Journal of Adhesion Science and Technology.* 21(7): 575-588.

Jousseaume, V., Fayolle, M., Guedj, C., Haumesser, P.H., Huguet, C., Pierre, F., Pantel, R., Feldis, H., Passemard, G. (2005) Pore sealing of a porous dielectric by using a thin PECVD a-SiC:H conformal liner. *Journal of the Electrochemical Society.* 152(10): F456-F161.

Kajtna, J., Golob, J., Krajnc. M. (2009) The effect of polymer molecular weight and crosslinking reactions on the adhesion properties of microsphere water-based acrylic pressure-sensitive adhesives. *International Journal of Adhesion and Adhesives.* 29: 186-194.

Keizai, F. (2011) Special Adhesive and Passivation Materials Market Outlook and Application 2012, Tokyo.

Kessler, D., Roth, P.J., Theato, P. (2009) Reactive surface coatings based on polysilsesquioxanes: controlled functionalization for specific protein immobilization. *Langmuir.* 25: 10068−10076.

Khan, I., Poh, B.T. (2011) Effect of molecular weight and testing rate on peel and shear strength of epoxidized natural rubber (ENR 50)-based adhesives. *Journal of Applied Polymer Science.* 120: 2641-2647.

Kim, S., Lim, D.-H, Oh, J.-K, Cho, Y.-S., Park, J.-W., Kim, H.-J. (2008) The curing behavior and PSA performance of acrylic pressures sensitive adhesives using aluminum acetylacetonate. *Journal of Adhesion and Interface.* 9(3): 27-33.

Kohl, P.A. (2011) Low-dielectric constant insulators for future integrated circuits and packages. *Annual Review of Chemical and Biomolecular Engineering.* 2: 379-401.

Kristensen, S.B., Kunov-Kruse, A.J., Riisager, A., Rasmussen, S.B., Fehrmann, R. (2011) High performance vanadia-anatase nanoparticle catalysts for the selective catalytic reduction of NO by ammonia. *Journal of Catalysis.* 284(1): 60-67.

Kuo, C.-F.J., Chen, J.-B., Chang, S.-H. (2018) Low corrosion optically clear adhesives for conducting glass: I. Effects of N,N-diethylacrylamide and acrylic acid mixtures on optically clear adhesives. *Journal of Applied Polymer Science.* 135(21): 46277.

Lu, Z., Lanagan, M., manias, E., Macdonald, D.D. (2009) Two-port transmission line technique for dielectric property characterization of polymer electrolyte membranes. *The Journal of Physical Chemistry B.* 113: 13551-13559.

Lee, J.-H., Lee, T.-H., Shim, K.-S., Park, J.-W., Kim, H.-J., Kim, Y., Jung, S. (2016) Molecular weight and crosslinking on the adhesion performance and flexibility of acrylic PSAs. *Journal of Adhesion Science and Technology.* 30(21): 760-766.

Lee, J.-H., Lee, T.-H., Shim, K.-S., Park, J.-W., Kim, H.-J., Kim, Y., Jung, S. (2017) Effect of crosslinking density on adhesion performance and flexibility properties of acrylic pressure sensitive adhesives for flexible display applications. *International Journal of Adhesion and Adhesives.* 74: 137-143.

Lee, J.H., Myung, M.M., Baek, M.J., Kim, H.-S., Lee, D.W. (2019a) Effects of monomer functionality on physical properties of 2-ethylhexyl acrylate based stretchable pressure sensitive adhesives. *Polymer Testing.* 76: 305-311.

Lee, J.-H., Shim, G.-S., Park, J.-W. Kim, H.-J., Kim, Y. (2019b) Adhesion performance and recovery of acrylic pressure-sensitive adhesives thermally crosslinked with styrene–isoprene–styrene elastomer blends for flexible display applications. *Journal of Industrial and Engineering Chemistry.* 78: 461-467.

Lee, S.-W., Park, J.-W., Park, C.-H., Kim, H.-J. (2014) Enhanced optical properties and thermal stability of optically clear adhesives. *International Journal of Adhesion and Adhesives.* 50: 93-95.

Lee, Y.K., Murarka, S.P., Jeng, S.-P., Auman, B. (1995) Investigations of the low dielectric constant fluorinated polyimide for use as the interlayer dielectric in ULSI. *Materials Research Society Proceedings.* 381: 31−43.

Lei, L., Wang, N., Zhang, X.M., Tai, Q., Tsai, D.P., Chang H.L.W. (2010) Optofluidic planar reactors for photocatalytic water treatment using solar energy. *Biomicrofluidics.* 4: 043004.

Lew, C.M., Li, Z., Li. S., Hwang, S.-J., Liu, Y., Medina, D.I., Sun, M., Wang, J., Davis, M.E., Yan, Y. (2008) Pure-silica-zeolite MFI and MEL low-dielectric-constant films with fluoro-organic functionalization. *Advanced Functional Materials.* 18(21): 3454-3460.

Li, C., Li, Z., Ren X., (2019) Preparation and characterization of polyester fabrics coated with TiO_2/benzotriazole for UV protection. *Colloids and Surfaces A-Physicochemical and Engineering Aspects.* 577: 695-701.

Li, L., Tirrell, M., Korba, G.A., Pocius, A.V. (2001) Surface energy and adhesion studies on acrylic pressure sensitive adhesives. *The Journal of Adhesion.* 76: 307-334.

Liaw, D.-J., Wang, K.-L., Huang, Y.-C., Lee, K.-R., Lai, J.-Y., Ha, C.-S. (2012) Advanced polyimide materials: syntheses, physical properties and applications. *Progress in Polymer Science.* 37: 907−974.

Liang, Y., Xie, W.J., Pakdel, E., Zhang, M.W., Sun, L., Wang, X.G. (2019) Homogeneous melanin/silica core-shell particles incorporated in poly(methyl methacrylate) for enhanced UV protection, thermal stability, and mechanical properties. *Materials Chemistry and Physics.* 230: 319-325.

Lim, K., Chow, W.S., Pung, S.Y. (2019) Accelerated weathering and UV protection-ability of poly(lactic acid) nanocomposites containing zinc oxide treated halloysite nanotube. *Journal of Polymers and the Environment.* 27: 1746-1759.

Liu, Y., Lee, B.P. (2016) Recovery property of double-network hydrogel containing mussel-inspired adhesive moiety and nano-silicate. *Journal of Materials Chemistry B.* 4(40): 6534-6540.

Liu, Y., Zhang, Y., Lan, Q., Liu, S., Qin, Z., Chen, L., Zhao, C., Chi, Z., Xu, J., Economy, J. (2012) High-performance functional polyimides containing rigid nonplanar conjugated triphenylethylene moieties. *Chemistry of Materials.* 24: 1212−1222.

Liu, Y., Qian, C., Qu, L., Wu, Y., Zhang, Y., Wu, X., Zou, B., Chen, W., Chen, Z., Chi, Z., Liu, S., Chen, X., Xu, J. (2015) A bulk dielectric polymer film with intrinsic ultralow dielectric constant and outstanding comprehensive properties. *Chemistry of Materials.* 27: 6543−6549.

Long, T.M., Swager, T.M. (2003) Molecular design of free volume as a route to low-*k* dielectric materials. *Journal of the American Chemical Society.* 125: 14113-14119.

Maex, K., Baklanov, M.R., Shamiryan, D., Iacopi, F., Brongersma, S.H., Yanovitskaya, Z.S. (2003) Low dielectric constant materials for microelectronics. *Journal of Applied Physics.* 93(11): 8793-8841.

Mahdavian, M., Yari, H., Ramezanzadeh, B., Bahlakeh, G., Hasanmi, M. (2018) Immobilization of ultraviolet absorbers on graphene oxide nanosheets to be utilized as a multifunctional hybrid UV-blocker: A combined density functional theory and practical application. *Applied Surface Science.* 447: 135-151.

Mai, Z.H., Xiong, Z.W., Shu, X., Liu, X., Zhang, H.W., Yin, X.Z., Zhou, Y.S., Liu, M., Zhang, M., Xu, W.L., Chen, D.Z. (2018) Multifunctionalization of cotton fabrics with polyvinylsilsesquioxane/ZnO composite coatings. *Carbohydrate Polymers.* 199: 516-525.

Maier, G. (2001) Low dielectric constant polymers for microelectronics. *Progress in Polymer Science*. 26: 3-65.

McConnell, B.K., Pethrick, R.A. (2010) A dielectric study of hydrolytic ageing and the effects of periodic freezing in carbon fibre reinforced plastic jointed structures. *International Journal of Adhesion and Adhesives.* 30: 214-224.

Meador, M.A.B., Wright, S., Sandberg, A., Nguyen, B.N., Van Keuls, F.W., Mueller, C.H., Rodríguez-Solís, R., Miranda, F.A. (2012) Low dielectric polyimide aerogels as substrates for lightweight patch antennas. *ACS Applied Materials & Interfaces.* 4: 6346−6353.

Miller, R.D. (1999) In search of low-*k* dielectrics. *Science.* 286: 421-423.

Miyamoto, M., Ohta, A., Kawata, Y., Nakabayashi, M. (2007) Control of refractive index of pressure-sensitive adhesives for the optimization of multilayered media. *Japanese Journal of Applied Physics.* 46(6B): 3978-3980.

Morgen, M., Ryan, E.T., Zhao, J.-H., Hu, C., Cho, T., Ho, P.S. (2000) Low Dielectric Constant Materials for ULSI Interconnects. *Annual Review of Chemical and Biomolecular Engineering.* 30: 645-680.

Nikafshar, S., Zabihi, O., Ahmadi, M., Mirmohseni, A., Taseidifar, M., Naebe, M. (2017) The effects of UV light on the chemical and mechanical properties of a transparent epoxy-diamine system in the presence of an organic UV absorber. *Materials.* 10(2): 180.

Nitto, “Adhesive Design Technology” 2019년 12월 21일 접속, https://www.nitto.com/kr/ko/rd/base/adhesive/specificat/.

Othman, M.B.H., Ramli, M.R.R., Ahmad, L.Y.Z., Akil, H.M. (2011) Dielectric constant and refractive index of poly (siloxane-imide) block copolymer. *Materials and Design.* 32: 3173-3182.

Park, C.-H., Kim, H.-J. (2015) Optical bonding materials for touch screen panel. *Polymer Science and Technology.* 26(4): 313-322.

Park, C.-H., Lee, S.-J., Lee, T.-H., Kim, H.-J. (2015) Characterization of an acrylic polymer under hygrothermal aging as an optically clear adhesive for touch screen panels. *International Journal of Adhesion and Adhesives.* 63: 137-144.

Park, C.-H., Lee, S.-J., Lee, T.-H., Kim, H.-J. (2016) Characterization of an acrylic pressure-sensitive adhesive blended with hydrophilic monomer exposed to hygrothermal aging: assigning cloud point resistance as an optically clear adhesive for a touch screen panel. *Reactive and Functional Polymers.* 100: 130-141.

Pellerin, J., Fox, R., Ho, H.M. (1997) Low dielectric constant fluorinated polyimides for interlayer dielectric applications. *Materials Research Society Proceedings.* 476: 113−119.

Peng, T.-Y., Lv, H.-J., Zeng, P., Zhang, X.-H. (2011) Preparation of ZnO nanoparticles and photocatalytic H_2 production activity from different sacrificial reagent solutions. *Chinese Journal of Chemical Physics.* 24(4): 464-470.

Pfeffer, A., Mai, C., Militz, H. (2012) Weathering characteristics of wood treated with water glass, siloxane or DMDHEU. *European Journal of Wood and Wood Products.* 70: 165-176.

Qian, C., Bei, R., Zhu, T., Zheng, W., Liu, S., Chi, Z., Aldred, M.P., Chen, X., Zhang, Y., Xu, J. (2019) Facile strategy for intrinsic low-*k* dielectric polymers: molecular design based on secondary relaxation behavior. *Macromolecules.* 52: 4601-4609.

Ren, Y., Lam, D.C.C. (2008) Properties and microstructures of low-temperature-processable ultralow-dielectric porous polyimide films. *Journal of Electronic Materials*. 37(7): 955-961.

Riedel, J.-H., Hocker, H. (1994) Preparation and characterization of polymers with pending UV-absorber groups. I. Polymers based on polydimethylsiloxane. *Journal of Applied Polymer Science.* 51: 573-579.

Rodil, R., Moeder, M., Altenburger, R., Schmitt-Jansen, M. (2009) Photostability and phytotoxicity of selected sunscreen agents and their degradation mixtures in water. *Analytical and Bioanalytical Chemistry.* 395: 1513-1524.

Samsung Display Newsroom (2017a), "[디스플레이 톺아보기] 디스플레이 기술의 기원 Part. 1", 2017년 2월 9일, 2019년 5월 7일 접속, http://news.samsungdisplay.com/326.

Samsung Display Newsroom (2017b), "[디스플레이 톺아보기] 디스플레이 기술의 기원 Part. 2", 2017년 2월 23일, 2019년 5월 7일 접속, http://news.samsungdisplay.com/316.

Samsung Display Newsroom (2018), "[디스플레이 톺아보기] PID (Public Information Display), 2018년 9월 13일, 2019년 5월 8일 접속, http://news.samsungdisplay.com/16236.

Sano, M., Oguma, H., Sekine, M., Sato, C. (2013) High-frequency welding of polypropylene using dielectric ceramic compounds in composite adhesive layers. *International Journal of Adhesion and Adhesives.* 47: 57-62.

Sano, M., Oguma, H., Sekine, M., Sata, C. (2014) High-frequency welding of glass-fiber-reinforced polypropylene with a thermoplastic adhesive layer including SiC. *International Journal of Adhesion and Adhesives.* 54: 124-130.

Sano, M., Oguma, H., Sekine, M., Sekiguchi, Y., Sato, C. (2015) High-frequency welding of glass-fibre-reinforced polypropylene with a thermoplastic adhesive layer: Effects of ceramic type and long-term exposure on lap shear strength. *International Journal of Adhesion and Adhesives.* 59: 7-13.

Satas, D. (1999) Handbook of Pressure-sensitive Adhesive Technology. 3rd ed. Van Nostrand Reinhold, New York.

Shamiryan, D., Abell, T., Iacopi, F., Maex, K. (2004) Low-*k* dielectric materials. *Materials Today.* 7: 34-39.

Silaghi, M.A. (2012) Dielectric Material., Chapter 1, Ahmad, Z. Polymeric Dielectric Materials. IntechOpen, London.

Sperling, L.H. (2006) Introduction of Physical Polymer Science. 4th ed. John Wiley & Sons, New Jersey.

Suyal, N., Krajewski, T., Menning, M. (1999) Microstructural and dielectric characterization of sol-gel derived silicon oxycarbide glass sheets. *Journal of Sol-Gel Science and Technology.* 14(1): 113-123.

Sydlik, S.A., Chen, Z., Swager, T.M. (2011) Triptycene polyimides: soluble polymers with high thermal stability and low refractive indices. *Macromolecules.* 44: 976−980.

Tao, L., Yang, H., Liu, J., Fan, L., Yang, S. (2010) Synthesis of fluorinated polybenzoxazoles with low dielectric constants. *Journal of Polymer Science Part A: Polymer Chemistry.* 48: 4668−4680.

Tummala, R.R., and Rymaszewski, E.J. (1989) Microelectronics Packaging Handbook. Van Nostrand Reinhold. New York.

Volksen, W., Miller, R.D., Dubois, G. (2010) Low dielectric constant materials. *Chemical Reviews.* 110: 56-110.

Vu, M.C., Bae, Y.H., Yu, M.J., Choi, W.-K., Islam, M.A., Kim, S.-R. (2019) Thermally conductive adhesives from covalent-bonding of reduced graphene oxide to acrylic copolymer. *The Journal of Adhesion.* 95(10): 887-910.

Wang, C., Sheng, X., Xie, D., Zhang, X., Zhang, H. (2016) High-performance TiO_2/polyacrylate nanocmposites with enhanced thermal and excellent UV-shielding properties. *Progress in Organic Coatings.* 101: 597-603.

Wang, J., Zhou, J., Jin, K., Wang, L., Sun, J., Fang, Q. (2017) A new fluorinated polysiloxane with good optical properties and low dielectric constant at high frequency based on easily available tetraethoxysilane (TEOS). *Macromolecules.* 50: 9394−9402.

Wang, S.Q., Balagula, Y., Osterwalder, U. (2010) Photoprotection: a review of the current and future technologies. *Dermatologic Therapy.* 23: 31–47.

Wypych, A., Wypych, G. (2015) Databook of UV Stabilizaers. ChemTec Publishing, Canada.

Xiong, M., Ren, Z., Liu, W. (2019) Fabrication of superhydrophobic and UV-resistant surface on cotton fabric via layer-by-layer assembly of silica-based UV absorber. *Journal of Dispersion Science and Technology.* (https://doi.org/10.1080/01932691.2019.1634589).

Xu, W., Yu, Y., Zhang, C., He, H. (2008) Selective catalytic reduction of NO by NH_3 over a Ce/TiO_2catalys. *Catalysis Communications.* 9: 1453-1457.

Yuan, B.N., Ji, X.D., Nguyen, T.T., Huang, Z.H., Guo, M.H. (2019) UV protection of wood surfaces by graphitic carbon nitride nanosheets. *Applied Surface Science.* 467: 1070-1075.

Yuan, C., Jin, K., Li, K., Diao, S., Tong, J., Fang, Q. (2013) Non-porous low-*k* dielectric films based on a new structural amorphous fluoropolymer. *Advanced Materials.* 25: 4875−4878.

Zhang, K., Han, L., Froimowicz, P., Ishida, H. (2017) A smart latent catalyst containing o-trifluoroacetamide functional benzoxazine: precursor for low temperature formation of very high performance polybenzoxazole with low dielectric constant and high thermal stability. *Macromolecules.* 50: 6552−6560.

Zhang, X., Ding, Y., Zhang, G., Li, L., Yan, Y. (2011) Preparation and rheological studies on the solvent based acrylic pressure sensitive adhesives with different crosslinking density. *International Journal of Adhesion and Adhesives.* 31: 760-766.

Zhang, X., Liu, H., Yue, L., Bai, Y., He, J. (2019a) Fabrication of acrylic pressure-sensitive adhesives containing maleimide for heat-resistant adhesive applications. *Polymer Bulletin.* 76: 3093-3112.

Zhang, X., Wang, F., Zhu, Y., Qi, H. (2019b) Cyanate ester composites containing surface functionalized BN particles with grafted hyperpolyarylamide exhibiting desirable thermal conductivities and a low dielectric constant. *RSC Advances.* 9(62): 36424-36433.

Zhu, T., Li, S., Huang, J., Mihailiasa, M., Lai, Y. (2017) Rational design of multi-layered superhydrophobic coating on cotton fabrics for UV shielding, self-cleaning and oil-water separation. *Materials and Design.* 134: 342-351.

Zuo, X., Morlet-Savary, F., Graff, B., Blancharde, N., Goddard, J.-P., Lalevee, J. (2016) Fluorescent brighteners as visible LED-light sensitive photoinitiators for free radical photopolymerizations. *Macromolecular Rapid Communications.* 37(10): 840-844.

초록

다양한 정보를 화면에 출력하는 표시 장치를 디스플레이라고 정의한다. 기종 디스플레이는 TV 와 컴퓨터 모니터로 제한되었지만 21 세기에는 휴대 전화 및 테블릿까지 응용 범위가 확장되었다. 따라서, 디스플레이를 위한 다양한 기능이 요구된다. 기존의 점착제 (PSA)는 디스플레이를 구성하는 각층을 고정시키는 역할을 했다. 그러나, 디스플레이가 발전됨에 따라 PSA 의 다양한 기능이 요구되고 있다. 현재 디스플레이용 PSA 에 요구되는 대표적인 기능성은 투명성, 복원 특성, 낮은 유전율 및 자외선 (UV) 흡수 등이 있다.

디스플레이를 구성하는 각 층은 아크릴 PSA 에 의해 고정되기 때문에, 충분한 점착력이 요구된다. 특히, 유연 디스플레이용 아크릴 PSA 는 점착력 뿐만 아니라 연신 및 복원 특성도 필요하다. 이러한 이유로, 아크릴계 PSA 상에 고/저 가교도 영역을 갖는 패턴을 제조하여 UV 패턴 효과를 확인하였다. 가교제 함량 및 UV dose 에 따른 Gel fraction 측정 결과, 가교제 함량 1 phr 및 1600 mJ/cm^2 의 UV dose 에서 가장 높은 Gel fraction 값이 얻어졌다. 최적의 낮은 가교도 영역을 제조하기 위해, 회색 및 흑색 명암에 따른 패턴 필름을 이용하였다. UV intensity 측정 결과, 회색 50 %는 가장 큰 가교도 차이를 나타냈다. 패턴 형성의 가시화를 위해, 발광 화합물인 2,5-bis(5-tert-butyl-benzoxazol-2-yl)thiophene (BBT)를 첨가하였고, 최적 함량은 0.001 phr 임을 확인하였다. 패턴 크기에 따른 UV 패턴 아크릴 PSA 의 Peel

strength 및 Pull-off 측정 결과, 패턴이 형성됨에 따라 감소하는 경향을 보였다. 허나, 패턴 사이즈가 2 mm 로 감소하였을 때, 점착력이 증가하였다. 한편, Lap shear 시험 결과, 패턴이 형성되었을 때, 최대 전단 응력 및 전단 변형이 감소하였다. 패턴 사이즈가 감소에 따른 큰 차이는 보이지 않았다. 응력 완화를 통한 복원 측정 결과, 패턴 사이즈가 4 mm 이하로 감소하였을 때, 특정 변형을 견디기 시작하였다. 또한, 패턴 사이즈가 2 mm 로 감소하였을 때, 복원이 약 60 %로 증가하였다. 이 결과를 통해, 아크릴 PSA 의 점착력 및 복원에 대한 UV 패턴의 가능성을 확인하였다.

스마트 장비의 터치 패널을 부드럽게 구동하려면 PSA 의 유전율을 조절할 수 있어야 한다. 이러한 이유로, 아크릴 프리폴리머를 합성하였고, 4 가지 종류의 Low-*k* 단량체를 선택하였다. 아크릴 프리폴리머를 Low-*k* 단량체와 혼합하고 UV 가교를 통해 PSA 필름을 제조하였다. 제조한 필름의 점착력 및 유전율을 측정하였다. 아크릴 PSA 는 Hexamethyldisiloxane (HMDS)의 함량이 증가함에 따라, 점착력이 감소하였으나, N-vinylcaprolactam (NVC)의 함량이 증가함에 따라, 점착력이 증가하였다. Low-*k* 단량체의 함량이 증가함에 따라, 아크릴 PSA 의 유전율은 감소하는 경향을 보였지만, 다른 물성들은 단량체의 종류에 따라 다른 경향을 보였다. 이 결과를 통해, Low-*k* 단량체의 종류 및 함량에 따라 자유 부피 형성의 차이로 인해 아크릴 PSA 의 점착력 및 유전율이 조절될 수 있음을 확인하였다.

최근 디스플레이는 야외에서 널리 이용되고 있다. 이러한 이유로, 디스플레이는 UV 조사로 인한 노화 및 신뢰성 문제를 야기할 위험이 있다.

이러한 문제로 인해 디스플레이의 각 층을 고정하는 PSA 에도 UV 흡수 특성이 필요하다. 광중합을 통해, 아크릴 프리폴리머를 제조하였고, UV 흡수제 (UVA) 및 가교제를 이용하여 아크릴계 PSA 를 제조하였다. UVA 의 종류 및 함량에 따라 가시 영역에서의 색상 변화 및 투과율 측정 결과, 큰 차이를 보이지 않았다. UVA 의 종류 및 함량에 따른 UV 흡수을 측정한 결과, 아졸기를 갖는 UVA 가 벤젠기를 갖는 UVA 보다 효과적이었다. 아졸기를 갖고 비교적 분자량이 작은 Benzotriazole 의 효율이 더 높고 즉각적이었다. UVA 의 종류 및 함량에 따른 점착력 특정 결과, 큰 차이를 보이지 않았다. 그러나, 분자량이 큰 Triazine 함량 3 phr 에서 응집력 감소로 인해 점착력이 급격히 감소하였다. 즉, 일정 함량의 UVA 는 점착력 및 투명성을 감소시키지 않으면서 UV 흡수가 가능하였다. 다양한 종류의 UVA 중에서도, 아졸기를 갖고 분자량이 작은 UVA 가 UV 흡수에 가장 효과적이었다.

디스플레이 적용을 위한 아크릴 PSA 의 기능성 향상 및 점착력에 미치는 영향에 대한 연구가 앞으로 보다 심화된 연구를 진행하는데 참고될 수 있기를 바랍니다.

주요어: 아크릴 점착제, 점착력, 기능성, 패턴, 복원 특성, 유전율, UV 흡수

학번: 2015-30381